EVALUATION OF MODELS FOR SUBSURFACE DISPERSANT INJECTION

FINAL REPORT

E. Eric Adams, PhD, PE

Scott A. Socolofsky, PhD

Michel Boufadel, PhD, PE

Submitted to

American Petroleum Institute

Oil Spill Response Joint Industry Task Force (JITF)

D3 Subsea Dispersant Injection Modeling Team

Suzanne M. Lemieux [LemieuxS@api.org]

Colin Frazer [FrazierC@api.org]

June 30, 2017

(Revised July 27, 2017)

Introduction

Since the fall of 2012, we have reviewed models and supporting experimental data to predict the sizes of droplets resulting from oil jetted into seawater due to an accidental deep ocean oil well blowout. Many of the studies we have reviewed were conducted by SINTEF, sometimes in collaboration with other institutions, under support of API D3. We have also developed our own droplet model (VDROP-J) and coupled it with both analytical and numerical models (TAMOC model) of buoyant jet dynamics. Through variation in the interfacial tension (IFT) between oil and water, these models also address the effectiveness of subsurface dispersant injection as was exercised during the Deepwater Horizon oil spill. Our work is described in a series of ten progress reports. Outlines of each report are provided at the end of this report, and the reports themselves are provided as an appendix. A brief summary of our review, and its major conclusions, are listed below, with emphasis on those items that were of particular interest to API as expressed to us. We also include a modest sensitivity study comparing the SINTEF and ASA models. More information is provided in the progress reports.

Summary and Conclusions

- There are two basic types of droplet models. The first includes equilibrium (or modified Weber number) correlation equations, as typified by the SINTEF model (Johansen et al., 2013; reviewed in PR1) and the ASA model (Li et al., 2017; reviewed in PR9 and PR10), that predict a characteristic droplet size and spread coefficient of a size distribution. The second class includes dynamic (or population) models as typified by VDROP-J (Zhao et al., 2014; reviewed in PR3, PR6 and PR9) and Oildroplets (Nissank and Yapa, 2016; reviewed in PR9), that dynamically solve for the time-evolving size distribution. Most operational oil spill models use size distributions from equilibrium models.
- The SINTEF model predicts the volume median droplet size

  $$d_{50}/D = A\{We_{SIN}/[1+BVi(d_{50}/D)^{1/3}]\}^{-3/5}$$

  where $We_{SIN} = \rho_o U^2 D/\sigma$ is the Weber number (the subscript SIN is used to distinguish this definition from the one below attributed to ASA), $Vi = \mu U/\sigma$ is the viscosity number, D is the orifice diameter, U is the exit velocity, σ is the interfacial tension (IFT) between oil and water, μ is the viscosity of oil, ρ_o is the density of oil, and A, B are empirical coefficients. The ASA model predicts d_{50} as

  $$d_{50}/d_o = r\, We_{ASA}^{q}\, (1 + 10Oh)^{p}$$

where $We_{ASA} = \rho_w U^2 d_o/\sigma$ is ASA's Weber number, $Oh = \mu/(\rho\sigma d_o)^{0.5}$ is the Ohnesorge number, and r, q and p are empirical coefficients or exponents. Finally, d_o is a characteristic length equal to the smaller of the orifice diameter D or the maximum stable droplet size d_{max} given by

$$d_{max} = 4\{\sigma/[g(\rho_w-\rho_o)]\}^{0.5}$$

While the number of input parameters to these models is small, there may be uncertainty as to the viscosity and IFT under field conditions, especially when chemical dispersants are used. Both models assume the spread coefficient of the size distribution is independent of scale and given by experiment.

- Equilibrium models assume droplets form due to turbulence produced by the jet, balanced by IFT and/or viscosity. Because turbulence varies with distance z along the trajectory, one could expect model coefficients (e.g., A, r) to depend on the relative distance z/D at which droplet size is measured. Population models, discussed below, show that DSDs, including d_{50}, do vary with trajectory length, at least over a short distance, but there are insufficient experimental data to show conclusively if, and if so by how much, d_{50} varies with distance in the lab (where it is difficult to make measurements close to the source).
- The two unknowns in SINTEF's model (A and B) were calibrated to measured oil droplet sizes from two studies conducted by the same researchers in the same facility (Tower Basin). In the earlier study Johansen et al., (2013) arrived at A = 15 and B = 0.8, while in the latter study Brandvik et al. (2014) found A = 24.8 and B = 0.08. In the sensitivity study below, one can see that the two coefficients steer the droplet size in different directions. Unless otherwise stated we refer to the second pair (A = 24.8 and B = 0.08) as the "SINTEF" model, since this version has received the most model verification.
- The ASA model has two exponents and one constant. The exponents (p = 0.46 and q = -0.518) were calibrated to data from *surface* oil slicks, and the same values are used for *subsurface* oil. The goal was to create a unified model, but we wonder if this is possible, given the somewhat different break-up mechanisms (turbulence due to wave breaking versus jet-induced turbulence). Meanwhile ASA's constant (r) was calibrated to droplet sizes measured during the DeepSpill field study. Two different values of r were determined based on two different estimates of observed d_{50}: Spaulding et al. (2016) report r = 9.67 while Li et al., (2017) report r = 14.05. As with the SINTEF model, the variation in the coefficient is a reflection of the uncertainty in their model. As a note, we looked at the same DeepSpill data (Release 2 involving methane and natural gas; PR1, PR3, and PR10) and concluded that, on this basis, r should really be closer to the smaller value. However, the overall agreement with data was better with r = 14.05 and we take this as the "ASA" model. See further discussion under sensitivity study.
- The SINTEF model does not explicitly account for the maximum stable droplet size, but one can override predictions of d_{50} if they exceed d_{max}. The ASA model accounts for the

maximum stable droplet size by using d_{max} rather than D as their length scale (to normalize d_{50} and for use in We_{ASA} and Oh) when $D > d_{max}$. This certainly reduces the magnitude of d_{50} predicted by their equation, but it is possible that for certain parameters, d_{50} could exceed d_{max}, even if $d_{max} < D$. This is most likely at field scale (where D is large) and for small U. See sensitivity study.

- Theoretically, *D may be the better normalizing length scale* to use because the magnitudes of We, on which both models depend, reflect the level of turbulence which, in a jet, is proportional to U^3/D. Li et al. (2017) justify their use of d_{max} by referring to Hinze (1955), who defined a critical We based on the diameter of the largest droplet (roughly d_{95}) that can survive in a turbulent environment. But d_{95} is fundamentally different from d_{max}, which is the diameter of the largest droplet that can survive free ascent in a quiescent environment. Also, SINTEF is following Hinze (1955) more closely when they assume that d_{95} is proportional to d_{50} and that the We based on D is proportional to Hinze's critical We since turbulent dissipation, which gives the critical We, is proportional to U^3/D. Their assumption starts to breakdown, though, if breakup occurs outside of the zone of flow establishment ($z = 6D$) since turbulent dissipation decays rapidly along the jet centerline for $z > 6D$.
- Both log-normal and Rosin-Rammler distributions have been fit to measured *volume* distributions of droplet sizes. Data from Johansen et al. [2013] suggest that the former provides the better fit at large droplet sizes, while the latter is better at smaller sizes. Arguably the larger droplets are more important because they will surface more readily, suggesting a slight preference for the log-normal distribution. It is also easier to determine parameters for the log-normal distribution. (For example the peak of the volume distribution is identically d_{50}.) To apply these distributions to the field, Johansen et al. [2013] suggest that the standard deviation is scale independent. The lack of available field data makes it difficult to test this hypothesis. Occasionally a *number* distribution for droplet size is provided. Due to processes such as tip-streaming or shearing, a large number of droplets with very small diameter might be created. Because of their small size, they would be able to enter and remain in sub-surface intrusions caused by density stratification, and hence contribute to measured CDOM profiles in the field. However, their contribution to the volume distribution might still be negligible. Indeed they may not be resolvable with the LISSST instrumentation commonly used to measure droplet sizes.
- Gas often accompanies oil in a blowout. *If the gas and oil flow together* (in parallel, as opposed to a series of separated slugs), the gas will squeeze the oil into a smaller cross-sectional area of the orifice. SINTEF handles this by defining a modified exit velocity $U_n = U/(1-n)^{1/2}$, which *conserves momentum*. Here n is the void ratio, assumed to be equal to GOR/(1+GOR), where GOR is the *in situ* gas-oil ratio in volume units. The ASA model handles this effect somewhat differently by using conservation of mass, giving an oil *exit velocity*, $U_n = U/(1-n)$. In PR1 and PR10 we explored these—and other—ways to

account for flow blockage due to gas, and found that the SINTEF correction worked best. However, this was based on limited data (a subset of data contained in SINTEF/SwRI's API D3 Phase V study; Brandvik, 2017). Other data showed less decrease (or even an increase) in droplet size with increasing gas flow.

- Gas is also highly buoyant, so a discharge of oil and gas is more plume-like than the oil-only discharges for which equilibrium models were calibrated, yielding a slower decay of the turbulent dissipation with distance from the source and potentially increasing the breakup. This effect varies with the non-dimensional distance along the trajectory (z/D), and SINTEF focuses on the non-dimensional distance l_M/D where l_M is the "momentum length" given by $l_M = M^{3/4}/B^{1/2}$ where M and B are the kinematic momentum and buoyancy fluxes of the oil and gas discharge. The SINTEF model accounts for gas buoyancy by calculating an effective exit velocity, U_C, that gives the same jet velocity at l_M, as would be given for a plume with discharge velocity U_n. The concept of l_M has been used for *single phase* buoyant jets which are directed either vertically or with a horizontal angle, but its application to multi-phase jets is untested. Also, SINTEF's buoyancy adjustment assumes that droplet size is determined by the level of jet energy dissipation at an elevation of precisely l_M. (Why not 0.5 l_M or 2 l_M?) Finally, the effects of gas on flow blockage and buoyancy both ignore gas momentum. Gas density, of course, increases with depth and could contribute up to ~ 15% of the total momentum in the case of DWH (PR 10).
- The models discussed above pertain to oil droplets from oil jets, with or without co-flowing gas. It would be tempting to apply them to pure gas discharges, but Weber number scaling does not apply to a pure gas release because the low density prevents the gas from forming jets. It is unclear how well We number models do in predicting gas bubble sizes in a gas-liquid mixture. The ASA model (Spaulding, 2015) was apparently applied to DeepSpill Release 4 (LNG mixed with seawater; discussed in PR3 and PR 9), but no results are presented, although the combined seawater likely did produce a jet in this case.
- Population models are a more physically-based alternative to equilibrium models, as they simulate actual droplet break-up and coalescence. As such they can compute *spatially varying* droplet size *distributions* as opposed to simply characteristic sizes (d_{50}). VDROP-J and the recent model Oildroplets each have a calibrated coefficient (one to adjust breakup efficiency in VDROP-J and one to adjust the jet's energy dissipation rate in the case of Oildroplets). We believe adjusting the energy dissipation contradicts studies on jet and plume hydrodynamics, whereas using a parameter that applies only on oil breakup is more physically-based. Both models require judicious selection of the initial droplet size, which introduces some degree of empiricism in these models. However, once calibrated they have been shown to simulate measured droplet size distributions quite well.

- The models discussed above describe droplet breakup due to turbulence (i.e., dynamic breakup). Additional breakup, called tip-streaming, is associated with capillary instability on the surface of a droplet. Using an inverted cone with recirculating seawater, Nagamine (2014) observed that tip-streaming caused oil droplets, with initial diameters of several millimeters and impregnated with high concentration of dispersants (DOR > 1:50), to disappear over a time scale of minutes to 10s of minutes. However, these droplets were introduced directly to the cone and never experienced turbulent breakup. Follow-up experiments conducted at SINTEF with a different injection scheme, without recirculation, and at lower temperatures (hence higher viscosities), were not able to reproduce the same degree of breakup (Davies, et al., 2016). Zhao et al. (2017) injected oil as a horizontal jet into seawater and measured DSDs using a LISST instrument. Without dispersant, they measured a unimodal DSD with d_{50} = 114 μm, while with dispersant pre-mixed at a DOR of 1:20, the distribution was strongly bi-modal with d_{50} = 5.9 μm and a plurality of the droplets having diameters less than 2.7 μm. They were unable to directly separate the effects of dynamic and tip streaming breakup, but inferred that tip streaming did occur, because they could not simulate the DSD using VDROP-J, which only handled dynamic breakup. They subsequently introduced into VDROP-J a first order loss mechanism to handle tip-streaming and, with a calibrated rate constant, were able to reproduce the experimentally observed bi-modal DSD.
- It would be helpful to have more tests of tip-streaming. It is clear from any number of transport model simulations, that the very small droplets, attributed to tip-streaming in idealized laboratory experiments, would be advected far greater distances and have far longer time to biodegrade before surfacing, if indeed they did surface. Yet these experiments have been conducted with relatively high DOR (much greater than applied at DWH and hence of possible environmental and economic concern) and, in the case of Nagamine (2014), dynamic breakup most likely did not occur. Would the tip streaming be as strong if the dynamic breakup occurred first—or simultaneously?
- We also recommend that future work on droplet formation revisit the behavior of gas mixed with oil. First, it would be helpful to know under what conditions gas and oil exit the orifice together or as separate slugs. If not together, there is less concern over the role of gas in oil droplet formation. Also, there has only been one experiment that shows convincingly how droplet size decreases with increasing gas flow rate. Ability to measure droplet sizes when oil and gas are co-mixed has been hampered by the inability to distinguish droplets and bubbles, but SINTEF's SilCam seems to have addressed this problem, and it would be helpful to have some confirmatory experiments. Because oil in water experiments will always be extrapolated to field scale parameter space, it would help to have these tests conducted at the largest scale possible, and short of a second DeepSpill field experiment, the OHMSETT facility, with towed jets, seems best suited.
- Finally, related to the last bullet, ASA's assumption that dmax serves as the appropriate length scale, rather than D, could be tested by conducting experiments in a large facility

with constant oil properties and constant U, but variable D in the range where D > d_{max}. Does d_{50} remain constant as D increases?

Sensitivity study involving ASA and SINTEF models

The two equilibrium models exhibit different sensitivity when extrapolated from lab to field conditions and in comparing treated and untreated oil. Table 1 at the back of this report illustrates some simple sensitivity using an oil only discharge (no gas) with typical parameters for the laboratory and the field. Laboratory conditions are characterized by D=0.2 cm, U = 300 cm/s, ρ_w = 1.03 g/cm^3, ρ_o = 0.85 g/cm^3, σ = 23 dynes/cm (untreated), σ = 0.23 dynes/cm (treated), and μ = 0.1 g/cm-s. Field conditions are the same except D = 50 cm and U = 60 cm/s. For these conditions d_{max} = 1.44 cm and 0.144 cm for untreated and treated oil respectively. For **untreated oil in the laboratory** the SINTEF and the ASA models predict similar size droplets. For the SINTEF model the new coefficients produce droplets that are 23% larger than droplets produced with the old coefficients while the corresponding difference with the ASA model is about 45%. For **untreated oil in the field** the ASA model predicts droplets that are 12 times larger than in the lab. With r = 14.05, their prediction of d_{50} = 1.30 cm approaches, but is still smaller than d_{max}. If droplets were not constrained by d_{max}, the SINTEF model would predict untreated droplets in the field to be 20 times larger than those in the lab, but with the constraint, the predicted droplet size in the field is 14 times larger than in the lab. Because the droplets are limited to d_{max}, SINTEF's droplet size does not change with model coefficients. And, due to the limitation on d_{max}, SINTEF's droplets are only about 10% larger than those predicted by ASA. For **treated oil in the laboratory** the ASA model predicts droplets that are about 7 times smaller than if they were untreated, while the SINTEF model predicts droplets that are about 6 times larger. SINTEF's droplets are about 10% larger than ASA's. Finally, **for treated oil in the field** the ASA model shows a 15 fold decrease in droplet size compared with untreated oil in the field, while the SINTEF model shows an 11 fold decrease if d_{max} were not constraining, or a 10 fold decrease if d_{max} is constraining. SINTEF's droplets are about 60% larger than those of ASA. We conclude from the above that, using the more recent set of coefficients for both models, and for the conditions tested, the SINTEF model predicts generally larger droplets than the ASA model, but the difference varies with condition because the two models have different numbers of coefficients and because predicted droplets in the field run up against d_{max}.

This difference in the two models is pursued further in Tables 2a-d, which show predicted d_{50} for the two models for a range of U and D assuming untreated and treated oil, without and with gas (n = 0 and 0.6). Parameter combinations that lead to droplets outside of the atomization range (We_{SIN} < 324) are shaded in red. Note that, for certain parameters, both models predict values of d_{50} that are constrained by d_{max}. Parameter combinations when the SINTEF model is constrained by d_{max} are shaded in grey. For small values of D (as in the lab) the two models predict comparable droplet sizes, but as D increases, SINTEF's droplets become larger, which can be

explained by the fact that the length scale in ASA's model reverts to d_{max} at large D. (When D > d_{max}, the ASA model predicts values of d_{50} that are totally independent of D, all else equal.) Under these (field) conditions the ASA model predicts both smaller droplets in general, and a greater decrease in droplet size when oil is treated. Finally, both models predict smaller droplets when oil of a given flow rate (given U and D) is accompanied by gas. The SINTEF model predicts smaller droplets as the result of increased effective exit velocity needed to conserve momentum and the increase in velocity needed to account for gas buoyancy. The ASA model accounts for only the former effect, but by conserving mass, their effective exit velocity is often even higher than SINTEF's.

Brief Summary of Our Progress Reports

- Progress Report 1 December 28, 2012
  - Reviewed SINTEF's modified Weber number formula and its theoretical basis (as described in *Marine Pollution Bulletin* publication and API D3 Phase I report on effects of DOR and geometry)
  - Discussed SINTEF'S approach to correcting for co-flowing gas, and suggested an alternative approach
  - Compared SINTEF model predictions of median droplet diameter with lab data (SINTEF's Tower Basin, U. Hawaii), and Field data (DeepSpill experiment)
  - Extrapolated SINTEF's predictions to field scale (DWH)
- Progress Report 2 February 25, 2013
  - Discussed droplet size distributions observed in the lab and field
  - Reviewed Bandera and Yapa's population based model
  - Summarized integrated models for oil fate and transport from sub-surface spills
  - Proposed test cases for model inter-comparison study
- Progress Report 3 May 23, 2013
  - Reviewed droplet size data from DeepSpill experiment
  - Reviewed, further, Bandera and Yapa's population model
  - Developed analytical expressions for plume energy dissipation rate, centerline velocity, width and flow rate for buoyant plumes.
  - Introduced our own population model (later known as VDROP-J) and compared predicted droplet size distributions with those measured at DeepSpill
- Progress Report 4 June 2, 2013
  - Reviewed droplet model of Boxall (2013) as applied by Paris et al. (2012)
  - Reviewed maximum entropy formalism model of Chen and Yapa (2007)
- Progress Report 5 November 30, 2013
  - Discussed planning for January 2014 workshop on integrated model inter-comparison

- Progress Report 6 March 12, 2014
  - Summarized January 2014 workshop on integrated models
  - Discussed draft manuscript on VDROP-J
  - Reviewed SINTEF's API D3 Phase II study.
- Progress Report 7 November 10, 2014
  - Reported on follow-up from January 2014 workshop
  - Submitted draft manuscript on VDROP-J to *Marine Pollution Bulletin*
  - Reviewed preliminary inverted cone results (SINTEF/U. Hawaii API D3 Phase IV study on latent breakup)
  - Reviewed SINTEF's unpublished report on effectiveness of different injection techniques
  - Reviewed SINTEF/SwRI's high pressure tests (API D3 Phase IIIa study on effects of high pressure)
- Progress Report 8 August 18, 2015
  - Coupled VDROP-J to TAMU's multiphase near field plume model
  - Compared SINTEF's model against data described in Belore (2014)
  - Published small article in *HydroLink*, a publication of IAHR, on the topic of Fluid mechanics of oil spilled form a deep ocean blowout: the role of chemical dispersants. Gave a plenary lecture on the topic at the 36th IAHR World Congress at the Hague (June 29-July 3, 2015).
- Progress Report 9 September 23, 2016
  - Reviewed RPS ASA' model and compared results from SINTEF and RPS ASA's formulas against median droplet size measured during five experiments
  - Reviewed Nissanka and Yapa (2016), a follow-up to Bandera and Yapa (2011).
  - Reviewed SINTEF/SwRI's API D3 Phase V study of oil droplets in the presence of co-flowing gas
  - Reviewed S.L.Ross/SINTEF's API D3 Phase VI study on upscaling using experiments with silhouette camera at OHMSETT facility
  - Compared VDROP-J predictions to the Phase VI results
  - Reported on further coupling of TAMOC and VDROP-J
- Progress Report 10 April 28, 2017
  - Provided additional discussion of the RPS ASA equations
  - Discussed various approaches to correct for co-flowing gas

References

Brandvik, P.J. O. Johansen, U. Farooq, G. Angell and F. Leirvik (2012), "Subsurface oil releases-experimental study of droplet distributions and different dispersant injection techniques." Final report version 2 prepared by SINTEF Materials and Chemistry, May 2014.

Brandvik, P.J., E. Davies, C. Storey, F. Leirvik, and D. Krause, (2017). “Subsurface oil releases - Verification of dispersant effectiveness under high pressure using combined releases of live oil and natural gas: A scaled experimental approach using the SwRIs 90" high pressure chamber” Final report prepared by SINTEF Materials and Chemistry, Mar 2017.

Davies, E. J., P.J. Brandvik, O. Johansen, I. Nagamine, D. Dunnebier, S. Masutani, and F. Leirvik (2016), “Fate of subsea dispersed oil droplets: an experimental study combining the SINTEF MiniTower (oil droplets created by a turbulent jet) and the concept of Univ. of Hawaii’s inverted cone system”, Draft report version 5 prepared by SINTEF Materials and Chemistry, June 2016.

Hinze, J.O. (1955). “Fundamentals of the hydrodynamic mechanisms of splitting in dispersion processes”. *AIChE Journal*, 1: 289-295.

Johansen, O., P. J. Brandvik, and U. Farooq (2013), “Droplet breakup in subsea oil releases - Part 2: Prediction of droplet size distributions with and without injection of chemical dispersants”, *Marine Pollution Bulletin, 73*, 327-335.

Li, Z., M.L. Spaulding, D. French McCay, D. Crowley, and J.R. Payne. (2017). “Development of a unified oil droplet size distribution model with application to surface breaking waves and subsea blowout release considering dispersant effects”. *Marine Pollution Bulletin* 114(1):247-257.

Nagamine, S.I. (2014) “The effects of chemical dispersants on buoyant oil droplets”. MS thesis, Dept of Mech Eng., U. Hawaii Manoa, HI.

Nissanka, I. D., P.D. Yapa. (2016) “Calculation of oil droplet size distribution in an underwater oil well blowout”, *J. Hydr. Res*, http://dx.doi.org/10.1080/00221686.2016.1144656.

Spaulding, M., D. Mendelsohn, D. Crowley, Z. Li, and A. Bird. (2015) “Technical Reports for Deepwater Horizon Water Column Injury Assessment, WC_TR.13: Application of OILMAP DEEP to the Deepwater Horizon Blowout, Appendix G: Development of OILMAP DEEP droplet size model”. Report prepared by RPS ASA, South Kingstown, RI 02879.

Zhao, L., M. C. Boufadel, S. A. Socolofsky, E. Adams, T. King, and K. Lee (2014), “Evolution of droplets in subsea oil and gas blowouts: Development and validation of the numerical model VDROP-J,” *Marine Pollution Bulletin*, 83(1), 58-69.

Zhao, L., F. Gao, M. C., Boufadel, T. King, B. Robinson, R. Conmy, and K. Lee. (2017) “Oil jet with dispersant: macro-scale hydrodynamics and tip streaming” *AIChE Journal* (in press).

Table 1 Predicted d50 (cm) with ASA and SINTEF models for oil only discharge (no gas) with and without treatment under lab and field conditions (more recent coefficient included in bold; earlier coefficients used for sensitivity)

	Untreated Lab	Untreated Field (no cons)	Untreat Field (const)	Treated Lab	Treated Field (no cons)	Treated Field (cons)
ASA						
r = 14.05	**0.106**	**1.305**	**1.305**	**0.017**	**0.089**	**0.089**
r = 9.67	0.073	0.898	0.898	0.012	0.061	0.061
SINTEF						
A = 24.8; B = 0.08	**0.103**	**2.083**	**1.444**	**0.018**	**0.187**	**0.144**
A = 15; B = 0.8	0.084	1.362	1.362	0.046	0.331	0.144

Table 2a Weber number (top), ASA predicted d50 (cm; middle), and SINTEF predicted d50 (cm; bottom) for oil only discharge (n = 0) without treatment (sig = 23 dynes/cm) for a range of U and D.

	U = 10 cm/s	20	50	100	200	500
D = 0.2 cm	2	5	23	83	313	1891
	1.444	1.444	0.678	0.331	0.161	0.062
	1.444	1.444	0.768	0.360	0.164	0.057
0.5	7	16	65	221	809	4792
	1.444	1.444	0.992	0.484	0.236	0.091
	1.444	1.444	1.030	0.498	0.231	0.081
2	60	110	347	1038	3529	19872
	1.444	1.444	1.444	0.769	0.375	0.145
	1.444	1.444	1.444	0.783	0.379	0.137
5	285	449	1161	3088	9714	51764
	1.444	1.444	1.444	0.769	0.375	0.145
	1.444	1.444	1.444	1.016	0.514	0.191
20	3474	4561	8710	18582	49412	230597
	1.444	1.444	1.444	0.769	0.375	0.145
	1.444	1.444	1.444	1.382	0.772	0.309
50	19446	23422	37567	68533	158184	648875
	1.444	1.444	1.444	0.769	0.375	0.145
	1.444	1.444	1.444	1.444	0.959	0.414

Table 2b Weber number (top), ASA predicted d50 (cm; middle), and SINTEF predicted d50 (cm; bottom) for oil only discharge (n = 0) with treatment (sig = 0.23 dynes/cm) for a range of U and D.

	U = 10 cm/s	20	50	100	200	500
D = 0.2 cm	186	494	2306	8282	31322	189136
	0.144	0.144	0.108	0.053	0.026	0.010
	0.144	0.144	0.081	0.045	0.025	0.012
0.5	685	1582	6489	22058	80915	479223
	0.144	0.144	0.108	0.053	0.026	0.010
	0.144	0.144	0.103	0.058	0.032	0.015
2	6011	10965	34699	103820	352932	1987224
	0.144	0.144	0.108	0.053	0.026	0.010
	0.144	0.144	0.141	0.083	0.047	0.022
5	28507	44871	116135	308822	971370	5176406
	0.144	0.144	0.108	0.053	0.026	0.010
	0.144	0.144	0.144	0.102	0.059	0.028
20	347380	456114	871012	1858161	4941154	23059699
	0.144	0.144	0.108	0.053	0.026	0.010
	0.144	0.144	0.144	0.132	0.082	0.040
50	1944565	2342159	3756680	6853346	15818416	64887541
	0.144	0.144	0.108	0.053	0.026	0.010
	0.144	0.144	0.144	0.144	0.097	0.050

Table 2c Weber number (top), ASA predicted d50 (cm; middle), and SINTEF predicted d50 (cm; bottom) for oil and gas (n = 0.6) without treatment (sig = 23 dynes/cm) for a range of U and D.

	U = 10 cm/s	20	50	100	200	500
D = 0.2 cm	5	14	61	213	794	4755
	1.390	0.678	0.262	0.128	0.062	0.024
	1.444	1.047	0.433	0.206	0.095	0.034
0.5	21	46	175	574	2066	12085
	1.444	0.992	0.384	0.187	0.091	0.035
	1.444	0.210	0.572	0.283	0.133	0.047
2	200	341	983	2792	9183	50530
	1.444	1.444	0.610	0.297	0.145	0.056
	1.444	1.444	0.809	0.435	0.215	0.079
5	988	1462	3437	8576	25785	132844
	1.444	1.444	0.610	0.297	0.145	0.056
	1.444	1.444	0.953	0.554	0.288	0.110
20	12579	15813	27733	54989	137221	605653
	1.444	1.444	0.610	0.297	0.145	0.056
	1.444	1.444	1.088	0.724	0.421	0.175
50	71771	83749	125227	212835	457344	1745219
	1.444	1.444	0.610	0.297	0.145	0.056
	1.444	1.400	1.101	0.803	0.510	0.231

Table 2d Weber number (top), ASA predicted d50 (cm; middle), and SINTEF predicted d50 (cm; bottom) for oil and gas (n = 0.6) with treatment (sig = 0.23 dynes/cm) for a range of U and D.

	U = 10 cm/s	20	50	100	200	500
D = 0.2 cm	550	1372	6057	21255	79369	475452
	0.144	0.108	0.042	0.020	0.010	0.004
	0.144	0.105	0.052	0.029	0.017	0.008
0.5	2128	4573	17452	57395	206574	1208460
	0.144	0.108	0.042	0.020	0.010	0.004
	0.144	0.123	0.064	0.037	0.021	0.010
2	20036	34054	98279	279235	918321	5052968
	0.144	0.108	0.042	0.020	0.010	0.004
	0.144	0.143	0.085	0.052	0.030	0.015
5	98832	146187	343684	857629	2578453	13284406
	0.144	0.108	0.042	0.020	0.010	0.004
	0.144	0.144	0.097	0.063	0.038	0.019
20	1257918	1581317	2773252	5498942	13722061	60565330
	0.144	0.108	0.042	0.020	0.010	0.004
	0.144	0.143	0.108	0.078	0.051	0.026
50	7177140	8374948	12522719	21283497	45734402	174521898
	0.144	0.108	0.042	0.020	0.010	0.004
	0.144	0.133	0.109	0.084	0.059	0.032

APPENDIX A

EVALUATION OF MODELS FOR SUBSURFACE DISPERSANT INJECTION

PROGRESS REPORT 1

E. Eric Adams, PhD, PE

Scott A. Socolofsky, PhD

Michel Boufadel, PhD, PE

Submitted to

American Petroleum Institute

Oil Spill Response Joint Industry Task Force (JITF)

D3 Subsea Dispersant Injection Modeling Team

Attn: Joe Twomey

p.twomey@ecosystem-management.net

November 20, 2012

Revised December 28, 2012

Introduction

Since initiation of the project we have worked on the following tasks of our Scope of Work: Tasks 1.1 (Identify droplet sub-models), Task 1.2 (Obtain model validation data), Tasks 1.3-5 (Program, run and evaluate droplet models) and Task 2.1 (Identify complete oil models). We also participated to the API Workshop in Houston on October 24-25. As agreed upon, we are focusing initially on the SINTEF droplet model (Section 8 of Brandvik, et al., 2012a; Johansen et al., 2012), and here we document our initial findings regarding this model. This revision (dated December 28, 2012, and marked with yellow background) corrects a few small errors in the November 20, 2012 progress report, and adds further discussion on the effect of gas on oil droplet size.

The SINTEF Model

When oil is jetted into water at sufficiently high velocity, it breaks into a number of small droplets, whose distribution can be characterized by a maximum droplet size, an average droplet size, etc. The SINTEF model focuses on the volume median droplet size, d_{50}, which means that half of the volume of oil is contained in larger-diameter droplets. While they discuss various distributions of droplet size surrounding d_{50} (e.g., Rosin-Rammler and log-normal), there is no theory suggesting which distribution, if any, is theoretically correct.

Following the classical study by Hinze (1955), droplets are assumed to form from turbulent break up due to pressure fluctuations and the characteristic droplet size reflects a balance between turbulent energy which wants to create small sizes and interfacial surface tension which resists the break-up. Under *stationary* conditions, the characteristic droplet size (d_{50} here) can be written:

$$d_{50} = c(\sigma/\rho)^{3/5}\varepsilon^{-2/5} \qquad (1)$$

where σ and ρ are the oil-water interfacial tension (IFT) and the oil density, ε is the fluid turbulent dissipation rate, and c is a constant. In a turbulent jet, an oil droplet experiences *time-varying* turbulent energy, as it moves along its trajectory. By dimensional reasoning, ε is proportional to the third power of the local jet mean velocity and inversely proportional to the local jet diameter. Representing these quantities by their discharge velocity U and orifice diameter D, where $U = 4Q/\pi D^2$, with Q being the volume flow rate,

$$\varepsilon \sim U^3/D. \qquad (2)$$

Combining Eqs (1) and (2),

$$d_{50}/D = AWe^{-3/5} \quad (3)$$

where We is the Weber number defined by

$$We = \rho U^2 D/\sigma \quad (4)$$

Because ε varies with distance along the trajectory, and Eq (2) merely provides a proportionality for ε at the orifice, Eq (3) is semi-empirical, and the coefficient A must be determined through comparison with data. To the extent that oil droplets break up due to the time variation of turbulent energy along the jet trajectory, and because ε varies with distance z along the trajectory, we might expect that A depends on the relative height z/D at which droplet size is measured.

Dispersants decrease IFT, and as σ becomes smaller, Eq (3) predicts that d_{50} decreases continuously. But for small σ, viscosity becomes important and ultimately controls droplet size. Following earlier work by Wang and Calabrese (1986), a unified model combining the limiting conditions of both surface tension and viscosity control is

$$d_{50}/D = AWe^{*-3/5} \quad (5)$$

where the modified Weber number is given by

$$We^* = We/[1+BVi(d_{50}/D)^{1/3}] \quad (6)$$

and Vi is the viscosity number defined by

$$Vi = \mu U/\sigma \quad (7)$$

where μ is the dynamic viscosity of oil. Combining Eqs (5) and (6) gives

$$d_{50}/D = A\{We/[1+BVi(d_{50}/D)^{1/3}]\}^{-3/5} \quad (8)$$

While the form of We* is based on theory, the coefficient B (as well as A) is empirical. Because there are two coefficients, it is difficult to obtain a unique calibration. For example, using data from their recent Tower Basin experiments, Brandvik et al. (2012a) found A = 24.8 and B = 0.08, while using data from their earlier Tower Basin experiments, Johansen et al. (2012) found A = 15 and B = 0.8. And while they studied a different flow condition (induced by an impellor rather than jet), Wang and Calabrese (1986) found significantly different values of A and B for their experiments. We also note that d_{50}/D appears on both sides of Eq (8) making the calculation of d_{50}/D implicit.

The above theory, and most of the SINTEF Tower Basin laboratory experiments, are based on a single dispersed phase (oil) discharging into a continuous phase (seawater). However, in the field oil is often accompanied by gas, which can affect the break-up dynamics in two ways. First, because gas has negligible density compared with oil, it creates a void, squeezing oil into a

smaller cross-sectional area of the orifice. Gas is also highly buoyant, so a discharge of oil and gas is more plume-like than an oil-only discharge.

Considering the first effect, if n is the void fraction occupied by gas, then the actual oil velocity, effective orifice diameter, kinematic momentum flux, and dissipation rate (denoted by primes) are given by

$$U' = U/(1-n);\ \ D' = D(1-n)^{1/2};\ \ M' = M/(1-n);\ \ \varepsilon' = \varepsilon(1-n)^{-7/2} \qquad (a)$$

where the unprimed quantities represent nominal conditions with no gas. SINTEF argues that droplets produced by an oil and gas jet should be similar to those produced by an oil only jet with the same kinematic momentum as the oil and gas jet, which requires that the velocity in the former be modified to a value U_n which is in between the nominal and actual velocity,

$$U_n = U/(1-n)^{1/2} = U'(1-n)^{1/2} \qquad (9)$$

U_n is then used to adjust the value of We in Eq (3) (if viscosity is negligible) or We* in Eq (5) (if viscosity is important). Considering the former, for simplicity,

$$d_{50}/D = AWe^{-3/5}(1-n)^{3/5} \qquad (b)$$

This is a reasonable adjustment based on momentum conservation. However, it does not take into account the possibility that oil droplets in an oil-gas discharge will be smaller when they exit a constricted nozzle and hence may have a head start in their break-up compared with droplets in an oil only discharge. This situation can be analyzed by using ε' in Eq (1) which, if viscosity is again negligible, leads to

$$d_{50}/D = AWe^{-3/5}(1-n)^{7/5} \qquad (c)$$

This is equivalent to using Eq (3) if the velocity in We is given by

$$U_n' = U/(1-n)^{7/6} = U'(1-n)^{-1/6} \qquad (d)$$

In order to see if Eq (b) or (c) or perhaps some other adjustment is appropriate requires some tests with oil and gas. A few such Tower Basin experiments were conducted, but these were not fully analyzed or discussed in Brandvik et al (2012a). Because Eqs (b) and (c) depend directly on n, it might be helpful if additional tests were performed with the same orifice diameter and oil flow and a range of gas flows (hence values of n). As an indication of anticipated sensitivity, if n = 0.5, Eq (b) suggested by SINTEF results in characteristic droplets that are $(1-n)^{1/2}$ = 66% of the size for an oil only jet, while Eq (c) introduced here suggests the droplets would be $(1-n)^{7/5}$ or 38% of their nominal size. This is a significant variation which should be discernable with more tests. Such tests might also reveal other aspects of oil-gas behavior.

Moving to the second effect of adding gas, a buoyant (oil-gas) jet will experience higher velocity along its trajectory than a non-buoyant (or much less buoyant) oil only jet with the same

momentum flux. This effect varies with the non-dimensional distance along the trajectory (z/D) and SINTEF focuses on the elevation l_M/D where l_M is the "momentum length" given by

$$L_M = M^{3/4}/B^{1/2} \quad (10)$$

where M and B are the kinematic momentum and buoyancy fluxes of the oil and gas discharge. Their doubly modified jet exit velocity that gives the same velocity at l_M as that of a buoyant jet is given by

$$U_C = U_n(1+Fr^{-1}) \quad (11)$$

where Fr is the densimetric Froude number given by

$$Fr = U_n/\{g[\rho_w-\rho(1-n)]/\rho_w D\}^{1/2} \quad (12)$$

where ρ_w is the density of the receiving water. Eq (11) assumes that the effect of voids is given by Eq (b). If we assume Eq (c) instead, then the U_n in Eq (11) could be replaced by U_n'.

The concept of l_M has been used for *single phase* buoyant jets which are directed either vertically or with a horizontal angle. The concept seems useful for vertically directed multi-phase jets, but it is not clear to what extent it applies to horizontally directed multi-phase jets as it is possible that the dominant dispersed phase (here the gas bubbles) will separate from the top (convex side) of the buoyant jet and rise more rapidly. Some theoretical calculations, or simple experiments, could be made to test this effect. It should also be mentioned that the proposed buoyancy adjustment (Eq 11) is based on the assumption that droplet size is determined by the level of jet energy dissipation at elevation l_M. The validity of this assumption might be evaluated by looking at the droplet size distribution at different relative elevations z/D.

Finally we note the obvious: prediction of d_{50}/D via Eq. (8) requires knowledge of oil properties σ, μ and ρ. All three properties are generally well-known for oil from production wells, not exposed to dispersants. When dispersants are added, σ drops dramatically, and a predictive relationship for σ must be determined. Viscosity can also be important, and the value of μ may not be known for an exploratory well, though it is mainly oils of low μ that are at most risk for high flow rate blowouts.

Comparison with Experimental Data

We look at data from three basic sources: SINTEF's Tower Basin Experiments, U. Hawaii's smaller scale lab experiments, and the Deep Spill field experiments. Our analysis uses a simple spreadsheet, summarized in the appendix and Figure 1.

SINTEF Tower Basin Experiments

SINTEF conducted two sets of experiments: an earlier set supported by BP and described in a two-part paper (Brandvik et al., 2012b and Johansen et al. 2012), and a later set supported by API and described in Brandvik et al. (2012a). These are probably the best set of data for oil droplet size distributions, being based on high quality LISST measurements in a series of tests involving oil jetted vertically upward at rates of 1.7 to 83 cm^3/s through nozzles with diameters 0.05 to 0.3 cm. Gas was not included, but some experiments introduced dispersants with dispersant-oil-ratios (DOR) ranging from 0 to 1:25. The IFT of oil droplets was measured from droplets extracted from the tank, allowing calculation of the Weber number. Measurements were made at a constant height of about 3 m above the release point, and the values of We exceeded 324 for all experiments, suggesting conditions were in the atomization regime (Tang and Masutani, 2003). More information is available in Brandvik et al. (2012a and b).

Data from the more recent experiments supported by API are shown in Block A of the appendix table. Following p 71 of Brandvik et al. (2012a), d_{50} is approximated as the reported peak diameter d_p divided by 1.2, consistent with droplet sizes fitting a Rosin-Rammler distribution. Data for d_{50}, normalized by orifice diameter D, are plotted against We* (computed with A = 24.8 and B = 0.08) as green dashes in Figure 1. Values for IFT, We and Vi were taken from Table 8.1 of Brandvik et al. (2012a) and values of d_{50}/D were computed implicitly from Eq (8). The average ratio of observed to predicted d_{50}/D is 1.02 (last column of appendix table), suggesting that the calibrated values of A and B are very close to, if not exactly, optimal. It is possible that we made some slightly different assumptions in our analysis or plotting.

Brandvik et al. (2012a) provide data for droplet distributions, which are compared with Rosin-Rammler and log-normal distributions. Theory suggests that turbulent pressure variations cause an oil droplet to break into daughter droplets of different sizes, while viscosity stretching causes droplets to break into daughters of similar size. As the DOR increases (IFT decreases), and viscosity becomes relatively more important (Eqs 6 and 7), one might expect to see a narrower droplet size distribution. However, Figure 6.8 of Brandvik et al. (2012a) shows distributions for a standard discharge condition (D = 0.15 cm and Q = 25 cm^3/s) and with varying DOR; little change in distribution can be observed.

Data from SINTEF's earlier BP-supported experiments are presented in Johansen et al. (2012) and summarized here in Block B of the appendix table. They are also plotted in Figure 1 as red dashes. Data are similar to the more recent experiments except that, following Johansen et al. (2012; pg 6), d_{50} is approximated as the peak diameter d_p, rather than the peak value divided by 1.2; d_{50} should be equal to d_p if the distribution is log-normal (Johansen, et al., 2012). The data match the theoretical trend reasonably well, but are somewhat higher than predicted, especially for experiments involving dispersant application. From the appendix table, the average ratio of observed to predicted d_{50}/D is 1.75. The somewhat different results for the two sets of experiments is reflective of the fact that different values of the calibration coefficients A and B were found by Johansen et al. (2012). (Note that the values of We* in Figure 1 have been calculated with A = 24.8 and B = 0.08 in all cases.) Also note that, if d_{50} were taken as $d_p/1.2$

rather than d_p, the agreement would be somewhat better: the ratio of observed to predicted d_{50}/D would decrease by up to about 17%.

As stated above, spatially-varying plume turbulence might cause droplet size to vary with elevation above the orifice. This could be tested, in principle, by making measurements at different elevations above the release. Measurements at low elevations above the orifice are hampered by high oil concentrations affecting the laser light transmission. However, a similar test of the effect of the relative height of measurement can be made by comparing data with different discharge diameter D. Figure 2 plots the ratio of observed to predicted d_{50} versus D for those SINTEF experiments tabulated in the appendix table which were conducted without chemical dispersants. There is a mild upward trend suggesting that the observed characteristic droplet diameter decreases slightly (relative to the predicted diameter) as the normalized measurement height increases (i.e., as one moves to the left on the graph). This could suggest that droplet splitting was still taking place at the height of the SINTEF measurements. Because it is much more convenient to predicted droplet size based on conditions at a single (discharge) location, it is worthwhile examining if this trend of observed droplet height with measurement elevation is actually real, or, if instead, predictions made with a single value for ε may be appropriate.

U. Hawaii smaller scale experiments

As part of the Deep Spill JIP, S. Masutani and graduate student L. Tang conducted a number of experiments to measure droplet sizes for oil jetted vertically upward in a smaller, 400L atmospheric tank. Four different types of oil and one silicone fluid were used, without accompanying gas or dispersant. Nozzle diameters ranged from 0.1 to 0.5 cm, and flow rates ranged up to 50 cm^3/s, which produced turbulent (atomized), transitional and laminar (discrete) droplet conditions, but only those in the atomization range have been considered. Measurements were made with a combination of a phase Doppler particle analyzer (PDPA) and video imaging. Eight different measures of "mean" droplet diameter were recorded in Table III.1.3 of Masutani and Adams (2000), and we have used the volume mean diameter (identified as d30) with "probe volume correction". We note that there is very little difference among the various measures of mean diameter for a given experiment, or for that matter, the estimates of mean diameter for *different* experiments. Data for all measurements in the atomization range are summarized in Block C of the appendix table.

Figure 1 plots, separately, data from the oil (blue x's) and the silicone fluid (red squares). Observed values of d_{50} for the oil are generally well above the theory with an average ratio of observed to predicted d_{50}/D of 3.29. When used with oil, the PDPA was based on the monitoring of reflected light and by comparing PDPA measurements and video records, the researchers conclude (p. 52 of Masutani and Adams, 2000) that "the instrument is extremely biased toward large droplets and is not capable of providing accurate size statistics for polydispersed opaque fluids such as crude oil". They attribute the problem to beam attenuation in the highly

concentrated oil cloud. For this reason, the oil data should be significantly discounted. By contrast, the observed values of d_{50} for the silicone fluid agree reasonably well with theory, with an average ratio of observed to predicted d_{50}/D of 1.28. For clear fluids such as silicone oils, the PDPA was based on monitoring of refracted light and the researchers observed that the PDPA results correlated well with the video records. The researchers did note that in the mode of PDPA operation used for the silicone fluid, it was not possible to record droplet sizes greater than about 2 mm. Thus while data for the silicone fluid are probably better than data for the oil, the observed mean diameters are likely biased to low values.

Masutani and Tang also analyzed droplet size distributions and for some experiments noticed that the distribution was bi-modal, much different from either a Rosin-Rammler or log-normal distribution. They speculated that a bi-modal distribution could be the result of large droplets formed from a pressure-type break-up consistent with Weber number models (as described above), and smaller droplets formed from a shearing mechanism in which droplets are peeled from the side of the jet. Such shearing might be most likely to occur in larger diameter jets, such as those experienced in the field. However, the only field scale experiment with reliable droplet size data is the DeepSpill experiment (described next), and in that experiment only video observations were available for droplet size analysis. Unfortunately, such observations tend to miss the smaller droplet sizes. That said, it is not clear how much the smallest droplets would contribute to the *volume* and opposed to simply the *number* diameter distribution.

DeepSpill Field Experiment

The centerpiece of the DeepSpill JIP was a series of four one hour field experiments in which gas and gas/oil mixtures were injected through a 12 cm nozzle at a depth of 840 m off the Norwegian Coast (Johansen et al., 2001, 2003). Among other measurements, droplet sizes were measured by video imaging from an ROV with use of a scale. Droplet volume distributions were reported on pages 63 and 64 of Johansen et al. (2001) for elevations of 4-5m, 9-10m, 14-22m, and 34-55m above the discharge (designated as Cases 5-8 respectively). For each height range we have determined the value of d_{50} as the median of the respective volume distribution and summarized it in Block D of the appendix table. Observed droplet sizes are plotted in Figure 1 as green triangles and are shown to be somewhat smaller than predictions, with the average ratio of observed to predicted d_{50}/D being 0.63. Combined with the U. Hawaii experiments with silicone fluid and the Tower Basin experiments, these data suggest that the SINTEF model may slightly under-predict droplet size at small scale (small We*) and slightly over-predict droplet size at large (field) scale (large We*).

We also plotted (solid blue diamonds) observed d_{50}/D against the doubly modified We based on Eq (11) where U_C is computed with U_n' (from Eq (d), rather than U_n). While we aren't claiming this is necessarily a better way to represent the void spaced caused by gas, the fit does appear better, with the average ratio of observed to predicted d_{50}/D being 0.9.

While measurements were collected at only four heights, there does not appear to be any consistent variation in droplet size with measurement height.

Extrapolation to Field Experiments

Laboratory data from SINTEF and U. Hawaii were characterized by small orifice diameters and the absence of gas, while field scale blow-outs have much larger diameters and include gas. Predicted d_{50} agrees reasonably well with the only reliable field data that is available, i.e., that from the Deep Spill field experiment.

Limited measurements of droplet distributions were available for the Deepwater Horizon spill (OBC, 2010), but these are not considered reliable for several reasons. Most importantly, the oil was collected in Nisken bottles and brought to the surface prior to measurement with a LISST. The maximum recorded droplet size was 157 microns (0.0157 cm), but larger droplets were most likely present but not sampled. In addition, the measurements were all taken at a considerable distance from the release point(s) and the trajectory from source to measurement point is not known. Finally, dispersants were added sub-surface at many times throughout the spill and it is not clear if measured droplets reflected oil that was or was not treated by dispersant.

Despite the fact that there is no reliable data against which to compare, it is still worth considering the predicted characteristic droplet sizes for Deepwater Horizon conditions. We have used the SINTEF model to predict d_{50} for three leaks during the Deepwater Horizon spill, each without chemical dispersants. Conditions are assumed based on FRTG (2010) and OBC (2010) and include 1) the horizontally directed Riser End Jet (REJ), which occurred for approximately the first half of the spill, and had an effective orifice diameter of 35 cm and an oil flow rate of 103,000 cm^3/s, 2) the largest of several diagonally directed leaks in the riser kink (RKL), which also occurred during the first half of the spill, and had an effective orifice diameter of 1.9 cm and an oil flow rate of 10,000 cm^3/s, and 3) the vertically directed Post Riser Cut Jet (PRCJ), which took place during the second half of the spill, with an effective orifice diameter of 49 cm and an oil flow rate of 126,000 cm^3/s . The oil was accompanied by natural gas, as well as some seawater and possibly some hydrates. From a dynamic standpoint, the most important of these constituents is gas. The flow of gas is known to vary through the process of slugging as illustrated in Figure 2, App 6 of FRTG (2010). In order to account for this variability, two conditions were considered for each leak: a gas flow rate of 55 percent of the total flow (n=0.55) and no gas flow (n = 0). For conditions with gas, calculations were made with the correction for both gas buoyancy and void fraction, as well as corrections for void fraction only. A total of nine values of d_{50} were thus calculated (Table 1).

The predicted diameters for the RKJ release show a narrow spread from 0.009 to 0.01 cm, within the range of the LISST measurements. However, flow from the riser kink jets, collectively, represents a relatively small proportion (~20%) of the total release during the period of leakage, and it is not possible to tell if these droplets were the ones actually measured by the LISST. For

the horizontally directed REJ, predicted diameters varied from 0.77 to 2.7 cm, while for the vertically directed PRCJ, the predicted diameters varied from 1.0 to 5.7 cm. The largest of these predicted droplet sizes are likely to exceed the maximum stable droplet size. Clift et al. (1978) summarize data on jet break-up, concluding that the maximum stable droplet size is given approximately by

$$d_{max} = 4(\sigma/g\Delta\rho)^{0.5} \quad (13)$$

where $\Delta\rho$ is the density difference between oil and water. Using values of σ = 23 dynes/cm and $\Delta\rho$ = 0.18 g/cm^3 for the Deepwater Horizon spill yields maximum diameters of about 1.4-1.5 cm. Given that the SINTEF model predicts median diameters, and the fact that the maximum diameter will be larger than the median, this suggests that the maximum predicted droplet diameters for field scale oil only releases may not be achieved, and that an upper bound should be established on predicted droplet diameter. If an additional field test were to be conducted, it would help to include tests without any gas to test this extreme.

Table 1 Predicted d_{50} (cm) for oil released from three Deepwater Horizon jets

	Gas void and buoyancy corrections	Gas void correction only	No gas
REJ	0.77	1.7	2.7
RKJ	0.009	0.009	0.01
PRCJ	1.03	3.5	5.7

Summary

1. The SINTEF model is an elegant, semi-empirical theory to predict characteristic droplet size. The approach is implicit, but relatively easy to solve.
2. Predicted median droplet diameters with the model, as calibrated, compare reasonably well with available data, but the model has not been tested in situations where the predicted droplet size is large (e.g., large flow rates through large orifices without gas or dispersants).
3. The theory is based on an oil-only jet, but adjustments have been made for the void space and buoyancy effects in an oil and gas jet. These corrections appear rational, but there are other possible corrections that give somewhat different results. As model calculations are quite sensitive to both factors, more insight could be gained by conducting experiments with both oil and gas, and by making measurements at different elevations.
4. The model does not predict droplet size distribution. Observed distributions appear reasonably constant, which could provide an empirical basis for prediction.
5. The model requires a value for the oil-water interfacial tension. Sigma is known for oils without dispersants, but relations for sigma as a function of dispersant flow rates and method of injection are necessary to make the approach totally predictive.

References

Brandvik, P.J., O. Johansen, U. Farooq, G. Angell and F. Leirvik (2012a), "Sub-surface oil releases-experimental study of droplet distributions and different dispersant injection techniques. A scaled experimental approach using the SINTEF Tower basin", Draft report prepared by SINTEF Materials and Chemistry, Aug 2012.

Brandvik, P.J., O. Johansen, F. Leirvik, U. Farooq, and P. S. Daling (2012b), "Droplet breakup in subsea oil releases – Part 1: Experimental study of droplet breakup and effectiveness of dispersant injection", *Marine Pollution Bulletin* (submitted October 2012).

Clift, R., J. R. Grace and M. E. Weber (1978), *Bubbles, Drops and Particles*, Academic Press, New York.

FRTG (2010), "Deepwater Horizon Release Estimate of Rate by PIV", July 2010

Hinze, J. O. (1955), "Fundamentals of the hydrodynamic mechanism of splitting in dispersion processes", *Amer. Inst. Chem. Eng. J.*,1**,** 289–295.

Johansen, O., P.J. Brandvik and U. Farooq (2012), "Droplet breakup in subsea oil releases – Part 2: Prediction of droplet size distributions with and without injection of chemical dispersants" ,*Marine Pollution Bulletin* (submitted October 2012).

Johansen, O., H. Rye, and C. Cooper (2003), "DeepSpill - Field study of a simulated oil and gas blowout in deep water", *Spill Sci Technol B, 8*(5-6), 433-443.

Johansen, O., H. Rye, A. G. Melbye, H.V. Jensen, B Serigstad, and T. Knutsen (2001), "Deep Spill JIP- Experimental dishcarges of gas and oil at Helland Hansen—June 200", Technical Report STF66F01082 by SINTEF Applied Chemistry, June 2001.

Masutani, S.M. and E. E. Adams (2002), "Experimental study of multiphase plumes and application to deep oil spills", Final report to the U.S. Dept. of Interior Minerals Management Service, Contract no. 1435-01-98-CT-30946.

OBC (2010), "Oil Budget Calculator Deepwater Horizon", Federal Interagency Solutions Group, Oil Budget Calculator Science and Engineering Team, November 2010.

Tang, L., and S. M. Masutani (2003), "Laminar and turbulent flow liquid-liquid jet instability and breakup", *Proc. 13th Int'l Offshore and Polar Engineering Conf.*, Honolulu, HI, 317-324.

Wang, C.Y. and R.V. Calabrese (1986), "Drop breakup in turbulent stirred-tank reactors. Part II: relative influence of viscosity and interfacial tension", *Amer. Inst. Chem. Eng. J.*, 32, 667-676.

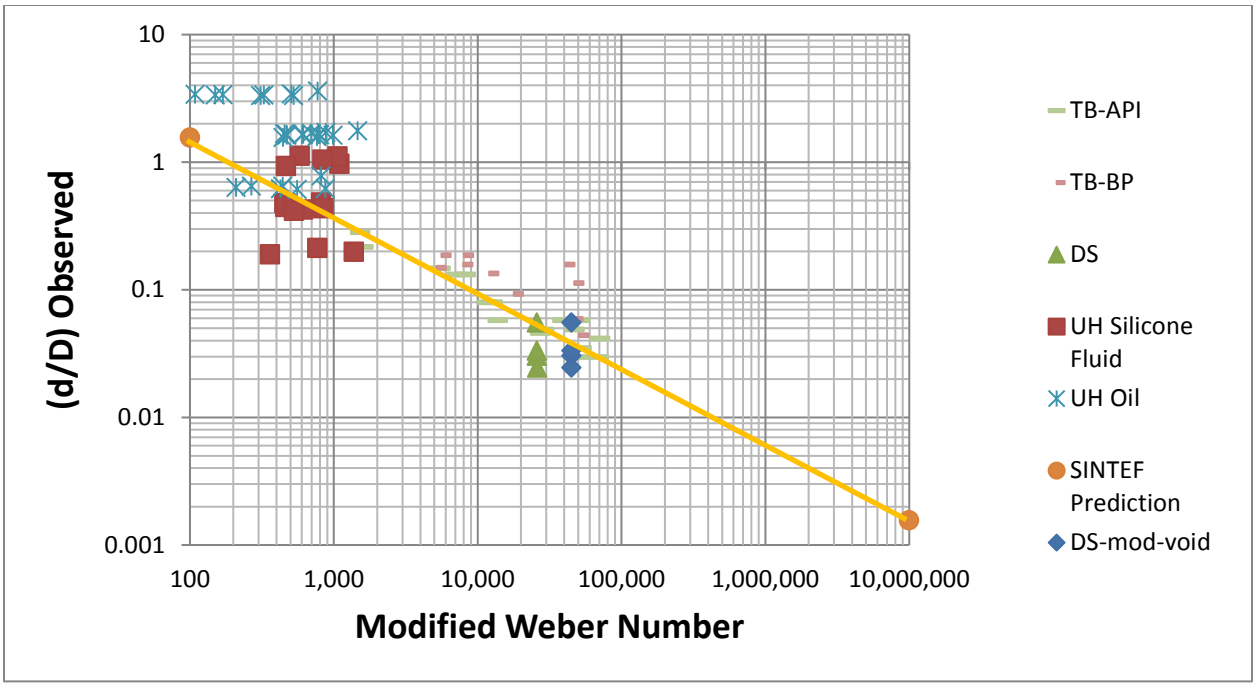

Figure 1 Comparison of SINTEF model against available experimental data

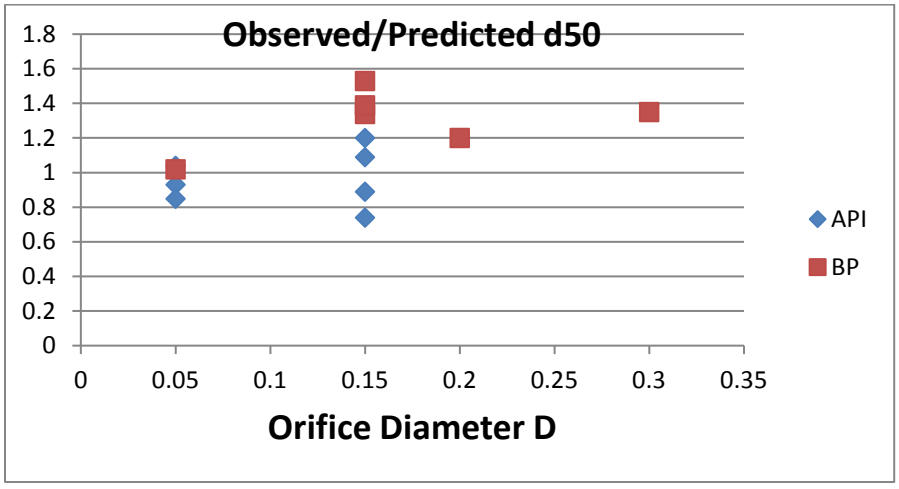

Figure 2 Effect of measurement height on droplet diameter for SINTEF Tower Basin experiments without dispersants. Because droplet size measurements were made at a constant elevation (z ~ 3 m above the discharge), the horizontal axis is inversely proportional to z/D. The mild increase in the ratio of observed to predicted d_{50} with D thus suggests a mild decrease in observe droplet size with increasing relative measurement height

Appendix: SINTEF Model Data Comparison

(all data in cgs units)

A Tower Basin Large Scale Lab Experiments conducted for API

n 0

Run	DOR	Q	D	U	Un	Fr	UC	rho	sigma	mu	We	Vi	d (obs)	d/D (obs)	LHS	d/D (pred)	We*	O/P
2604-1	-	8.3	0.15	472	472	91	477	0.84	15.315	0.0964	1.9E+03	3	0.03258	0.217222		0.294988	1612.306	0.74
2604-2	-	20.0	0.15	1132	1132	219	1137	0.84	15.081	0.1061	1.1E+04	8	0.01975	0.131667		0.11	8263.979	1.20
2604-3	-	46.7	0.15	2641	2641	510	2646	0.84	15.054	0.1024	5.9E+04	18	0.00867	0.057778		0.042658	38971.08	1.35
0305-1	-	1.7	0.05	849	849	284	852	0.84	15.087	0.1063	2.0E+03	6	0.01417	0.283333		0.304909	1526.604	0.93
0305-2	-	3.3	0.05	1698	1698	568	1701	0.84	15.052	0.0974	8.1E+03	11	0.00735	0.147		0.14077	5534.696	1.04
0305-3	-	8.3	0.05	4244	4244	1420	4247	0.84	15.032	0.0991	5.0E+04	28	0.00230	0.046		0.05402	27278.73	0.85
2806-1	-	20.0	0.15	1132	1132	219	1137	0.84	18.259	0.0964	8.9E+03	6	0.01975	0.131667		0.120527	7209.423	1.09
2806-5	1:100	20.0	0.15	1132	1132	219	1137	0.84	0.091	0.1007	1.8E+06	1258	0.00867	0.057778		0.036729	51898.75	1.57
2806-6	1:50	20.0	0.15	1132	1132	219	1137	0.84	0.071	0.1003	2.3E+06	1617	0.00525	0.035		0.035688	52936.18	0.98
2806-7	1:25	20.0	0.15	1132	1132	219	1137	0.84	0.050	0.1004	3.2E+06	2264	0.00448	0.029833		0.035094	53507.87	0.85
1704-1	-	25.0	0.15	1415	1415	273	1420	0.84	16.560	0.105	1.5E+04	9	0.01200	0.08		0.089629	11599.46	0.89
1704-2	1:1000	25.0	0.15	1415	1415	273	1420	0.84	14.769	0.104	1.7E+04	10	0.01200	0.08		0.084561	12727.26	0.95
1704-3	1:500	25.0	0.15	1415	1415	273	1420	0.84	13.272	0.1028	1.9E+04	11	0.00867	0.057778		0.081177	13856	0.71
1704-4	1:250	25.0	0.15	1415	1415	273	1420	0.84	4.536	0.099	5.6E+04	31	0.00735	0.049		0.052028	29064.62	0.94
1704-5	1:100	25.0	0.15	1415	1415	273	1420	0.84	1.512	0.1001	1.7E+05	94	0.00735	0.049		0.038737	47361.21	1.26
1704-6	1:50	25.0	0.15	1415	1415	273	1420	0.84	0.002	0.1004	1.3E+08	70730	0.00623	0.0415		3.04E-02	71193.02	1.00
1704-7	1:25	25.0	0.15	1415	1415	273	1420	0.84	0.071	0.1004	3.6E+06	2021	0.00448	0.029833		0.030881	69520.19	0.97
Average																		**1.02**

B Tower Basin Large Scale Lab Experiments conducted for BP

n 0

Run	DOR	Q	D	U	Un	Fr	UC	rho	sigma	mu	We	Vi	d (obs)	d/D (obs)	LHS	d/D (pred)	We*	O/P
1	0	3.3	0.05	1699	1699	568	1702	0.84	15.569	0.1098	7810	12	0.00745	0.14900		0.146392	5184.967	1.02
2	0	16.7	0.15	944	944	182	949	0.84	15.688	0.1157	7230	7	0.02805	0.18700		0.139788	5601.076	1.34
3	0	25.0	0.15	1415	1415	273	1421	0.84	15.600	0.1098	16300	10	0.0201	0.13400		0.087589	12024.46	1.53
4	0	83.3	0.2	2654	2654	444	2660	0.84	15.578	0.1113	76300	19	0.0088	0.04400		0.036671	50679.26	1.20
5	0	83.3	0.3	1180	1180	161	1187	0.84	15.706	0.1059	22600	8	0.0279	0.09300		0.068742	17902.32	1.35
6	0	20.0	0.15	1132	1132	219	1138	0.84	15.677	0.1103	10400	8	0.0237	0.15800		0.113553	7938.067	1.39
7	1000	20.0	0.15	1132	1132	219	1138	0.84	15.527	0.1092	10500	8	0.02805	0.18700		0.112839	8018.379	1.66
8	100	20.0	0.15	1132	1132	219	1138	0.84	0.506	0.1099	322000	247	0.0237	0.15800		0.042477	40750.16	3.72
9	50	20.0	0.15	1132	1132	219	1138	0.84	0.050	0.1097	3230000	2472	0.01695	0.11300		0.04	47012.2	2.83
19	25	20.0	0.15	1132	1132	219	1138	0.84	0.091	0.1099	1790000	1373	0.00885	0.05900		0.04	46366.96	1.48
																		1.75

C U Hawaii Small Scall Lab Experilments

n 0

Run	DOR	Q	D	U	Un	Fr	UC	rho	sigma	mu	WeC	Vi	d (obs)	d/D (obs)	LHS	d/D (pred)	We*	O/P
G2T	-	9.1	0.2	290	290	55	295	0.88	25	0.18	5.7E+02	2.13	0.32460	1.623		0.598518	495.9034	2.71
G2T	-	10.5	0.2	335	335	63	340	0.88	25	0.18	7.6E+02	2.45	0.33180	1.659		0.506257	655.5637	3.28
G2T	-	11.8	0.2	377	377	71	382	0.88	25	0.18	9.6E+02	2.75	0.31740	1.587		0.441151	824.7143	3.60
G5T	-	32.6	0.5	166	166	20	174	0.88	25	0.18	4.6E+02	1.26	0.30960	0.6192		0.655984	425.8311	0.94
G5T	-	37.3	0.5	190	190	23	198	0.88	25	0.18	6.1E+02	1.43	0.30620	0.6124		0.557497	558.469	1.10
M2T	-	9.2	0.2	292	292	55	297	0.88	25	0.24	5.8E+02	2.85	0.33470	1.6735		0.606566	485.2051	2.76
M2T	-	10.7	0.2	342	342	65	347	0.88	25	0.24	8.0E+02	3.33	0.33000	1.65		0.505347	657.3192	3.27
M2T	-	12.5	0.2	397	397	75	402	0.88	25	0.24	1.1E+03	3.86	0.32830	1.6415		0.427797	867.8939	3.84
M2T	-	14.3	0.2	454	454	86	459	0.88	25	0.24	1.4E+03	4.41	0.32470	1.6235		0.367634	1117.516	4.42
M5T	-	33.6	0.5	171	171	20	179	0.88	25	0.24	5.0E+02	1.72	0.32560	0.6512		0.640503	443.3443	1.02

M5T	-	46.7	0.5	238	238	28	246	0.88	25	0.24	9.6E+02	2.37	0.38970	0.7794	-146579	#NUM!	0.00
M5T	-	48.1	0.5	245	245	29	253	0.88	25	0.24	1.0E+03	2.43	0.30940	0.6188	0.421488	890.0961	1.47
N1T	-	3.5	0.1	442	442	111	446	0.86	25	0.13	6.5E+02	2.32	0.34300	3.43	0.554551	563.1434	6.19
N1T	-	4.4	0.1	562	562	141	566	0.86	25	0.13	1.1E+03	2.94	0.36030	3.603	0.420739	892.491	8.56
N1T	-	2.6	0.1	337	337	84	341	0.86	25	0.13	3.8E+02	1.77	0.33280	3.328	0.759204	333.7998	4.38
N1T	-	2.7	0.1	346	346	87	350	0.86	25	0.13	4.0E+02	1.82	0.33690	3.369	0.735703	351.7605	4.58
N1T	-	3.5	0.1	451	451	113	455	0.86	25	0.13	6.7E+02	2.37	0.33300	3.33	0.542675	583.8435	6.14
N2T	-	8.9	0.2	285	285	50	291	0.86	25	0.13	5.4E+02	1.51	0.33030	1.6515	0.6051	487.1701	2.73
N2T	-	11.1	0.2	352	352	62	358	0.86	25	0.13	8.2E+02	1.86	0.33940	1.697	0.472517	735.7207	3.59
N2T	-	12.6	0.2	401	401	71	407	0.86	25	0.13	1.1E+03	2.11	0.34280	1.714	0.407437	941.8475	4.21
N2T	-	16.7	0.2	531	531	94	537	0.86	25	0.13	1.9E+03	2.79	0.35360	1.768	0.294224	1619.443	6.01
N2S	-	8.7	0.2	276	276	49	282	0.86	25	0.13	5.1E+02	1.46	0.31290	1.5645	0.627144	458.9635	2.49
N2S	-	11.9	0.2	378	378	67	384	0.86	25	0.13	9.5E+02	1.99	0.32960	1.648	0.4349	844.8182	3.79
P1T	-	3.8	0.1	486	486	152	489	0.92	25	1.96	8.4E+02	38.35	0.33740	3.374	1.014064	205.7539	3.33
P1T	-	2.9	0.1	373	373	117	376	0.92	25	1.96	4.9E+02	29.49	0.34000	3.4	1.28691	138.5204	2.64
P1T	-	4.2	0.1	541	541	169	544	0.92	25	1.96	1.0E+03	42.67	0.33970	3.397	0.923836	240.4992	3.68
P5T	-	33.8	0.5	172	172	24	179	0.92	25	1.96	5.3E+02	14.05	0.32420	0.6484	0.894463	253.5226	0.72
P5T	-	28.8	0.5	147	147	21	154	0.92	25	1.96	3.8E+02	12.09	0.31770	0.6354	1.054553	193.0372	0.60
																	3.29
S1T	-	3.2	0.1	403	403	190	405	0.98	21	0.19	7.6E+02	3.67	0.11270	1.127	0.528164	611.1182	2.13
S1T	-	4.5	0.1	577	577	272	579	0.98	21	0.19	1.6E+03	5.24	0.09750	0.975	0.353084	1195.646	2.76
S1T	-	4.5	0.1	571	571	269	573	0.98	21	0.19	1.5E+03	5.19	0.11110	1.111	0.356917	1174.329	3.11
S1T	-	2.8	0.1	354	354	167	356	0.98	21	0.19	5.8E+02	3.22	0.09350	0.935	0.612437	477.4669	1.53
S1T	-	3.9	0.1	495	495	234	497	0.98	21	0.19	1.1E+03	4.50	0.10510	1.051	0.418462	898.1944	2.51
S2T	-	7.4	0.2	235	235	78	238	0.98	21	0.19	5.1E+02	2.15	0.09550	0.4775	0.636802	447.6466	0.75
S2T	-	7.4	0.2	237	237	79	240	0.98	21	0.19	5.2E+02	2.17	0.08910	0.4455	0.630385	455.1904	0.71
S2T	-	10.1	0.2	323	323	108	326	0.98	21	0.19	9.7E+02	2.95	0.09700	0.485	0.441671	823.0597	1.10
S2T	-	8.7	0.2	276	276	92	279	0.98	21	0.19	7.1E+02	2.52	0.08520	0.426	0.529332	608.5665	0.80
S2T	-	7.5	0.2	239	239	80	242	0.98	21	0.19	5.3E+02	2.19	0.09440	0.472	0.625611	460.9371	0.75
S2T	-	8.0	0.2	255	255	85	258	0.98	21	0.19	6.0E+02	2.33	0.08310	0.4155	0.580537	521.7124	0.72
S2T	-	10.3	0.2	328	328	109	331	0.98	21	0.19	1.0E+03	2.99	0.08740	0.437	0.434329	846.3923	1.01
S5T	-	25.1	0.5	128	128	27	133	0.98	21	0.19	3.8E+02	1.20	0.09520	0.1904	0.73734	350.5684	0.26
S5T	-	37.1	0.5	189	189	40	194	0.98	21	0.19	8.3E+02	1.75	0.10660	0.2132	0.466627	751.2666	0.46

S5T	50.2	0.5	256	256	54	261	0.98	21	0.19	1.5E+03	2.36	0.0993	0.1986		0.327904	1353.757	0.61
average																	**1.28**

D Deep Spill Small Scale Field Experiment

n 0.33

Run	**DOR**	**Q**	**D**	**U**	**Un**	**Fr**	**UC**	**rho**	**sigma**	**mu**	**WeC**	**Vi**	**d** (obs)	**d/D** (obs)	**LHS**	**d/D** (pred)	**We***	**O/P**
Case5	-	16667	12	147	180	2.48	253	0.85	25	0.039	2.6E+04	0.39	0.36500	0.030417		0.056773	25814.04	0.54
Case6	-	16667	12	147	180	2.48	253	0.85	25	0.039	2.6E+04	0.39	0.66667	0.055556		0.056773	25814.04	0.98
Case7	-	16667	12	147	180	2.48	253	0.85	25	0.039	2.6E+04	0.39	0.40000	0.033333		0.056773	25814.04	0.59
Case8	-	16667	12	147	180	2.48	253	0.85	25	0.039	2.6E+04	0.39	0.29500	0.024583		0.056773	25814.04	0.43
Average																		**0.63**

APPENDIX B

EVALUATION OF MODELS FOR SUBSURFACE DISPERSANT INJECTION

PROGRESS REPORT 2

E. Eric Adams, PhD, PE

Scott A. Socolofsky, PhD

Michel Boufadel, PhD, PE

Submitted to

American Petroleum Institute

Oil Spill Response Joint Industry Task Force (JITF)

D3 Subsea Dispersant Injection Modeling Team

Attn: Joe Twomey

p.twomey@ecosystem-management.net

February 25, 2013

Introduction

In our previous progress report we described the "SINTEF Model", provided a theoretical critique of several aspects of the model, and compared *characteristic* droplet sizes (i.e., d_{50}) predicted by the model against available data. Here we follow up with some brief observations regarding droplet size *distributions*, including information gleaned from the Gulf of Mexico Oil Spill & Ecosystem Science Conference held recently in New Orleans. Next we discuss an alternative model framework (Bandara and Yapa, 2011) that allows droplet size distributions to be computed. We have coded their model and are comparing our results with theirs, including the data from the DeepSpill field experiment. A more complete reporting will be provided in our next progress report. The above efforts relate to Task 1 of our proposal. We conclude with a discussion of integrated models of oil fate and transport, including a brief description of available models (addressing Task 2.1 of our proposal), a discussion of data for model validation (Task 2.2), and a straw man proposal for test cases of integrated models (Tasks 2.2 and 2.3).

Observed Droplet Size Distributions

The SINTEF model simply predicts the characteristic droplet size (d_{50} in their case) of oil jetted in the atomization (high Weber number) regime. They do not predict droplet size distributions, but data collected in their Tower Basin provide many empirical distributions, and they have fit these data to empirical distributions (log-normal and Rosin-Rammler). These distributions are all uni-modal and their characteristic spread seems quite constant among runs with different exit conditions and dispersant-oil-ratios. We also note that measurements were taken at the same elevation (~3m) above the nozzle release, so that potential shifts in the droplet distributions with time of travel cannot be observed.

By contrast to the SINTEF experiments, other observations show bi-modal droplet size distributions (Li et al., 2007) or even tri-modal distributions (Mukharje and Wrenn, 2011). Results from the former study (where M. Boufadel was a co-author) from the Bedford Institute of Technology were obtained from wave tank studies (see their Figure 8) while the latter study used jars stirred by impellers. At the recent Gulf of Mexico Oil Spill & Ecosystem Science Conference (abstracts available at http://program.gulfofmexicoconference.org/) , the Bedford Institute of Technology team (Brian Robinson's presentation) showed results similar to their 2007 study: in essence, when dispersant was added, droplets became smaller AND there was a large number at very small diameter. In another presentation, Joseph Katz from Johns Hopkins University also observed lots of small droplets, but the basic size distribution did not change significantly with dispersant addition. He explained the presence of small droplets by observing

that long thin threads of oil tended to be attached to the parent oil droplet. While these threads were observed both with and without dispersant, the smaller surface tension associated with the dispersed oil resulted in less resistance to the strands breaking off, allowing small droplets to be formed. This mechanism of breakup is known as "tip-streaming" (e.g., DeBruijn, 1993), and occurs in the presence of a surfactant gradient on the droplet surface. However, tip streaming is more important in quiescent conditions than in turbulent conditions. Finally, recent experiments from Steve Masutani (University of Hawaii; summarized at the Gulf of Mexico Conference in the presentation by Tim Nedwell) showed that individual oil droplets, exposed to dispersants and stabilized in a counter-flowing Imhoff Cone, disappeared within 25 minutes. The smaller oil droplets were observed to fall off the parent droplet and then gradually disappear, presumably by dissolution. Meanwhile similar droplets introduced to the Imhoff Cone without being exposed to dispersants remained essentially unchanged for as long as 24 hours. Twenty-five minutes is well less than the rise time to the surface, for a field scale release, implying that the droplet diameters that SINTEF were seeing in their experiments might change (droplets shrinking) over time. Of course, because of the recirculating (closed) nature of the apparatus, droplets in Masutani's apparatus undoubtedly experienced higher residual dispersant concentrations than would droplets in a wide-open ocean.

We note that each of the above experimental observations were under conditions significantly different from those of jetted oil. However, Steve Masutani also observed bi-modal distributions in his earlier work with atomized oil jets without dispersants (Masutani and Adams, 2002) and argued that the small droplets were formed from a surface instability that might be scale dependent (i.e., it would be more likely to take place in a large diameter field scale release than a small scale laboratory release such as SINTEF's).

Each of the above observations suggests the possibility of some time (space) varying behavior that might be significant, yet beyond the range of SINTEF's observations that were all made at one elevation above the release point. They also suggest the need to reconcile theories of equilibrium droplet size, fundamental to steady-state models such as the one developed by SINTEF, with theories based on continuous droplet aggregation and break-up, embodied in time-varying models, such as the one presented by Bandara and Yapa (2011)

A Simple Time-varying Model of Droplet Size Distributions

Bandara and Yappa (2011) presented a droplet size distribution model, which is largely based on the work of Prince and Blanchard (1990). The model accounts for breakup due to interaction of turbulent eddies with droplets. The model also accounts for coalescence of droplets as a result of differential velocities due to both turbulent mixing and buoyancy rise. The model was compared to the DeepSpill field experiment where good agreement was noted. Bandara and Yapa (2011), however, does not explain in detail how the model was implemented. For example, they used the mixing energy at the orifice, but to account for coalescence (especially due to buoyancy) one

would need to consider spatially-varying mixing energy, which was not discussed. In addition, the model considers that the only resisting force for the breakup of droplet is surface tension, which might not be correct when dispersants are added, especially if they reduce the surface tension by several orders of magnitude. In such a case, the viscosity of the fluid would need to be considered.

We have coded the Bandara and Yapa (2011) model and are attempting to reproduce their results, including comparison against available data. We will report our results in our next progress report.

Summary of Integrated Models of Oil Fate and Transport (Task 2.1)

There are a large and growing number of models to predict the transport of oil from spills in the oceans. We limit our focus here to models that consider subsea spills, and we limit our analysis of model capabilities to processes occurring before the first surfacing or boundary interaction of spilled oil and gas. Hence, we will not evaluate surface fate models, boundary resuspension models, or mixing of oil from a surface slick back into the water column by wind and wave dispersal. Further, there are a large number of models developed around the world to satisfy the needs of various non-US government agencies. We limit our model evaluation to models that have had wide use in the United States or are otherwise well known through the research literature or through foreign companies operating in US oil fields.

Before discussing the individual models, a brief review of subsurface processes is warranted. When oil and gas are spilled, their collective buoyancy forms a plume of rising hydrocarbons and entrained water. Such plumes are much smaller than the resolution of the best ocean circulation models, and are generally treated using a separate near-field model. Most near-field models are based on integral modeling techniques. Models that developed out of (or were improved through) the DeepSpill JIP are of the integral plume type and include the Clarkson CDOG and SINTEF DeepBlow models. As the plume rises through the water column, two physical processes affect its trajectory and composition. First, crossflows tend to deflect the plume downstream and separate the faster-rising gas from the slower-rising oil droplets and entrained seawater. Both CDOG and DeepBlow account for this crossflow separation by algorithms validated to experiments in Socolofsky and Adams (2002). Second, ambient density stratification decelerates the entrained fluid by its negative buoyancy. In strong crossflows, this increases the degree to which the plume bends over, eventually creating a horizontal line-thermal type flow. This situation was characteristic of the DeepSpill field experiment, and both CDOG and DeepBlow are validated to this dataset. In weaker crossflows, the plume rises nearly vertically and dense entrained seawater is ejected from the plume periodically (peels from the plume), descending to form distinct intrusion layers. Socolofsky et al. (2011) suggest that the Deepwater Horizon accident behaved in this way. Because the large oil droplets and gas bubbles

do not leave the plume at the peeling events, a coherent plume continues to rise through the water column, and multiple intrusion layers can be formed. Neither CDOG nor DeepBlow have the capability of modeling periodic peeling, at least in their state as described in the literature.

Once the plume rise is arrested by the crossflow and/or stratification and an intrusion begins to form, the near-field plume stage ends and the flow transitions to a far field behavior that lacks an entraining and dynamic plume. Models of the far-field transport are usually based on some form of Lagrangian particle tracking, or random walk/flight. These models advect oil, gas, and dissolved hydrocarbon as a result of ambient currents and the terminal rise velocity of the oil and gas fluid particles. Ambient currents can either be specified by a single vertical profile of velocity or provided from numerical CFD simulations of the ocean currents. For integral models such as CDOG and DeepBlow, where the plume stage ends at the formation of the lowest intrusion layer, this Lagrangian transport phase accounts for the majority of the oil and gas transport in the model.

Along with the near-field plume physics and far-field transport, oil and gas fluid particles undergo physical changes due to release of pressure, dissolution, possible hydrate formation, and a host of physical, chemical and biological degradation processes, which we will call simply weathering. Many models account for dissolution of the gas and weathering of the oil. Some models consider dissolution of the oil and hydrate formation of the gas.

Although there are many different integrated oil spill models, each is based on a few key model elements, including an integral plume stage, transition to a far-field transport model, particle tracking in the far-field, and modeling and mass balancing of the transformation processes of the oil and gas fluid particles. Moreover, the fundamental equations governing each of these modeling components should be very similar across all modeling platforms. Differences arise through numerical implementation of the solution, simplifications or deletions by the modelers, and the levels of spatial and temporal resolution of the models. The models listed below meet the minimum standards identified in the opening paragraph of this section; the models are presented in alphabetical order.

1. **CDOG** – Comprehensive Deepwater Oil and Gas Model

http://www.clarkson.edu/cee/faculty/yapa.html

CDOG is developed by Poojtha Yapa and his students at Clarkson University. The model includes an integral plume model, transition to the far field, and Lagrangian particle tracking of oil and gas particles to the surface. CDOG itself has limited capability for interface in CFD models of ocean circulations, but can have an applied velocity profile that varies with depth. While CDOG has been developed and used for response, its primary purpose is for research, and it has been extensively described in the research literature. Dissolution and hydrate formation of

the gas is considered; however, no publications describe fate processes for oil in CDOG. An older version of CDOG (Version 2.02) is available in the public domain but is no longer supported by Yapa. Application of the current version of CDOG is accomplished by contracting with Yapa at Clarkson.

2. **COSIM** – Chemical/Oil Spill Impact Module

http://www.erm.com

http://www.nukaresearch.com/projects/aira/documents/ERMsOilSpillModelingServices.pdf

COSIM is developed and applied by ERM, Inc. and is a sub-module of their Generalized Environmental Modeling System for Surfacewaters (GEMSS), a hydrodynamic model that can be run for one-, two-, or three-dimensional simulations. The COSIM module is responsible for solution of the reactive advection diffusion equation for fate and transport of spilled oil or chemicals. Details of the numerical scheme are lacking in the COSIM literature. The fate components of the model include full dissolution and weathering. While spills may originate subsurface, it is unclear whether the model includes a nested plume stage module or whether the spill is treated as a tracer in the transport equation. From their literature, it appears the latter is the case. COSIM is the only model listed that is explicitly designed to nest with a specific hydrodynamic model (GEMSS). It appears the nesting is one-way (e.g., the hydrodynamic computations are independent of the transport calculations for the modeled chemicals/spilled oil). COSIM can be licensed from ERM or ERM can be contracted to apply the model.

3. **ERO3S** – EPA Research Object-Oriented Oil Spill

http://www.epa.gov/athens/publications/reports/Weaver_600_R04_120_Characteristics_oil_3a.pdf

http://yosemite.epa.gov/sab/sabproduct.nsf/0/177EF331F2AD57CB85257798006BD42A/$File/Draft%2BOil%2BSpill%2BResearch%2BStrategy.pdf

ERO3S is a modeling framework developed by the US EPA. The model is built using the concepts of object-oriented programming where surface oil patches can be objects (containing a specific set of properties) that break up into additional patches, inheriting the parent properties at formation. The model is further designed as a framework that can handle several different aspects of spill simulation. The backbone of the model is a mass balance-based approach, capable of predicting dissolution and weathering of oil with or without dispersant application. ERO3S does not appear to be available for download, nor is it listed under any of the modeling resources on the EPA website (as far as we could ascertain). Review of published EPA reports

indicate that to-date it has been exclusively design for surface slicks, including the capability of dispersal into the water column, but without a subsurface spill modeling component. ERO3S is listed as a model under current development in the 2011 Oil Spill Research Strategy document, but the model does not appear to be currently operational.

4. **GNOME** – General NOAA Operational modeling Environment

http://response.restoration.noaa.gov/oil-and-chemical-spills/oil-spills/response-tools/gnome.html

GNOME is the modeling framework developed and used by NOAA for oil spill response. Currently, NOAA Response and Restoration (R&R) is undertaking a complete update of GNOME, primarily to refactor the code, separating physics calculations from the model GUI, and to update components of the code that are outdated or inadequate. The revised model version should be available in 2014. The current model version includes CDOG for the plume stage and a simplified Lagrangian particle tracking scheme for the far field. The model can be rapidly interfaced with a wide variety of CFD output for ocean circulations and can be run with or without the CDOG plume stage. GNOME is in the public domain and is freely available. NOAA R&R applies the model to aid response during spills in US waters.

5. **OILMAPDEEP** – Deep Water Oil Spill Model and Analysis System

http://www.asascience.com/software/oilmap/oilmapdeep.shtml

OILMAPDEEP is the modeling system developed by Applied Science Associates (ASA) for predicting fate and transport of subsea releases. This model complements ASA's comprehensive spill modeling system SIMAP. The model includes an integral plume stage, transition to the far field, and Lagrangian particle tracking in the far field. The plume stage can be modeled either using CDOG Version 2.02 or by a similar integral plume model developed in-house by ASA. Fate processes are included for both gas and oil, though the details of the modeling algorithms are not publically available and are based on an extensive database of chemical properties of hydrocarbons maintained by ASA. OILMAPDEEP can be nested in two- or three-dimensional CFD predictions of ocean circulations. The model can be licensed from ASA or ASA can be contracted to apply the model.

6. **OSCAR** – Oil Spill Contingency and Response

http://www.sintef.no/home/Materials-and-Chemistry/Software/OSCAR--Oil-Spill-Contigency-and-Response/

http://www.sintef.no/home/Materials-and-Chemistry/Marine-Environmental-Technology/Environmental-modelling/Numerical-models/OSCAR-Oil-Spill-Contingency-And-Response/

OSCAR is a comprehensive oil spill simulation platform developed by SINTEF. The model is similar to GNOME in its purpose and scope. The subsea plume state and Lagrangian particle tracking is accomplished by DeepBlow, a submodule of OSCAR. DeepBlow is similar in physics to the CDOG model and has also been described in detail in the research literature. Gas dissolution and hydrate formation are considered; algorithms in OSCAR accomplish oil dissolution and weathering. Gas fate is described in the research literature, whereas fate processes for oil are proprietary to SINTEF and based on their libraries of hydrocarbon properties. OSCAR can be nested in CDF predictions of ocean circulations. Both OSCAR and DeepBlow can be licensed from SINTEF or SINTEF can be contracted to apply the model.

7. **OSIS** – Oil Spill Information System

http://www.bmtargoss.com/?/2025/1912/2856

OSIS is a comprehensive oil spill simulation platform developed by BMT Group, Ltd. The OSIS literature states that it is the primary oil spill modeling system used in the UK, filling a similar niche as the GNOME model for the U.S. and the OSCAR model in Norway. The model has been extensively validated to 30 years of laboratory and field scale experiments. The literature focuses on its performance on surface spills; it is unknown to us at this time what sub-modules are in operation for subsurface spills. The model includes full chemical dissolution and weathering and can be integrated with current fields from CFD models. OSIS can be licensed from BMT ARGOSS or BMT can be contracted to apply the model.

8. **SIMAP** – Integrated Oil Spill Impact Model System

http://www.asascience.com/software/simap/index.shtml

SIMAP is ASA's comprehensive modeling system for fate and transport of spill oil, extended beyond the subsurface and including aspects beyond OILMAPDEEP, such as biological impacts, exposure, and effects modeling and surface processes. The model includes a subsurface plume stage, transition to the far field, and Lagrangian particle tracking in the far field. Oil and gas fate are modeled as in OILMAPDEEP. The ASA literature does not specify whether the subsurface modeling algorithms are the same in SIMAP and OILMAPDEEP; ASA will be contacted to address this question. Based on available information, it is assumed that these models behave identically in the subsurface for the initial transport of oil from the wellhead to its first

interaction with the boundary (e.g., free surface or sea bed). Like OILMAPDEEP, SIMAP can be licensed from ASA or ASA can be contracted to apply the model.

9. **SIMP** – Stratified Integral Multiphase Plume

https://ceprofs.civil.tamu.edu/ssocolofsky/

SIMP is developed by Scott Socolofsky and his students at Texas A&M University. The model includes an integral plume model and transition to the far field. The model was developed specifically for low-current environments and, hence, does not include the effect of crossflow. However, SIMP is the only model capable of predicting multiple subsurface intrusion layers due to the effects of stratification. Far field transport must be accomplished by a separate modeling platform. This model has not been designed or applied for response, but rather is a research model. The model physics are described in Socolofsky et al. (2008). Recent updates to include oil and gas chemistry are yet unpublished. SIMP is also the only model listed not in the public domain; the model can be applied by contracting with Socolofsky at Texas A&M.

The Excel worksheet at the end of this report presents an inter-comparison matrix summarizing the data presented in this section.

Data for Model Validation

The focus of this project is to compare each of the above models to understand their respective limitations and differences, not to conduct a comprehensive model validation for each model. However, several papers in the literature present validations of some of the above listed models. A future progress report will summarize the model validation exercises that have already been published for these models and use this information to help inform the results of the model inter-comparison.

Proposed Test Cases for Integrated Oil Fate and Transport Models

The models identified in Task 2.1 will be evaluated and inter-compared using a consistent set of test cases. For the most part the model runs will be made by the model developers themselves. The purpose of the model inter-comparison is to identify differences in model predicted output and to link those differences to differences among the algorithms each model uses for oil fate and transport. As identified in the proposal, initial model inter-comparisons will use oil droplet size distributions provided to the modelers, while subsequent inter-comparisons will use oil droplet size distributions generated by modelers' algorithms. To provide realistic, yet efficient inter-comparisons, the model test cases should capture the full-field physics, yet in an idealized

manner—e.g., by having smooth and deterministic boundary and initial conditions, and thus allowing results in some cases to be compared to analytical and empirical predictions.

As a starting point, we propose the following suite of eight experiments which span expected blowout types in the deep Gulf of Mexico. This exceeds the five experiments suggested in the proposal, and we welcome feedback regarding if/how our number might be reduced. For these cases, three different blowout depths would be modeled, each with its own GOR. For each depth, one experiment will simulate an untreated release (no dispersant) and another experiment will simulate the initial droplet size distribution with optimal wellhead dispersant application. For the initial tests, the oil and gas particle size distributions for each of these modeled cases will be specified based on the results of Task 1, and each integrated transport model will use the same flow rates and sizes. To test the integrated model transport algorithms, the experiments for the mid-depth case will first be run with all fate processes for the oil turned off (i.e. no dissolution or degradation of oil). Fate processes for gas must remain active otherwise gas bubbles will become unrealistically large due to expansion as pressure is relieved. A second set of tests for the mid-depth case will include all fate processes for oil. Table 1 summarizes the proposed model test matrix.

Table 1. Summary of the model test cases proposed for evaluation and inter-comparison of integrated oil fate and transport models

Case	Depth	Oil Flux	Gas Flux	Flow Rate	GOR	Dispersant	Oil Fate
	[ft]	[kg/s]	[kg/s]	[bbo/d]	[scf/bbl]	[yes/no]	[yes/no]
1	3,000	14.6	14.7	35,000	5,200	No	Yes
2	3,000	14.6	14.7	35,000	5,200	Yes	Yes
3	6,000	160	48.9	100,000	2,800	No	No
4	6,000	160	48.9	100,000	2,800	No	Yes
5	6,000	160	48.9	100,000	2,800	Yes	No
6	6,000	160	48.9	100,000	2,800	Yes	Yes
7	10,000	161	2.0	100,000	640	No	Yes
8	10,000	161	2.0	100,000	640	Yes	Yes

The cases in Table 1 are the same base cases (depth, GOR and flow rate) as reported in Anderson et al. (2012). For each case, the outlet diameter will be 10 in and the expelled fluids will be assumed to be at 250°F. Gas will be 86% methane, 9% ethane, and 7% propane and the crude oil will be taken as Louisiana sweet crude.

Ambient stratification and currents will be provided as a smooth temperature, salinity, and current speed profile based on profiles in the deep Gulf of Mexico. Current speed will decrease with depth, but to simplify analysis of the model predictions, will be in the same direction at all depths. All test Cases in Table 1 will use the same ambient conditions profile.

Again, this test matrix has been offered as a starting point, and we welcome feedback.

References

Anderson, K., Bhatnagar, G., Crosby, D., Hatton, G., Manfield, P., Kuzmicki, A., Fenwick, N., Pontaza, J., Wicks, M., Socolofsky, S., Brady, C., Svedeman, S., Sum, A. K., Koh, C., Levine, J., Warzinski, R. P., and Shaffer, F. (2012). "Hydrates in the ocean beneath, around, and above production equipment." *Energy & Fuels*, 26(7), 4167-4176.

Bandara U. C., and Yapa, P. D. (2011). "Bubble sizes, breakup, and coalescence in deepwater gas/oil plumes." *J. of Hydraul. Eng,-ASCE*, 137(7), 729-738.

De Bruijn, R. A. (1993). "Tipstreaming of drops in simple shear flow", *Chemical Engineering Science*, 48(2), 277-284.

Li, Z, Kepkay, P., Lee, K., King, T., Boufadel, M., and Venosa, A. (2007). "Effects of chemical dispersants and mineral fines on crude oil dispersion in a wave tank under breaking waves." *Marine Pollution Bulletin*, 54, 983-993.

Prince, M. J., and Blanch, H.W. (1990). "Bubble coalescence and break-up in air-sparged bubble columns." *AIChE J.*, 36(10), 1485–1499.

Masutani, S.M. and Adams, E.E. (2002). "Experimental study of multiphase plumes and application to deep oil spills", Final report to the U.S. Dept. of Interior Minerals Management Service, Contract no. 1435-01-98-CT-30946.

Mukherjee , B. and Wrenn, B.A., (2011). "Effects of physical properties and dispersion conditions on the chemical dispersion of crude oil" *Environmental Engineering Science*, 28(4), 263-273.

Socolofsky, S. A., and Adams, E. E. (2002). "Multi-phase plumes in uniform and stratified crossflow." *J Hydraul Res*, 40(6), 661-672.

Socolofsky, S. A., Adams, E. E., and Sherwood, C. R. (2011). "Formation dynamics of subsurface hydrocarbon intrusions following the Deepwater Horizon blowout." *Geophys Res Lett*, 38, L09602.

Socolofsky, S. A., Bhaumik, T., and Seol, D. G. (2008). "Double-plume integral models for near-field mixing in multiphase plumes." *J. Hydraul. Eng.-ASCE*, 134(6), 772-783.

APPENDIX A Summary of Integrated Models

Integrated Model System	Developer	Nearfield Plume	Farfield Transition	Lagr. Particle Tracking	Gas Dissolution	Gas Hydrate Formation	Oil Dissolution	Oil Weathering	Simple Currents Only	Currents from CFD Sim.	Response Ready Model	Research Model	Notes
CDOG	Yapa, Clarkson University	X	X	X	X	X			X			X	Supported only through contracting with Yapa.
COSIM	ERM, Inc.	?	X	?	X		X	X		X*	X		*COSIM only integrates with the GEMSS CFD model.
ERO3S	U.S. EPA				X		X	X		X			Not currently available online from EPA servers.
GNOME	U.S. NOAA R&R	X	X	X	X	X		X		X	X		Current version uses CDOG 2.02 for plume model. Undergoing complete revision.
OILMAPDEEP	ASA	X	X	X	X	X	X	X		X	X		Subsurface version of SIMAP.
OSCAR	SINTEF	X	X	X	X	X	X	X		X	X	X	Is used as a response model. Submodules (e.g. DeepBlow) also research oriented.
OSIS	BMT Group, Ltd.	?	?	?	X	?	X	X		X	X		Billed as comprehensive oil spill response model. No subsurface spill examples available.
SIMAP	ASA	X	X	X	X	X	X	X		X	X		Comprehensive oil spill modeling system. Unknown if subsurface modules identical to OILMAPDEEP.
SIMP	Socolofsky, Texas A&M	X	X		X	X			X			X	Supported only through contracting with Socolofsky.

APPENDIX C

EVALUATION OF MODELS FOR SUBSURFACE DISPERSANT INJECTION

PROGRESS REPORT 3

E. Eric Adams, PhD, PE

Scott A. Socolofsky, PhD

Michel Boufadel, PhD, PE

Submitted to

American Petroleum Institute

Oil Spill Response Joint Industry Task Force (JITF)

D3 Subsea Dispersant Injection Modeling Team

Attn: Joe Twomey

p.twomey@ecosystem-management.net

May 23, 2013

Introduction and Background

In our first progress report we described the "SINTEF Model" (Johansen et al., 2013; Brandvik et al., 2012), a semi-empirical (or phenomenological) model that predicts a characteristic non-dimensional droplet size (specifically the volume median diameter d_{50} normalized by the orifice diameter) as a function of a modified Weber number. The model applies to oil jetted into ambient seawater at high velocities (atomization regime) and the "modification" takes into account the role of viscosity which is expected to come into play when chemical dispersants are applied and interfacial tension (IFT) drops significantly. The model showed reasonably good agreement in comparison with all available laboratory and field data, including recent laboratory data from SINTEF's Tower Basin (Brandvik et al., 2012) where chemical dispersants were added to the jetted oil.

Several limitations of the model were also pointed out. Firstly, the model only predicts a characteristic droplet diameter and not the distribution of diameters. At this point the distribution must be prescribed independently. Secondly, the model implicitly assumes equilibrium between droplet break up and coalescence characterized by conditions at the orifice. By contrast, we know that both turbulent energy (responsible for droplet breakup) and droplet concentration (responsible for droplet coalescence) decrease along the trajectory of a rising plume so, depending on the relative change of these two factors, we might expect the characteristic droplet diameter and the distribution about this diameter to evolve with time (i.e., distance beyond the orifice). Thirdly, the basic model and most of the experimental data to which it is calibrated, apply only to a single dispersed phase (oil), whereas most real-world releases include a combination of both oil and gas. However, SINTEF has made two adjustments to their model to account for the increased momentum and the increased buoyancy of an oil and gas plume (relative to an oil-only plume with equal oil flow rate), and in our first progress report we offered a variant on one of the adjustments.

In our second progress report, we alluded to an alternative class of models which are based on time-varying droplet/bubble "population dynamics". Such models have been applied in the past, but mostly to confined flows such as found in a reactor or a bubble column, rather than unbounded flows such as plumes. Prince and Blanch (1990) and Tsouris and Tavlarides (1994) are the "main stream" models, where the breakage relies on interaction of turbulent eddies with droplets, and where coalescence relies on the drainage of the film between intersecting droplets. These approaches are entrenched in physics, and are therefore promising not only for understanding processes but also for predictions. Luo and Svendsen (1996) made some improvements within this thrust of models, where they eliminated various empirical constants,

and developed an even more physically-based breakage function. We note, however, that none of these models applies directly to a dispersed phase in a jet or plume.

There are two population models that have been used to model a dispersed phase in a jet or plume: one is by Martínez-Bazán et al., (1999a, b), and the other is by Bandara and Yapa (2011). Martínez-Bazán et al. (1999a, b) developed a bubble model, and applied it to experiments where a water jet with air at a small holdup (ratio of air volume to water volume of the jet) was released in a water tank. The bubble distribution was measured using cameras. As the holdup was small (around 10^{-5}), coalescence was negligible. For this reason, the model developed by Martínez-Bazán et al. did not have a coalescence component in it. Good agreement was achieved between the model and the experimental observations. Unfortunately, such a model cannot be used to simulate a blowout, where the holdup starts from nearly 100%, at which point coalescence is clearly important. Another limitation of the Martínez-Bazán et al. model is in its formulation of the breakage function, which formally represents the likelihood of breakage as a function of the bubble diameter. Their breakage function increases with the bubble diameter until reaching a critical diameter, where the breakage decreases with an increase in the diameter. The decrease does not seem physical, as one expects the probability of breakage to increase with the diameter (i.e., larger bubbles break more easily).

Bandara and Yapa (2011) used the formulation of Prince and Blanch (1990) combined with the model of Tsouris and Tavlarides (1994) for the droplet model. They coupled the resulting model with the Combined Deep Oil and Gas (CDOG) model (Chen and Yapa, 2003; Zheng et al., 2003). They have applied it directly to oil released from a deep ocean blowout and have made comparisons against three datasets including the Deep Spill field experiment off the coast of Norway (Johansen, et al., 2001, 2003). As such, this appears to be the most relevant model of its class to discuss further. We have implemented a simplified version of the Bandara and Yapa (2011) model and are comparing it with Bandara and Yapa's published results (to make sure we are doing similar things) as well as measured droplet size distributions from Deep Spill and elsewhere. The following includes a brief summary of the Bandara and Yapa (2011) model, as well as an initial assessment of the model's strengths and weakness in relation to phenomenological models such as that of SINTEF. More complete results will be presented in future progress reporting, and we plan to make a presentation of the two model types in the forthcoming workshop scheduled for June in Tampa, FL.

Data from Deep Spill

It is worth discussing briefly the Deep Spill field experiment, because it is the best set of field (or field-scale) data available, and because it is one of the data sets used by Bandara and Yapa (2011) to test their model. We will address specifically the measurements of droplet and bubble sizes. Four experimental releases were made of oil and/or gas through an orifice 12 cm in

diameter, at a depth of 844 m in the Norwegian Sea. The two releases for which measurements of droplet or bubble sizes are provided are Release 2 (designated Exp-A by Bandara and Yapa) consisting of a mixture of marine diesel discharged at a rate of 60 m^3/hr and LNG discharged at a rate of 0.6 Sm^3/s, and Release 4 (designated Exp-C by Bandara and Yapa) consisting of seawater discharged at a rate of 60 m^3/hr and LNG discharged at a rate of 0.7 Sm^3/s. For Release 2, measurements were made of both diesel droplet size and diesel droplet volume distributions at four elevation ranges above the release point: 4-5 m, 9-10 m, 14-22 m and 34-55 m. Data are displayed in Figures 7.1.18 and 19 of Johansen et al. (2001) and are reproduced here as Figure 1. For Release 4, measurements were made of both methane bubble size and methane bubble volume distributions. Data are displayed as Figures 7.1.13 and 14 of Johansen et al. (2001) and are reproduced here as Figure 2. Measurements were made using a video camera mounted on an ROV with the help of a ruler as a scale. While Johansen et al. (2001) report some issues with camera focus and lighting, at least 100 droplets or bubbles were measured at each elevation range, sufficient to develop histograms. They also likely missed some of the smallest droplets and bubbles, which would affect the droplet size distributions but probably not the volume distributions, which we rely on here.

Based on Figures 1 and 2 we have also determined the median droplet/bubble diameter at each elevation as shown in Table 1.

We note that neither Table 1 nor Figures 1 or 2 indicate any consistent trend in the characteristic droplet/bubble size or the droplet/bubble size distributions with elevation above the release. But we emphasize that no dispersants were used for the Deep Spill experiments. Recent work by Masutani in a water tunnel suggests that significant evolution of the size distribution may occur when dispersants are added. We also note from the figures that, while there is randomness in the distributions at a given elevation, when the data are averaged over the four elevations, the two distributions are clearly uni-modal.

Table 1 Volume Median Diesel Droplet Sizes and Methane Bubble Sizes (d_{50}) as Functions of Measurement Elevation

Release	Fluid	Height Range (m)	d_{50} (mm)
2	Diesel	4-5	3.6
	Diesel	9-10	7.2
	Diesel	13-22	4.0
	Diesel	34-55	3.0
4	Methane	8-18	4.3
	Methane	18-22	5.4
	Methane	38-57	5.1
	Methane	64-84	3.4

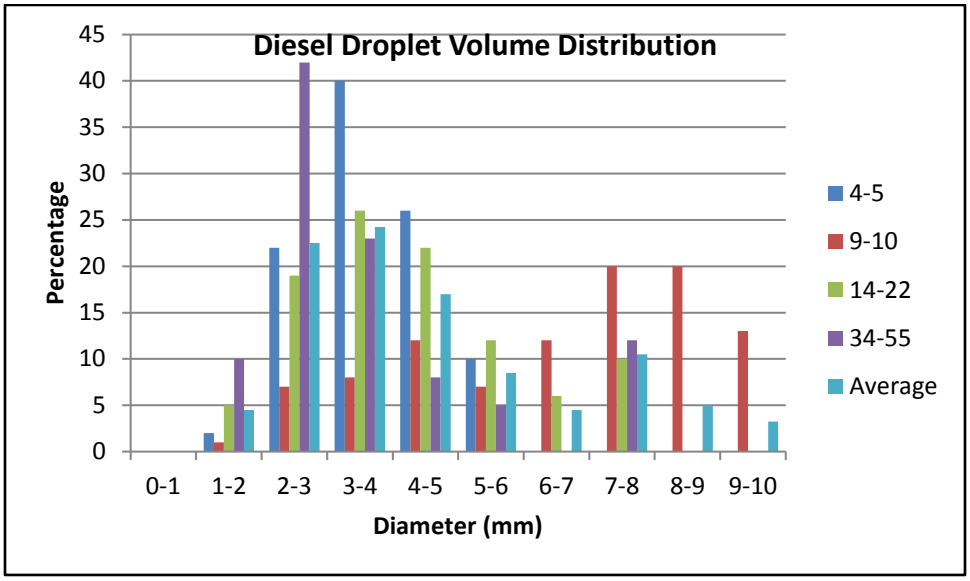

Figure 1 Diesel droplet volume distributions at different elevation ranges above the orifice from Deep Spill Release 2

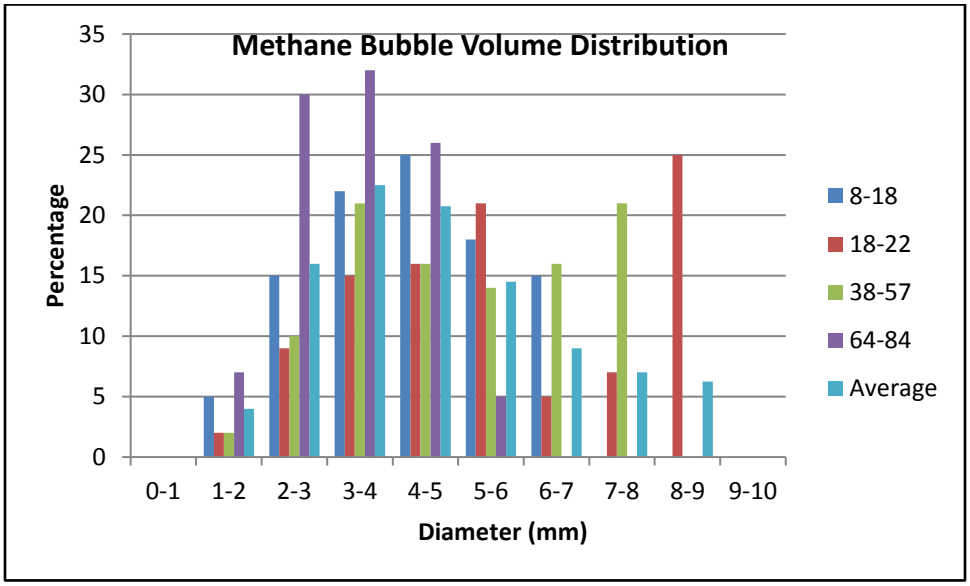

Figure 2 Methane bubble volume distributions at different elevation ranges above the orifice from Deep Spill Release 4

The Model of Bandara and Yapa

The Bandara and Yapa model applies to both oil droplets and gas bubbles but in our description we sometimes refer to droplets and bubbles interchangeably. The model divides droplets into a number of size classes (they use 10 for computational efficiency) each characterized by a single diameter. The model solves for the changing number of droplets in each size class as the result of droplet breakup and coalescence. Specifically, the number of droplets in a given size class can increase due to the breakup of larger size droplets and/or the coalescence of smaller droplets. Similarly the number of droplets of a given size can decrease due to breakup of droplets into droplets of smaller sizes and/or coalescence into larger sizes. Thus there are four terms in the droplet evolution differential equation. Simulations begin with all droplets having the same (seed) diameter, and after each time step newly created droplets, as a result of the four terms, are assigned to an appropriate size class in a manner consistent with conservation of mass.

Theoretical equations are given to compute breakup and coalescence. Breakup is probably the more important process and is due to the interaction of droplets with turbulent eddies. This depends strongly on the amount of turbulent kinetic energy, characterized by the energy dissipation rate, ε, as well as resistance to breakup due to interfacial tension (IFT) and/or viscosity. Bandara and Yapa use a formulation for ε that depends on the local jet velocity relative to the projection of the ambient velocity in the direction of flow. For a quiescent ambient $\varepsilon = cu^3/b$ where u and b are the local jet velocity and width, and c is an empirical coefficient. They use c = 2, which is significantly higher than implied by the near source dissipation rate measured by Martínez-Bazán et al. (1999a) for a water jet (Figure 3, which is adapted from Figure 3 of Martínez-Bazán et al.).

Figure 3 is for a jet with initial velocity of u_o = 17 m/s and plots ε versus a normalized and transformed distance, $x'/D_o = x/D_o - x_o/D_o$, where x is distance from the nozzle, D_o (they use D_j) is nozzle diameter (0.003 m), and x_o is a virtual origin, identified as $5.4D_o$. The data can be approximated by the red line consisting of a constant ε_o = 5E3 for x'/D_o less than about 10 and a decreasing function, $\varepsilon = 7E7\ (x/D_o)^{-4}$, at larger distances. The initial (constant) region is consistent with $\varepsilon_o = 0.003\ u_o^3/D_o$, while the latter (declining) region can be fit by $\varepsilon = 0.024u_c^3/b$, where u_c is the local centerline velocity and b is the half-width defined by $u/u_c = \exp(-r/b)^2$ where r is distance perpendicular to the centerline trajectory. The proportionality coefficient, c = 0.024, is deduced from empirical observations that, beyond the initial flow establishment region, $u_c/u_o = 6.2D_o/x$, and bx = 0.11. (Fischer, et al., 1979). The value of c = 0.024 is twice the value (0.012) used in earlier theoretical work by SINTEF (Rye et al., 1998). Figure 3 also plots ε using Bandara and Yapa's c = 2 (green line), which gives much larger dissipation rates. We note that Figure 3 applies to a non-buoyant jet, while the Bandara and Yapa model applies to bubble and droplet plumes. Plumes are known to display greater turbulent fluctuations than jets, though this difference is manifest more in the fluctuation of scalars (e.g., temperature), than velocity (Lee and Chu, 2003). Additional turbulence is no doubt added by the dispersed phase, especially the

bubbles, so it is possible that the "real" function is higher than that implied by the data of Martínez-Bazán et al. (1999a). It is also possible that Bandara and Yapa's definitions of u and b are slightly different from ours, thus affecting their constant c.

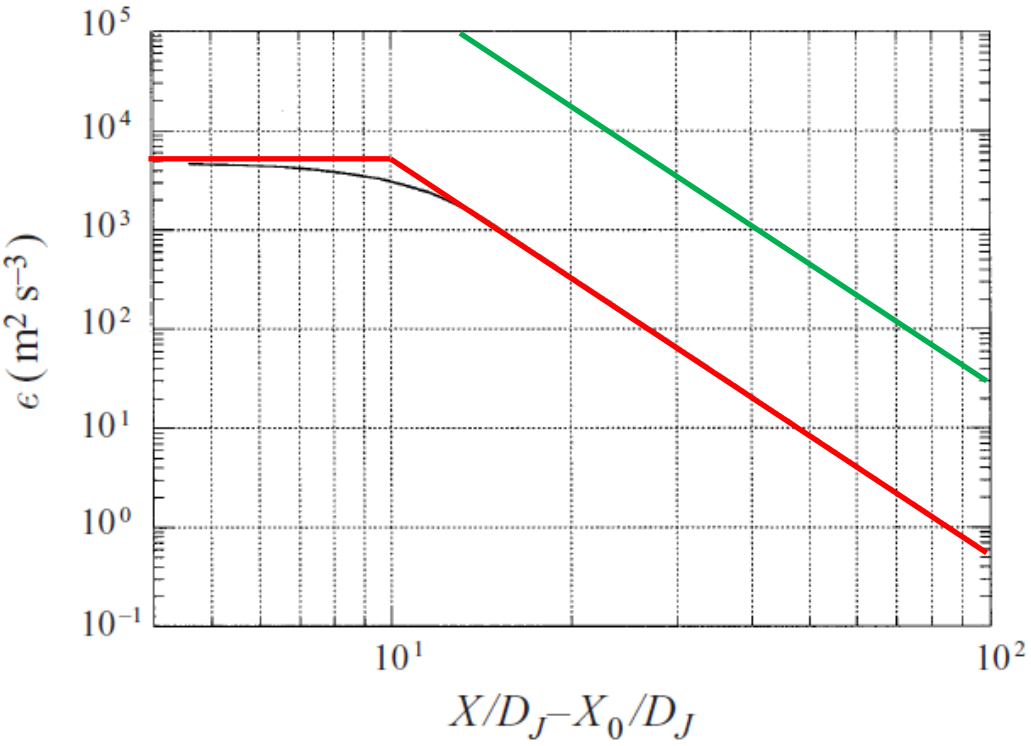

Figure 3 Dissipation rate, ε, modified from Martínez-Bazán et al. (1999a). See text for details.

It should also be mentioned that Bandara and Yapa (2011) assume that breakup is limited only by IFT resulting in a critical Weber number. This assumption may not be correct when dispersants are applied, because IFT can be reduced by several orders of magnitude, rendering viscosity as a contender for the resisting force. Presumably this could be accounted for by adopting some kind of modified Weber number as introduced by Hinze (1955), and used by Wang and Calabrese (1986) and the SINTEF model.

Coalescence results from the collision of two droplets as a result of differential velocities due to both turbulent mixing and buoyant rise, and depends both on collision frequency and coalescence efficiency, the former depending strongly on droplet concentration. Because both energy dissipation and droplet concentration decrease strongly along the axis of a plume, these processes are time-varying. Bandara and Yapa mention that this time variation is computed by coupling their droplet model to the plume model CDOG (Chen et al., 2003; Zheng, et al., 2003). While CDOG has been described in detail in prior works, Bandara and Yapa (2011) is shy on details regarding its coupling with their droplet model.

Bandara and Yapa (2011) compared predicted droplet/bubble size characteristics against three data sets. The first, reported by Hesketh et al. (1991), pertains to laboratory experiments on air bubbles injected through a 0.635 cm nozzle into a horizontal pipe of 3.8 cm diameter containing water recirculated at 398 cm/s. Hesketh et al. (1991) measured bubble distributions at different distances along their pipe, but reported that the distribution became constant after 1.33 m (about 200 nozzle diameters), suggesting that breakup and coalescence processes occurred close to the orifice. The authors defined a "breakage fraction", as a function of bubble size, as the ratio of the volumes of daughter bubbles breaking up and mother bubbles being broken up. Comparable calculations with the Bandara and Yapa model showed acceptable agree (their Figure 2), but a somewhat flatter distribution than indicated by the experiments.

The second data set includes laboratory experiments conducted at U. Hawaii, reported by Masutani and Adams (2001). Here, either crude oil or silicone fluid was injected through a 0.2 cm nozzle at one of three injection rates. The U. Hawaii data were expressed in terms of number (rather than volume) distributions, and measured and predicted distributions agreed well for all six cases cited by Bandara and Yapa (their Figures 3 and 4). However, we note that for both crude oil and silicone fluid, the experiment with smallest flow rate fell below the atomization range. Furthermore, the comparison involves only a small sub-set of the number of experiments conducted (the appendix to our first progress report lists 43 experiments in the atomization range) and it is not known if a good fit would have been obtained with some of the other experiments.

The last data set includes field measurements of both diesel droplets and methane bubbles from the Deep Spill experiment (Johansen et al., 2001), as described above. For the diesel droplets (Release 2) comparisons were made at the lowest (4-5 m) and the next to highest (14-22 m) of the four elevation ranges above the orifice at which measurements were made. For the methane bubbles (Release 4) comparisons were made at the lowest (8-18 m) and the highest (64-84 m) of the four elevation ranges above the orifice at which measurements were made. Coalescence rates were multiplied by a factor of 0.15 in all simulations, presumably to account for the decrease in coalescence in salt water. Reasonable agreement was obtained in all four cases (their Figures 5 and 6), but the following trends are noted. For diesel, the model shows an increase in droplet size as elevation increases from 4-5 m to 14-22 m above the nozzle while, as discussed above, no coherent trend is observed in the data. For methane, the model predicts no significant change in droplet size with elevation. Meanwhile the data for the two elevation ranges presented suggest a decrease in bubble size with increasing elevation, but if data from all four elevation ranges are considered, no such trend is apparent. It is not clear why all four elevation ranges were not included in their presentation, but perhaps they could be in the future.

Bandara and Yapa (2011) also performed several sensitivity studies to clarify aspects of their model. Simulations were made for both a pure gas and a pure oil release, using conditions in the same range as those at Deep Spill. Results for a pure gas release showed that above 2 m the gas volume distribution was independent of the initial (seed) diameter within the range of 1 to 10

mm (their Figure 7). Their Figure 8 shows that, while the four processes of birth and death by breakup and coalescence were very "active" at low elevations, they died down quickly to nearly zero by an elevation of 2 m, which can be explained by the rapid decrease in energy dissipation rate and bubble concentration, which they illustrate in their Figure 9 using CDOG. Meanwhile the overall gas volume distribution, which reflects a combination of the four processes, was shown to gradually shift to larger bubble sizes with elevation (their Figure 7). For example, peak diameters of 2, 3 and 4-5 mm were observed at elevations of 1, 2 and 50 m. No further increase was observed above an elevation of 50 m, and unfortunately no data were provided for elevations between 2 and 50 m.

Qualitatively similar results were found for runs with a pure oil release (their Figure 10). Again, there was no sensitivity to seed diameter beyond an elevation of 2 m, and the droplet volume distribution showed a gradual increase with the peak diameter shifting from 3 to 5 to 7 mm at elevations of 1, 2 and 50 m. For both gas and oil, the gradual increase in the bubble/droplet size distributions presumably represents the dominance of coalescence over breakup at larger distances, but this is not seen in their Figure 8 which plots the relative magnitudes of the four processes for a gas only release.

In conclusion, while additional sensitivity appears warranted, it is clear that most of the evolution of the bubble size distribution occurs near the origin. The dynamics of bubble breakup and coalescence are certainly important in this early evolution, but it is not clear if transient simulations are necessary. Because the kinetics are so fast, it may be that a properly calibrated steady state model could be sufficient for predicting the (steady state) bubble/droplet characteristics. Of course steady state models such as SINTEF's do not currently predict bubble/droplet size distributions so there is merit in further pursuing population based models.

Table 2 Qualitative comparison of SINTEF and Bandara and Yapa models

Attribute	SINTEF	Bandara and Yapa
Predicts droplet distribution?	No	Yes
Predicts time-varying behavior	No	Yes
Includes effect of gas	Yes	No
Includes effect of viscosity at low IFT	Yes	No
Degree of calibration/validation	Moderate	Moderate

Table 2 presents a qualitative comparison of the attributes of the steady state SINTEF model and the transient Bandara and Yapa model. More detailed comparison awaits more complete comparison of the Bandera and Yapa model against data and additional sensitivity study.

Our Reproduction of Bandara and Yapa's model

We have implemented a simplified version of Bandara and Yapa's droplet model, and have used it to simulate the droplet size distribution of the Deep Spill experiments off the coast of Norway. The reader can access the model interface by clicking:
https://dl.dropboxusercontent.com/u/83442/DropletModelv2.exe

We report herein our simulation results of Release 2 (diesel in water, reported in Figure 1 and in their Figures 5a and 5b), and compare them to the data, and by extension, their model. Bandara and Yapa (2011) coupled their droplet model to their transport model CDOG, and noted that the energy dissipation rate (ε) decreases sharply with the distance from the orifice. For example, for their sensitivity study using Scenario 3 conditions (similar to Scenario 2 except with crude oil replacing diesel), they reported that ε decreases from 450 W/kg to 2.0 W/kg (450 m^2/s^3 to 2 m^2/s^3) within two meters of the orifice. As stated above, their values of ε seem quite high. We have not formally coupled our droplet model with a transport model, but instead have used analytical expressions for a single phase plume to provide time-varying input to our droplet model. Our simplified plume dynamics seems justified in view of the fact that the measurements of droplet size at Deep Spill were taken at elevations before significant phase separation occured due to currents or stratification. Our model employs the following equations:

$$\varepsilon = \min\{0.024u_c^3/b,\ 0.003u_o^3/D_o\} \quad \text{(from above discussion)} \quad (1)$$

$$u_c = \min\{4.7B_o^{1/3}/x^{1/3},\ u_o\} \quad \text{(Fischer, et al., 1979)} \quad (2)$$

$$b = \max\{0.1x,\ D_o/2\} \quad \text{(Fischer, et al., 1979)} \quad (3)$$

$$Q = \max\{\pi u_c b^2,\ Q_o\} \quad \text{(Fischer, et al., 1979)} \quad (4)$$

Variable definitions and values for Deep Spill (from Socolofsky et al., 2011) are: x = plume height above origin, u_c and b = centerline plume velocity and half-width, Q_o = initial flow rate (0.024 m^3/s) including oil (0.017) and gas (0.07), D_o = orifice diameter (0.12 m), u_o = initial plume velocity (2.1 m/s), and B_o = initial plume kinematic buoyancy flux (0.095 m^4/s^3). These equations were integrated numerically with simple first order time-stepping using a time step of 0.01 sec. Figure 4 plots t, u, b, ε and the holdup, Q_{oil}/Q, as a function of x for conditions of Release 2 at Deep Spill. These results were input to the droplet model which we initiated with a seed size of 10 mm. Droplet distributions from our model (Figure 5) show reasonable agreement with field measurements taken at an elevation of 4-5 m above the source. Although our distribution is somewhat wider than observed, it is clearly uni-modal, and has the correct peak droplet diameter And this is without any attempt at calibration. Since Bandara and Yapa also obtained good agreement with similar data, this gives us confidence that we have programmed our model in a manner similar to theirs. Our next steps will be to conduct sensitivity tests, to complement those already conducted by Bandara and Yapa (2011), to better understand the relative importance of the break-up and aggregation processes inherent to this type of model.

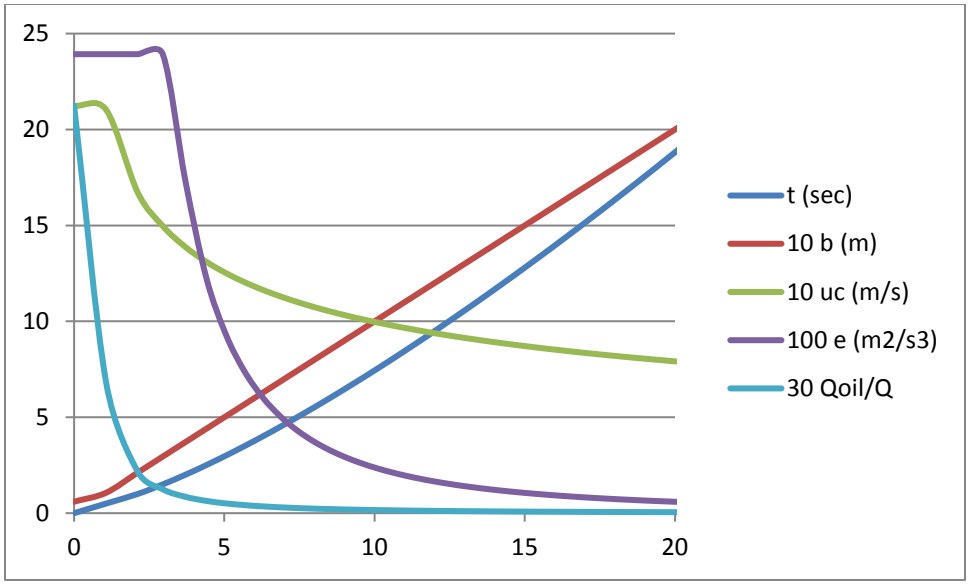

Figure 4 Calculated travel time (t in sec), plume half-width (b in m), plume centerline velocity (u_c in m/s), dissipation rate (ε in $m^2/s3$) and fractional oil flow rate (Q_{oil}/Q) plotted vertically as function of plume height x (in m) plotted horizontally.

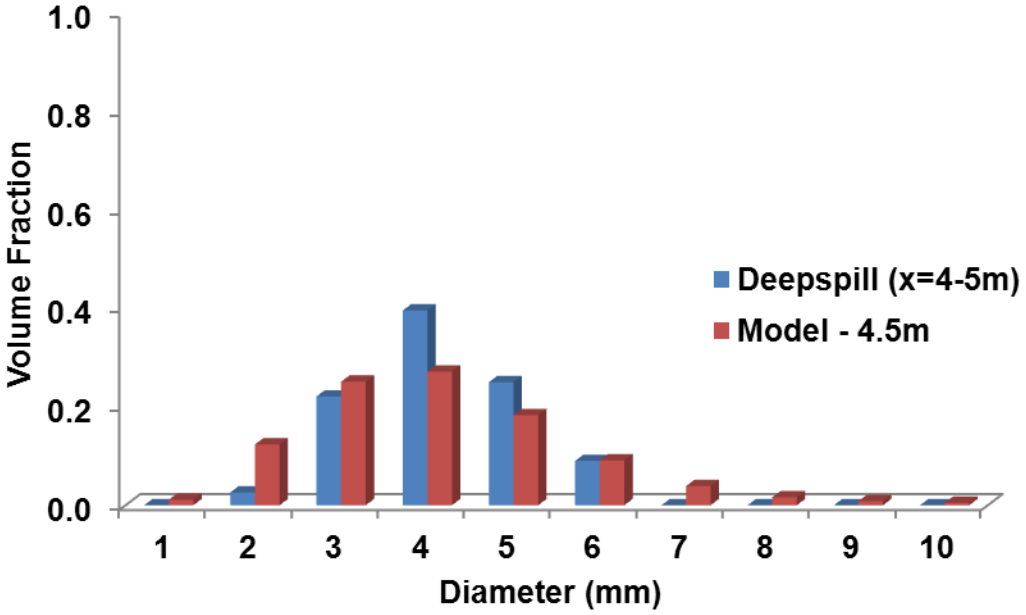

Figure 5 Droplet size distribution predicted by our simplified model (red) and measured during Release 2 at Deep Spill (blue) 4-5 m above orifice.

References

Bandara U. C., and P.D. Yapa, (2011). “Bubble sizes, breakup, and coalescence in deepwater gas/oil plumes.” *J. of Hydraul. Eng,-ASCE*, 137(7), 729-738.

Brandvik, P.J., O. Johansen, U. Farooq, G. Angell and F. Leirvik (2012). “Sub-surface oil releases-experimental study of droplet distributions and different dispersant injection techniques. A scaled experimental approach using the SINTEF Tower basin”, Draft report prepared by SINTEF Materials and Chemistry, Aug 2012.

Chen, F.H. and P.D. Yapa, (2003). "A Model for Simulating Deepwater Oil and Gas Blowouts - Part II : Comparison of Numerical Simulations with "Deepspill" Field Experiments", *Journal of Hydraulic Research, IAHR*, August, 41(4), 353-365

Fischer, H.B., E.J. List, R.C.Y Koh, J. Imberger, and N. H. Brooks, (1979) *Mixing in inland and coastal waters*, Academic Press, New York, NY.

Hesketh, R. P., A.W. Etchells, and T. Russell (1991). “Experimental observations of bubble breakage in turbulent flow” *Ind. Eng. Chem. Res*., 30(5), 835-841.

Hinze, J. O. (1955), “Fundamentals of the hydrodynamic mechanism of splitting in dispersion processes”, *Amer. Inst. Chem. Eng. J.*,1**,** 289–295.

Johansen, O., P.J. Brandvik and U. Farooq (2013), “Droplet breakup in subsea oil releases – Part 2: Prediction of droplet size distributions with and without injection of chemical dispersants”, *Marine Pollution Bulletin* (in press).

Johansen, O., H. Rye, and C. Cooper, (2003). “DeepSpill - Field study of a simulated oil and gas blowout in deep water”, *Spill Sci Technol B, 8*(5-6), 433-443.

Johansen, O., H. Rye, A. G. Melbye, H.V. Jensen, B Serigstad, and T. Knutsen (2001). “Deep Spill JIP- Experimental dishcarges of gas and oil at Helland Hansen—June 200”, Technical Report STF66F01082 by SINTEF Applied Chemistry, June 2001.

Lee, J., and H. Chu, (2003). *Turbulent jets and plumes: a Lagrangian approach*, Kluwer Academic Publishers Group, Dordrecht, Netherlands.

Luo, H., and H.F. Svendsen. (1996). “Theoretical model for drop and bubble breakup in turbulent dispersions.” *Amer. Inst. Chem. Eng. J* 42(5), 1225-1233.

Martínez-Bazán C., J. L. Montanes, and J. C. Lasheras, (1999a). “On the breakup of an air bubble injected into a fully developed turbulent flow. Part 1. Breakup frequency”. *J. Fluid Mech.*, 401, 157-182.

Martínez-Bazán C., J. L. Montanes, and J. C. Lasheras, (1999b). “On the breakup of an air bubble injected into a fully developed turbulent flow. Part 2. Size PDF of the resulting daughter bubbles”, *J. Fluid Mech.*, 401, 183-207.

Masutani, S.M. and E. E. Adams (2002). “Experimental study of multiphase plumes and application to deep oil spills”, Final report to the U.S. Dept. of Interior Minerals Management Service, Contract no. 1435-01-98-CT-30946.

Prince, M. J., and H.W. Blanch, (1990). “Bubble coalescence and break-up in air-sparged bubble columns.” *Amer. Inst. Chem. Eng. J*., 36(10), 1485–1499.

Rye, H., O. Johansen, and H. Kolderup, (1998). “Drop size formation from deep water blowouts” Technical Report STF66F98090 by SINTEF Applied Chemistry, Sept. 1998.

Socolofsky, S., E. Adams, and C. Sherwood, (2011). “Formation dynamics of subsurface hydrocarbon intrusions following the Deepwater Horizon blowout”. *Geo. Res. Lettr*. 38, L09602, Doi:10,1029/2011GLO47174, 2011.

Tsouris, C., and Tavlarides, L. L. (1994), “Breakage and coalescence models for drops in turbulent dispersions”. *Amer. Inst. Chem. Eng. J*, *40*(3), 395-406.

Wang, C.Y. and R.V. Calabrese (1986), “Drop breakup in turbulent stirred-tank reactors. Part II: relative influence of viscosity and interfacial tension”, *Amer. Inst. Chem. Eng. J*., 32, 667-676.

Zheng, L., Yapa, P. D., and F.H. Chen, (2003). "A Model for Simulating Deepwater Oil and Gas Blowouts - Part I: Theory and Model Formulation" *J. Hydraulic Research, IAHR*, August, 41(4), 339-351.

APPENDIX D

EVALUATION OF MODELS FOR SUBSURFACE DISPERSANT INJECTION

PROGRESS REPORT 4

E. Eric Adams, PhD, PE

Scott A. Socolofsky, PhD

Michel Boufadel, PhD, PE

Submitted to

American Petroleum Institute

Oil Spill Response Joint Industry Task Force (JITF)

D3 Subsea Dispersant Injection Modeling Team

Attn: Joe Twomey

p.twomey@ecosystem-management.net

June 2, 2013

Introduction

In this progress report we briefly review two additional "models". The first is that of Boxall et al. (2012), from the Colorado School of Mines, as applied by Paris et al. (2012). This is relevant because Paris et al. (2012) relied on the Boxall model, at least in part, to compute droplet sizes as input to a numerical transport model, which in turn was used to infer the effectiveness of chemical dispersants during the Deepwater Horizon oil spill. The second model is by Chen and Yapa (2007) who developed a procedure to predict oil droplet size distributions in deepwater oil spills using the concept of maximum entropy formalism (MEF). This approach is relevant because it can potentially be used to tie an estimate of characteristic droplet size (e.g., d_{50} or d_{max}) computed by models such as that of SINTEF (Brandvik et al., 2012; Johansen et al., 2013) to a distribution relative to the characteristic diameter, thus allowing prediction of a *complete droplet size distribution*.

The Model of Boxall (2012) as applied by Paris et al. (2012)

Boxall et al. (2012) report experiments on the dispersion of *water* droplets in *oil*, where the water was stirred with the oil by an *impeller* in a tank rather than by a jet. Thus it should be noted from the outset that these experiments differ from an oil blow out in two respects: 1) the dispersed and continuous phases are reversed, and 2) the method of injection is quite different. It is still possible that the basic theory could apply to oil jetted into water but, as found by SINTEF (Brandvik et al., 2012; Johansen et al. 2013) when they based their model on earlier work by Wang and Calabrese (1986), this would require calibration since one would not expect the same empirical relationships to apply exactly. This is discussed further below.

Boxall et al. (2012) fit their data to theoretical models of Shinnar (1961) giving droplet size for "large" and "small" droplets as

$$d/D \sim [\rho(ND)^2 D/\sigma]^{-3/5} \qquad (d > l_d) \qquad (1a)$$

$$(d/D)^2 \sim [\sigma/(\rho N^3 D^4 \mu)] \qquad (d < l_d) \qquad (1b)$$

where l_d is the Kolmogorov length scale (size of smallest eddy) given by

$$l_d = (\nu_c^3/\varepsilon)^{1/4} \qquad (2)$$

and ν_c and ε are the kinematic viscosity and energy dissipation rate, respectively, of the continuous phase. They applied their theory to mixing in reactors where D is the impeller diameter and N is the impeller frequency. ND is dimensionally a velocity (U) so the above equations can be recast as

$$d/D = C_{inertia}\, We^{-3/5} \qquad (d > l_d) \qquad (3a)$$

$$d/D = C_{viscous}\, Re^{1/2}\, We^{-1} \qquad (d < l_d) \qquad (3b)$$

where $We = \rho U^2 D/\sigma$ and $Re = \rho UD/\mu$ are the Weber and Reynolds numbers respectively. Similar proportionalities are expected for flow in a pipe where U and D are the pipe velocity and diameter. For experiments in a stirred reactor, Boxall et al. (2012) report that $C_{inertial} = 0.063$, and $C_{viscous} = 0.016$, when d is defined as the arithmetic mean water droplet diameter which is approximately $0.57 d_{max}$.

Paris et al. (2012) use the above equations but have a mistake in the text for small droplets. Their Equations S3 (large droplets) and S4 (small droplets) are

$$\text{Eq S3: } d/D = C_{inertia}(\rho_{eff}\, U^2 D/\sigma)^{-3/5} \quad \text{or } d/D = C_{inertial} We^{-3/5} \qquad (4a)$$

$$\text{Eq S4: } d/D = C_{viscous}(\rho_{eff}\, UD/\mu_{eff})^{-1}(\rho_{eff}\, U^2 D/\sigma)^{1/2} \quad \text{or } d/D = C_{viscous}\, Re^{-1}\, We^{1/2} \qquad (4b)$$

So the exponents on We and Re in their Eq S4 are switched in the text. However, it appears from Figure 1 of the main paper that their calculations use the correct equation. Also, Paris et al. refer to ρ_{eff}, υ_{eff} as the effective density and viscosity of the "oil/water mixture", which Boxall et al. (2012) say should reflect the continuous phase (oil for them, but water for us). It is not clear which medium Paris et al. (2012) use, though it does not make too much difference for the low viscosity oil released at high temperature at Macondo.

We note that Boxall's equation for large droplets (Eq. S3) has the same -3/5 power law dependence on Weber number used by SINTEF and others, which implies that droplets are broken down by ambient turbulence into smaller droplets until this break-up is resisted by surface tension. Since there is no dependency on the viscosity number, $Vi = \mu_d U/\sigma$, where μ_d is the viscosity of the dispersed phase (oil) and σ is the interfacial tension between oil and water, this equation would correspond to SINTEF's calculations for untreated oil (Eq. 3 in our Progress Report 1).

But as stated previously, Boxall's results were not for oil *jetted* into water, so one would not expect the same calibration coefficient so apply. Indeed, looking at Eq. 3a, the coefficient $C_{inertia} = 0.063$ for Boxall's stirred reactor is two and a half orders of magnitude smaller than the corresponding values of A = 15 and 24.8 found by SINTEF (Johansen et al. 2013, and Brandvik et al.,2012, respectively) for jet mixing! Because the SINTEF model agrees reasonably well with the data against which it has been compared, it can be concluded that the Boxall model, as applied to *oil jetted into water*, predicts droplets that are way too small.

It is also of interest to compare Eq S4 for "small" droplets with SINTEF's equation for droplets characterized by large viscosity number $V_i = \mu_d U/\sigma$. For very large V_i, SINTEF's formula (Eq 8 from our Progress Report 1) boils down to

$$d/D = CRe^{-3/4} \quad (5)$$

where $C = A^{5/4}B^{3/4}$. Using A = 24.8 and B = 0.08 (Brandvik et al., 2012) yields C = 8.3 while for A = 15 and B = 0.8 (Johansen, et al., 2013), C = 25. Assuming values representative of the Deepwater Horizon blowout post riser cut (σ = 23 g/s^2, D = 50 cm, U = 64 cm/s, μ_d = 0.04 g/cm-s, and ρ = 0.85 g/cm^3) yields Re = 68000 which gives d = 0.1 cm (C=8.3) to 0.3 cm (C=25). An indication of experimental uncertainty is the fact that separate calibrations, against similar measurements conducted in the same experimental facility (SINTEF's Tower Basin), lead to half an order of magnitude difference in characteristic droplet size. Meanwhile, for the same parameters, Eq S4 (with corrected exponents) gives a diameter of 0.028 cm which is one order of magnitude smaller.

The choice of Eq S3 or Eq S4 depends on whether the predicted droplet size is greater or smaller than the Kolmogorov length scale, which depends on the rate of energy dissipation ε. In Progress Report 3 we used data from Martínez-Bazán et al. (1999) to deduce that, near the jet,

$$\varepsilon = 0.003\ U^3/D \quad (6)$$

For the above values of U and D, ε = 16 cm^2/s^3, and using a value of kinematic viscosity for water of ν_c = 0.01 cm^2/s, Eq (2) gives a value of l_d = 160 μm. We noted in Progress Report 3 that the value of ε measured by Martínez-Bazán et al. (1999) seemed small, and that Bandera and Yapa (2011) assumed values that were several orders of magnitude larger. Using a value that is 100 times larger would reduce l_d to about 50 μm. We also note that, in the preparation of the Oil Budget Calculator (Lehr, et al., 2010), there was significant debate among the panel members over the magnitude of the energy dissipation rate, and conclude that this is an area that still needs further study. But uncertainly aside, even the larger 160 μm is probably smaller than most of the droplets produced at Deepwater Horizon (and certainly smaller those observed at DeepSpill), suggesting that the "large" droplet equation is most consistent with observations. This does not mean that there cannot be droplets with diameters smaller than l_d, formed by the asymmetrical break-up of droplets larger than l_d, but these would not be predicted by a model such as SINTEF's which presupposes only large droplets

Boxall et al. (2012) does not provide data on droplet distributions, but Paris et al. (2012) estimate the droplet distribution from experimental data on untreated oil reported by Greaves et al. (2008) and Aman, et al. (2010), also from the Colorado School of Mines. However neither of these studies applies to oil jetted into water. For dispersed oil, they refer to Li et al. (2008), and Chen and Yapa (2003). The former describes the effects of dispersants on treated *surface* oil, while the later compares predictions with the CDOG model against observations at DeepSpill. The CDOG model does have a Weber number based algorithm to predict droplet size, but one needs to know the corresponding reduction in interfacial tension.

The application of Paris et al. (2012) predicts much smaller droplets than were observed in DeepSpill. Reported droplets at DeepSpill were mainly in the range of 1 to 10 mm, and while there could have been smaller droplets that went undetected by the video observations, but it is doubtful that they contributed meaningfully to the droplet *volume* distribution. By contrast, Figure S3 shows that, without dispersants, predicted droplets were mostly less than 300 μm with a mode of 50-70 μm, while with dispersants the droplets were mostly below 200 μm with a mode of 10-20 μm. The authors state that larger droplets (1mm or larger) are doubtful because they would need to be nearly neutrally buoyant (SG > 0.9) in order to take three hours (inferred from Ryerson et al., 2012) to rise to the surface, and they feel this SG is too high. Indeed the SG of the Macondo oil was more like 0.85/1.027 = 0.83. However, using formulae from Zhang and Yapa (2000), and based on oil droplet and ambient densities of 0.85 and 1.027 g/cm^3, the rise velocities of 1, 3 and 10 mm oil droplets are roughly 3.4, 9.9 and 12.3 cm/s. Assuming these droplets rise as individual droplets over the entire water column (no interaction or plume effects), the surfacing times over a depth of 1500 m would be roughly 12, 4 hours, and 3 hours respectively. During the first part of their ascent, these droplets would have been part of a plume, so they would have travelled at a (much) faster velocity during the early stages of their ascent. Even if they were to have detrained with the first intrusion, at a depth of say 1100 m, the above travel times would have been reduced to about 9, 3 and 2.5 hours, quite consistent, on average, with inferences from Ryerson et al. (2012). Data from Chan (2012) suggests that oil droplets larger than about 2 mm would not have entered the intrusion, so under sufficiently quiescent conditions, these droplets could have benefited from further plume effects.

In conclusion, it appears that the data obtained by Boxall et al. (2012) for water stirred into oil in a reactor, is not suitable for estimating the size of droplets resulting from oil jetted into water.

The MEF Model of Chen and Yapa (2007)

Population based models such as Bandera and Yapa (2011), or our modification described in Progress 3, predict droplet size directly, but semi-empirical models such as SINTEF's predict only a characteristic droplet size. In the latter case, one could fit empirical data to an empirical distribution function (e.g., Rosin-Rammler or log-normal). An alternative is to use an optimization approach such as maximum entropy formalism (MEF).

MEF is an approach that can be used to estimate probability density functions under a set of user-defined constraints. Chen and Yapa have borrowed concepts developed in related areas of flow atomization and spray research to apply to the distribution of oil droplets. The potential advantage of their approach is that if avoids detailed simulation of the time-varying evolution of the distribution, but the disadvantage is that there is no clear cut way to choose the constraints.

Chen and Yapa identify a maximum droplet size based on standard Weber number scaling calibrated to droplet sizes observed at DeepSpill and then developed their distribution for smaller droplet sizes. Four physical constraints were identified—a normalization constraint, conservation of mass, conservation of momentum and conservation of kinetic and surface energy. In principle, these constraints are collectively satisfied by calculating four Lagrangian multipliers. When only two constraints were used (mass and specific energy) they were able to find a unique solution, but convergence was not always possible when using all four equations. The solution scheme was also sensitive to initial estimates of the Lagrangian multipliers, and it appears that some judgment is necessary in their selection. Thus is does not appear at present that this approach is any more reliable than assigning a distribution, à prior, based on experimental observations.

References

Aman, Z.M., L.E. Dieker, G. Aspenes, A.K. Sum, E.D. Sloan, and C.A. Koh (2010), "Influence of model oil with surfactants and amphiphilic polymers on cyclopentane hydrate adhesion forces", *Energy and Fuels* 24(10), 5441-5445.

Bandara U. C., and P.D. Yapa, (2011). "Bubble sizes, breakup, and coalescence in deepwater gas/oil plumes." *J. of Hydraul. Eng*, 137(7), 729-738.

Boxall, J.A., C.A. Koh, E. D. Sloan, A. K. Sum, and D. T. Wu (2012), "Droplet size scaling of water-in-oil emulsions under turbulent flow", *Langmuir* 28, 104-110.

Brandvik, P.J., O. Johansen, U. Farooq, G. Angell and F. Leirvik (2012). "Sub-surface oil releases-experimental study of droplet distributions and different dispersant injection techniques. A scaled experimental approach using the SINTEF Tower basin", Draft report prepared by SINTEF Materials and Chemistry, Aug 2012.

Chan, G.K.Y., (2013). "Effects of droplet size on intrusion of sub-surface oil spills". SM thesis, Dept of Civil and Environmental Engineering, Massachusetts Institute of Technology.

Chen, F. and P. Yapa, (2003). "A model for simulating deep water oil and gas blowouts - Part II: comparison of numerical simulations with "Deepspill" field experiments", *J. Hydraulic Res*. 41(4), 353-365.

Chen, F. and P. Yapa (2007). "Estimating the oil droplet size distributions in Deepwater oil spills", *J. Hydraul. Eng*. 133(2), 197-207.

Greaves, D., J. Boxall, J. Mulligan, D.E. Sloan, and C. Koh, (2008). "Hydrate formation from high water content-crude oil emulsions", *Chem. Eng. Sci*. 63, 4570-4579.

Johansen, O., P.J. Brandvik and U. Farooq (2013), "Droplet breakup in subsea oil releases – Part 2: Prediction of droplet size distributions with and without injection of chemical dispersants", *Marine Pollution Bulletin* (in press).

Lehr, B., et al. (2010) Oil Budget Calculator—Deepwater Horizon technical documentation: a report to the National Incident Comand, Coastal Response Res. Cent., Durham NH.

Li, Z., P. Kepkay, M.C. Boufadel, A.D. Venosa, and K. Lee, (2008). " Oil droplet size distribution as a function of energy dissipation rate in an experimental wave tank. *International Oil Spill Conference*, 1-6.

Martínez-Bazán C., J. L. Montanes, and J. C. Lasheras, (1999). "On the breakup of an air bubble injected into a fully developed turbulent flow. Part 1. Breakup frequency". *J. Fluid Mech*., 401, 157-182.

Paris, C. B., M. L. Hénaff, Z. M. Aman, A. Subramaniam, J. Helgers, D-P. Wang, V. H. Kourafalou, and A. Srinivasan, (2012). "Evolution of the Macondo well blowout: s\imulaitng the effects of the circulation and synthetic dispersants on the subsea oil transport", *Environmental Science and Technology* 46(24), 13293-13302.

Ryerson, T.B., R. Camilli, J.D. Kessler, E.B. Kujawinski, C.M. Reddy, D. L. Valentine, E. Atlas, D.R. Blake, J. de Gouw, S. Meinardi, D. D. Parrish, J. Peischl, J.S. Seewald, and C. Warneke. (2012), "Chemical data quantify Deewater Horizon hydrocarbon flow rate and environmental distributions", PNAS, doi:10.1073/pnas.1110564109.

Shinnar, R. (1961). "On the behavior of liquid dispersions in mixing vessels", *J. Fluid Mechanics* 10(2), 259-275.

Wang, C.Y. and R.V. Calabrese (1986), "Drop breakup in turbulent stirred-tank reactors. Part II: relative influence of viscosity and interfacial tension", *Amer. Inst. Chem. Eng. J.*, 32, 667-676.

Zhang, L. and P. Yapa (2000), "Buoyant velocity of spherical and non-spherical bubbles/droplets" *J. Hydraul. Eng*., 126(11), 852-854.

APPENDIX E

EVALUATION OF MODELS FOR SUBSURFACE DISPERSANT INJECTION

PROGRESS REPORT 5

E. Eric Adams, PhD, PE

Scott A. Socolofsky, PhD

Michel Boufadel, PhD, PE

Submitted to

American Petroleum Institute

Oil Spill Response Joint Industry Task Force (JITF)

D3 Subsea Dispersant Injection Modeling Team

Attn: Joe Twomey

patrick.twomey@hdrinc.com

November 30, 2013

Introduction

Since our last progress report (PR4, dated June 2, 2013) we have engaged in the following activities: a) continued our review of droplet models, b) worked on our own dynamic droplet model, c) attended the June 2013 API/GoMRI workshop in Tampa, FL, d) published a comment on the Paris article in ES&T, e) submitted abstracts for the January 2014 Gulf of Mexico Oil Spill and Ecosystem Science Conference in Mobile, AL and the May 2014 International Oil Spill Conference in Savanna, GA (the latter will be withdrawn as it was not accepted for oral presentation), and f) managed the initial phases of the January 2014 Workshop on Integrated Models to be held in Houston, TX. This progress report briefly summarizes our work to-date on the January 2014 workshop.

January 2014 Workshop on Integrated Models

Initial planning took place during the summer via a number of conference calls and email exchanges among ourselves and members of the API D3 Task Force. In September invitation letters, along with a white paper describing the workshop, were sent to approximately 40 individuals, including modelers, the evaluation team, members of the API D3 Task Force, federal agency representatives, and selected other researchers, including the GoMRI leadership. Nearly all of the invitees responded that they would like to attend the workshop, mostly in person, but a few remotely. The workshop had originally been planned for mid-January, but to minimize travel conflicts, the date was changed to January 31, immediately after the Gulf of Mexico Oil Spill and Ecosystem Science Conference in Mobile, AL.

Modelers were asked to simulate the fate of oil, released at a rate of 20,000 bpd from the seafloor, with hydrocarbon composition and ocean hydrographic conditions representative of the Gulf of Mexico. The white paper spelled out 14 separate scenarios involving different GOR, DOR, water depth, and ocean current speed that were to be simulated. The modelers were to provide their output in two steps. As a first step (Task 1), modelers were asked to predict the oil droplet size distributions near the point of release (distances of ~ 10s m). In Task 2 the modelers were asked to predict the transport and fate of oil in the near and intermediate fields (distances of ~ 100s to 1000s of m). For the latter task, the modelers were to use their own droplet size distribution model for some simulations, and a "common" droplet size distribution model for other simulations; the common model was designed to elucidate model differences other than those relating to determination of initial droplet size. Output for Task 2 was to be summarized in a set of metrics which we provided.

Shell provided a description of the oil for use in the modeling. We provided this data to all modelers upstream of the Task 1 deadline (droplet size distribution predictions), and all model

teams completed this task. However, not all modelers were able to input the exact oil composition into their models. This, and the use of different algorithms for droplet size, resulted in a range of predicted distributions among modelers. Based on an analysis of the results, we provided a "common" droplet size distribution model to the other modelers.

Our analysis of the Task 1 results shows that, even when modelers use the same model, they can arrive at differences that are significant (up to a factor of two). These differences are mostly due to differences in the assumed equation of state, which results in different densities or flow rates. A full analysis of the Task 1 results will be summarized in future reporting.

Results of Task 2 will be summarized ahead of the workshop using the metrics provided to the modelers. This analysis will be presented in graphical form, to facilitate discussion at the workshop. Following the workshop, we will prepare a summary progress report and, depending on the tone of the modelers, we intend to complete a journal article submission.

APPENDIX F

EVALUATION OF MODELS FOR SUBSURFACE DISPERSANT INJECTION

PROGRESS REPORT 6

E. Eric Adams, PhD, PE

Scott A. Socolofsky, PhD

Michel Boufadel, PhD, PE

Submitted to

American Petroleum Institute

Oil Spill Response Joint Industry Task Force (JITF)

D3 Subsea Dispersant Injection Modeling Team

Attn: Joe Twomey

patrick.twomey@hdrinc.com

March 12, 2014

Introduction

This progress report describes three efforts: a) the January 2014 Workshop on Integrated Models, held in Houston; b) preparation of a draft manuscript on our numerical droplet model, VDROP-J, and c) a brief review of the latest SINTEF report describing their API D3 Phase II experimental studies.

January 2014 Workshop on Integrated Models

A Model Intercomparison Workshop was held on January 31, 2014, at the Chevron offices in Houston, TX, and included an audience of modelers, industry representatives, federal agency participants, and academics. Minutes for the workshop were collected by HDR Ecosystem Management & Associates, and includes a list of attendees along with notes on the discussion. A list of all individuals contacted by Dr. Socolofsky with information about the workshop is included in Contact_List.xlss attached to this report. In addition, a post-doc and a grad student from TAMU and a grad student from MIT attended (but are not included on the list).

As described in our Progress Report 5, the model included two main tasks. For both tasks, 14 test cases of a blowout of 20,000 bbl/d were specified with a range of gas to oil ratios (GOR), water depths, and dispersant application rates (no dispersant or dispersant application at 2% dispersant to oil ratio, DOR). The file Intercomparison_Summary.doc attached to this report presents the description of the intercomparison exercise as it was presented to the modelers.

Five teams submitted results to Task 1, which required modelers to estimate the initial size distribution of oil and gas for each of the 14 test cases. Preliminary results of Task 1 were summarized in Progress Report 5. The attached Power Point presentation, Task_01.pptx, was presented at the January 31 workshop. The main conclusions of our analysis of the Task 1 results are as follows:

- Each modeling team employed a similar strategy for estimating initial droplet size distribution: A Weber number or modified Weber number model is used to estimate a characteristic droplet size (e.g., volume median diameter, d_{50}) as a function of oil properties (interfacial tension, viscosity and density) and orifice conditions (velocity and diameter). The size distribution is obtained using this characteristic size with an assumed distribution and spreading coefficient. All but DHI used volume droplet distributions that followed the Rosin-Rammler distribution; DHI used a droplet number distribution (e.g., as opposed to a volume distribution) following Chen and Yapa (2007).
- Results varied for a number of reasons:

    - Most teams used an oil equation of state that differed from that specified by us in the Intercomparison. This effect is described in our Progress Report 5.
    - Teams made different choices on which density (oil, gas, or seawater) to use in the Weber number model.
    - Teams treated the presence of gas with the oil differently.
    - Teams made different assumptions about the effect of dispersant on the interfacial tension.
    - The fitting coefficients for the Weber number model (A and B) were drawn from different experimental datasets, yielding differences in their values.
- The variability of the results among models was moderate, with differences being less than an order of magnitude (generally within a factor of 2 to 5), and with differences being the smallest for the test cases with zero gas flux at the wellhead (cases 3 and 4 with a GOR of 500 in 2000 m depth of ocean). The DHI results presented at the workshop contained an error; thus, their values are not included in reaching this conclusion.
- All of the predictions for field-scale conditions require an extrapolation in the non-dimensional Weber number and Reynolds number space above values achieved in the laboratory or in the Deep Spill experiment.
- Most modeling teams assume the gas bubbles are fixed at 10 mm diameter and are unaffected by dispersant. ASA estimates the gas bubble size from the Weber number model (reporting a diameter of 4.4 mm), but also assume no effect of dispersant.

Overall, the results were in agreement with our general expectations for droplet size, with all modeling teams reporting non-treated oil droplet sizes for d_{50} between 1 to 5 mm and treated oil droplet sizes consistently one order of magnitude smaller (100 to 500 micron).

Six teams submitted results to Task 2 in time to be included in the workshop comparison plots. Task 2 required teams to use API-specified, as well as their own user-specified, droplet and bubble sizes to simulate the fate of oil through a near field plume and subsequent Lagrangian drift through the water column under idealized stratification and crossflow conditions. Two of the teams (CMS and LTRANS) only submitting results for the plume stage of the model. The attached Power Point presentation, Task_02.pptx, was presented at the January 31 workshop. We have updated the figures in the presentation to reflect our best understanding of the modeler-reported results. These comparison plots and a data table summarizing the results will be sent to each modeling team shortly so that they can revise their model simulations or update the dataset with the correct model output (e.g., in the case that we misunderstood the model output or they reported the wrong metric). The attached Task_02_Metrics.doc file details what the modelers were asked to provide.

The main conclusions related to the near field plume modeling of Task 2 include the following:

- Models generally agree in predictions of the basic geometric features of the plume (trap height, maximum height of rise, etc.). This is mainly due to the inherent scaling of the

problem, since for a plume in stratification, the characteristic length scale depends on the buoyancy flux to the quarter power. Models may differ in how they allow bubbles to leave on the upstream side or in their simulation of dissolution, two processes that may reduce the buoyancy flux, but the prediction of geometric scales is largely insensitive to these differences as a result of this scaling.

- Models that include the effects of crossflow generally predict a lower trap height than those that do not since they accurately reflect greater entrainment throughout the plume stage resulting from the crossflow.
- Models that include gas dissolution or leakage of gas bubbles out of the plume by a crossflow generally predict a lower trap height than those that do not since the buoyancy flux accurately reduces with height in these models.
- Models differed the most in two main aspects:
    - Models varied in how they allowed gas to leak out of the plume on the upstream edge of the plume in a crossflow. Each model predicts a slightly different level and degree of upstream gas leakage, generally resulting from differing, proprietary numerical algorithms to capture this effect. Only the BLOSOM model appeared to predict unacceptable leakage; this is particularly evident in their predictions in the 200 m depth case with the plume trapping at 150 m depth or below and all other teams predicting the oil to reach the sea surface.
    - Models differed on when they stopped the near field plume calculations and passed the oil and gas off to the far field. Most teams employed a Lagrangian plume modeling approach, which in general, can be integrated well into the intrusion layer. Some models stop the near field model when the plume fluid first becomes neutrally buoyant, but this ignores the large, upward momentum still resident in the plume. Some models stop the near field model when this excess momentum is dissipated, but this ignores the plunging of the plume from this height of maximum rise to the subsequent intrusion layer. Only the OSCAR model appears to track the near field plume through these two end points and into the intrusion layer.
- Models generally agree on travel time for the oil and gas and rates of dissolution for the gas in the near field.
- Because all models stop their near field plume stage before the free surface is reached in a deep water blowout, new metrics need to be defined to identify the amount of oil transported to the surface near the response zone and the amount entering the intrusion layers. For the OSCAR model, it was possible to estimate the mass flux of oil into the intrusion, and those predictions agreed very well with the empirical prediction of the MIT model based on recent laboratory work by Chan et al. (2014) Results for other models will be obtained as we continue to work with the modeling teams.

For all of the models tested, the near field plume stage extends less than 1000 m above the release point, with an intrusion forming in the neighborhood of 300 m above the sea floor. In a

water depth of 2000 m, most of the oil transport takes place in these models within a Lagrangian particle tracking stage. The main conclusions of the Lagrangian far field modeling of Task 2 include the following:

- All models predict the radius to the surfacing zone of fresh oil to increase about an order of magnitude in the downstream direction when subsea dispersants are added. For the test cases without dispersant in deep water, surfacing zones predicted by the models range from 600 m to 4 km in the low crossflow (5 cm/s current) cases and 7 km to 10 km in the high crossflow (30 cm/s current) cases. When dispersants are added, the low crossflow surfacing zones move to 10 to 50 km downstream and the high crossflow surfacing zones move to 70 to 300 km downstream.
- The models predict the shallow plumes (200 m water depth) to go directly to the surface. Some models (notably OSCAR) predict much of the oil to remain dispersed in the upper mixed layer.
- The models vary significantly in the amount of oil predicted to eventually reach the water surface. This is most likely due to modelers simulating different time periods, since a steady state is not reached for the small droplets for a very long time. This metric will be reevaluated in the coming discussion with the modelers.

Hence, most models agree that the surfacing zone of free oil moves outside (more than 5 km downstream) of the response zone for a deep water blowout when dispersant is added, and that without dispersant, the free oil would surface much closer to the well (between 1 and 7 km downstream depending on the current). Models differ in their prediction of the amount of oil reaching the surface, mostly due to differences in how oil degrades in the water column and at what time in the simulation the mass of surfacing oil is estimated. The models are expected to give better consensus once a better metric is defined for this parameter since the simulations do not reach a steady state in a reasonable duration of simulation time.

During March 2014, the far field results for CMS and LTRANS, as well as modeling results for GNOME, will be added to the intercomparison. The plots and an associated metrics data table will also be provided to all modelers so that they can review whether the results of their simulations are accurately reflected in the intercomparison. Modelers will also be asked to provide more details on their simulation initial conditions, since none of the teams used the specified oil and differences in initial conditions may explain some of the model prediction spread. *These efforts will be summarized in a later progress report and will form the basis for a journal publication coauthored by all model teams and our group.*

Draft manuscript on our numerical model VDROP-J

We have been working on development of a droplet model that simulates the evolution of droplet sizes along the axis of a buoyant jet caused by an oil/gas blowout. The model computes droplet

size distributions taking into consideration the processes of jet breakup and coalescence, with resistance to breakup consisting of both fluid interfacial tension and viscosity. The model is an extension of Zhao et al. (2013) applied to the longitudinally-varying conditions of a buoyant multiphase jet.

We have submitted a draft first manuscript, referred to as Zhao et al. (2014), to *Marine Pollution Bulletin*, and the paper has just been accepted, subject to minor revision. We are still making changes to the model, some of which may be reflected in a revision to the first manuscript, while some may be discussed in a subsequent manuscript. We thought that including the attached draft copy would be the simplest way to convey our current status. We welcome your comments**.**

Among possible revisions to the model, we envision a major effort regarding the correlation of the droplet break-up parameter K_b with dimensionless quantities such as We and Re. Currently a strong correlation has been shown with the dynamic momentum. This is a dimensional quantity, which is not desirable, but we will continue using it until a good correlation with dimensionless quantities emerges. We also envision a comparison of the simulated droplet size distributions to log-normal and Rosin-Rammler distributions that have often been fit to experimentally determined droplet size distributions.

Review of latest SINTEF model study

Following their earlier (Phase I) testing for API D3 (Brandvik et al., 2013a), SINTEF has conducted additional droplet size experiments in their Tower Basin (Brandvik et al., 2013b). The aim of these experiments was to test the sensitivity of droplet size to a number of factors including: i) oil type, ii) dispersant type and dosage (i.e., DOR), iii) dispersant injection mode (upstream, simulated injection tool, and side of the jet at or slightly above the release elevation), iv) oil temperature, v) measurement height above the nozzle (as a test for spatial variation in droplet size), and vi) the presence of gas (air) discharged along with the oil. Their report largely speaks for itself, so we are going to focus on results relating to modeling, which mainly pertains to aspects iv), v) and vi).

As expected, droplet sizes were influenced by the type of oil, the type of dispersant and the dispersant to oil ratio (DOR), the method of injection, and the oil temperature (i, ii, iii, and iv). Perhaps the most striking result is that, when the temperature of oil increased, dispersant effectiveness dropped dramatically. This is mainly due to an *increase* in IFT with increasing temperature for dispersant treated oil. Compounding this is a modest *decrease* in IFT with temperature for untreated oil. Combining the two effects suggests a significant decrease in dispersant effectiveness for warm (hot) oils. Viscosity also decreases significantly with temperature, but no measurements are reported for the viscosity of treated oil, and viscosity has little effect on droplets of light oils that are untreated (e.g., Oseberg blend and Kobbe condensate). However, it should plan a role for heavy oils, such as the Grane or even the Norne

blend. Given the measured IFT and viscosity, the authors show that the "SINTEF model" was able to reproduce the measured d_{50}. There are actually two variants of the SINTEF model (Brandvik et al., 2013a; Johansen et al., 2013) with different empirical parameters (A and B) and the authors did not state which one they used.

Of course, one of the considerations with the SINTEF model, and indeed with any similar model, is that one needs to know the IFT. Earlier SINTEF results suggested that, at reasonable DOR, dispersants reduced the IFT by roughly a factor of 200, but a much smaller reduction was achieved here when the oil was heated. So it appears that the major uncertainty here is predicting IFT (as a function of temperature, oil type, dispersant type and dosage), rather than modeling droplets with a known IFT. One possible explanation for the observed temperature effect is that heating caused the oil to "weather", with some of the lower carbon fractions dissolving, leaving the remainder more resistant to change in IFT (harder to disperse). The IFT that SINTEF measured pertained to warm/hot oil that was heated, exposed to dispersant, injected into cold water, collected as droplets, then (after significant cooling) analyzed with a spinning drop tensiometer. It would be interesting to know how the IFT would differ for oil that was pre-mixed with dispersant, and then heated up. Or for oil that was treated, then heated then tested for IFT while still hot (e.g., by withdrawing small portions quasi-isothermally prior to insertion into the spinning drop tensiometer. Depending on how the IFT varied among different tests, one could suggest a protocol for future applications with the SINTEF, or similar, model.

Related to v), for some tests, measurements were conducted at two elevations within the Tower Basin (2 m and 5 m above the orifice). No significant differences in droplet sizes were observed, leading the authors to conclude that coalescence was not an important factor, at least for this part of the jet trajectory. In these tests the nozzle diameter was 1.5 mm, so the non-dimensional measurement heights (z/D) were approximately 1300 and 3300 which are huge. For a field scale orifice diameter of 50 cm (the case at Macondo after the riser was cut), the corresponding heights would be 660 to 1660 m, comparable to the total water depth! We recognize the difficulty in making measurements much closer to the orifice, but have to conclude that "the jury is still out" on this factor.

Related to vi), perhaps the most important factor studied was the presence of gas. SINTEF was hoping their experiments would determine if gas reduced the size of oil droplets in accordance with their model, and if gas influenced the effectiveness of dispersants in determining droplet size.

In Section 5.6 the authors mention that tests conducted in their Tower Basin were performed: a) with oil flow rate held constant and gas (air) flow varied without dispersant, b) same as a) but with dispersants, c) similar to a) and b), but using water instead of oil (the water contributing a similar effect on momentum as oil, but not creating droplets), and d) with oil and dispersant (similar to earlier tests). Unfortunately results are limited, possibly because of the acknowledged

difficulty in distinguishing oil droplets and gas bubbles using LISST instrumentation and cameras. However, some interesting data are provided in the various plots of Figures 5.35.

The red curve in Fig. 5.35b is for oil only and shows a d_{50} of about 260 microns. This curve serves as a reference point.

The green curve in Fig. 5.35a is for oil and air and shows $d_{50} > 400$ microns. On the face of it this could mean that the presence of air makes the droplets larger, whereas theory says they should be smaller, because the oil is being squeezed through a smaller cross-section and hence has greater momentum. However, it is likely that the data on the RHS of the curve is actually air bubbles. But if so, where are the oil droplets? There is certainly no dominant secondary peak.

The red curve in Fig. 5.35a is the same as the green curve except that water replaces oil; again it appears that $d_{50} > 400$ microns. Water should be similar to oil as far as its momentum is concerned, but it does not form droplets. Thus the red line in this figure should only represent the concentration of bubbles. In principle the distribution of bubbles from this figure might be subtracted from the distribution of oil droplets plus bubbles represented by the previous green curve, but this may not be possible in practice.

The blue line in Fig. 5.35b is for oil and dispersant and shows d_{50} of about 50 microns; the lower value of d_{50} compared with that of oil only (red curve in Fig 5.35b showing d_{50} of about 260 microns) suggests, as expected, that dispersant, without gas, helps to reduce droplet size.

Finally, the purple line in Fig. 5.35a is for oil, dispersant and gas. The distribution is bimodal, with peaks roughly at *both* 260 and 50 microns. To the extent that the peaks represent oil droplets (and not air bubbles), this suggests that the presence of air actually increases the average droplet size, rather than decreasing it as theory would suggest. The fact that the two peaks were at the same diameter as those observed when oil and oil plus dispersant were used, without air, suggests that the air might have prevented some of the dispersant from mixing effectively with the oil. That is, the portions of the oil that were effectively mixed with dispersant formed small droplets ($d_{50} = 50$ microns) while the portions of the oil that were not effectively mixed with dispersant formed large droplets ($d_{50} = 260$ microns).

Experiments conducted at TAMU with dye (representing dispersant) injected into a bubble plume above the orifice, show times when the dye is well mixed in the plume, and other times when the dye concentration is patchy, confirming that dispersant effectiveness could be intermittent. Because SINTEF was using either the simulated injection tool or an upstream injection (it is not clear from their Table 5.15), and the gas was introduced with the oil upstream of the orifice, the variability in dispersant effectiveness could be even greater. Did the flow in the pipe consist of oil droplets dispersed in gas, gas bubbles dispersed in oil, slugging oil and gas, gas flow in the center of the pipe with oil along the annulus, etc. The topology of the oil could probably be determined theoretically, but it might also be possible to observe it experimentally in the SINTEF experiments.

SINTEF did not perform tests with only air plus dispersant, so it is possible that one of the two peaks in the oil plus dispersant plus air tests actually corresponds to small bubbles. However, the congruence of the two peaks with the peaks obtained in separate tests with oil, and with oil plus dispersants, both without gas, suggests this is unlikely. In any case, contrary to theory, there is no evidence that air ever helped reduce droplet size.

Additional data are provided in Fig. 5.36 based on experiments in SINTEF's MiniTower. Results are shown for: a) oil only, b) oil (same flow rate as a) and two different flow rates of gas, and c) oil and gas (same flow rates as b) plus dispersant at DORs of 1 and 2%). The oil only release had a d_{50} of about 200-240 microns, which again serves as a baseline. Adding gas at the smaller of the two flow rates shifted the distribution slightly toward larger droplets, and added a much larger peak on the RHS which presumably is due to bubbles. Adding gas at the larger of the two flow rates appeared to flatten the distribution of droplets with greater numbers at both smaller and larger diameters compared with the oil only experiments; again the high concentrations on the RHS are probably due to bubbles. Results for oil, gas and dispersant were mildly bi-modal with a peak at slightly larger diameter than for pure oil, and a more pronounced peak at substantially smaller diameter. The bi-modality was stronger with a DOR of 2% compared with 1% with more droplets present at the smaller diameters. In conclusion, addition of dispersants at either DOR created smaller droplets, but the presence of gas had relatively little effect.

Another possible explanation for the apparent lack of reduction in droplet size when gas is added could be a result of scavenging of oil droplets by gas bubbles along their path to the measurement volume. If indeed small oil droplets are produced near the nozzle but these are then scavenged by larger gas bubbles moving quickly through the plume, the effect could be to increase the oil droplet size with height above the release. However, since the observed peaks in the gas plus oil plus dispersant case match closely the oil peaks with and without dispersant, the case can still be made that the observations are consistent with a lower dispersant mixing efficiency.

It is worth noting, again, that no results were presented with just gas and dispersants. Even though the gas in these experiments was air, considering gas and dispersants along with experiments with water and gas, would serve to isolate bubbles from droplets. It would also address the more fundamental question of the effect of dispersant on gas bubble size, which could affect overall plume dynamics, especially when the working gas is a hydrocarbon (which we understand is planned in later phases of the work).

Regarding the difficulty in distinguishing droplets from bubbles, it seems possible that the two phases might be made to separate spatially (i.e., fractionate) so they could be measured separately. In a buoyant plume comprising both gas and oil, the relatively large and buoyant bubbles will tend to spread less widely than the smaller and less buoyant droplets, such that measurements taken on the outside of the jet would be more likely to sample droplets. If the

air/water source were towed, e.g., in a circle at the bottom of the tank, the relative velocity would cause a stronger fractionation, with the faster rising bubbles leaving the plume closer to its source and the more slowly rising droplets leaving later. Fractionation might also be achieved by abruptly turning off the oil/gas source, allowing the more slowly rising droplets to lag at the back of the remnant plume, where they could be sampled without the presence of gas bubbles.

In conclusion, the predicted effect of gas on oil droplet size is significant. Table 1 of our Progress Report 1 shows that, for conditions at Macondo after the riser cut, d_{50} goes from about 1 cm with the two gas corrections to SINTEF's model, to over 5.7 cm without the corrections. (Of course the 5.7 cm exceeds the maximum stable droplet size, but the influence of gas is still apparent.) In view of the importance of gas, we would like to see if there are any additional results or interpretations added in SINTEF's final report.

References

Brandvik, P.J., O. Johansen, U. Farooq, G. Angell and F. Leirvik (2013a), "Sub-surface oil releases-experimental study of droplet distributions and different dispersant injection techniques. A scaled experimental approach using the SINTEF Tower basin", Report prepared for American Petroleum Institute by SINTEF, Trondheim, Norway.

Brandvik, P.J., O. Johansen, U. Farooq, E. Davies, F. Leirvik, and D. Krause (2013b), "Sub-surface oil releases-experimental study of droplet size distributions Phase-II. A scaled experimental approach using the SINTEF Tower basin", **Draft** report prepared for American Petroleum Institute by SINTEF, Trondheim, Norway.

Chan, G., Chow, A., Adams, E. 2014. "Effects of droplet size on intrusion of sub-surface oil spills", in preparation for *Environmental Fluid Mechanics*

Chen, F. and Yapa, P. 2007. "Estimating the oil droplet size distributions in Deepwater oil spills", *J. Hydraul. Eng*. 133(2), 197-207.

Johansen, O., P.J. Brandvik and U. Farooq (2013), "Droplet breakup in subsea oil releases – Part 2: Prediction of droplet size distributions with and without injection of chemical dispersants", *Marine Pollution Bulletin*, 73: 327-335.

Zhao, L., Torlapati, J., Boufadel, M.C., King, T. Robinson, B. Lee, K., 2013. VDROOP: a numerical model for the simulation of droplet formation from oils of various viscosities". *Environmental Modeling and Software* (submitted).

Zhao, L., Boufadel, M.C., Socolofsky, S., Adams, E.E., King, T., Lee, K., 2014. Evolution of droplets in subsea oil and gas blowouts: development and validation of the numerical mdoels VDROP-J. *Marine Pollution Bulletin*. (accepted subject to revision).

Attachments

A.1 Workshop Contact_List.xlss

A.2 Workshop Intercomparison_Summary.doc

A.3 Workshop Task_01.pptx

A.4 Workshop Task_02.pptx

A.5 Workshop Task_02_Metrics.doc

B Draft manuscript (Zhao, et al., 2014)

APPENDIX G

EVALUATION OF MODELS FOR SUBSURFACE DISPERSANT INJECTION

PROGRESS REPORT 7

E. Eric Adams, PhD, PE

Scott A. Socolofsky, PhD

Michel Boufadel, PhD, PE

Submitted to

American Petroleum Institute

Oil Spill Response Joint Industry Task Force (JITF)

D3 Subsea Dispersant Injection Modeling Team

Attn: Joe Twomey

patrick.twomey@hdrinc.com

November 10, 2014

Introduction

In the interval since Progress Report 6 we have been engaged in two major activities: a) follow up from the January 2014 Workshop on Integrated Models, held in Houston, and b) development and application of the dynamic droplet model VDROP-J. We have also reviewed several recent studies conducted by SINTEF through support of API.

Follow-up from January 2014 Workshop on Integrated Models

Results from the workshop have been compiled into a draft manuscript intended for submission to *Marine Pollution Bulletin*. The draft has benefited from feedback from API members and from the various modeling groups whose work is represented. We have received feedback from four of the modeling groups: 1) Claire Paris et al., from RSMAS, representing the model CMS; 2) Wolfgang Konkel from Exxon, representing ASA's model OILMAP Deep; 3) Lawrence Sim, from NETL, representing the model BLOSSOM; 4) Henrik Madsen, from DHI, representing the model MIKE; and 5) Mark Reed and CJ Beegle-Krause, from SINTEF, representing the model OSCAR. We have yet to receive feedback from U. Maryland, representing the model LTRANS, but expect to hear from them soon, and are making plans to submit the manuscript before the upcoming API workshop in Houston, November 18-19. The abstract of the paper is included as Attachment 1.

Draft manuscript on our numerical model VDROP-J

As described in our previous progress report, we have developed a model, called VDROP-J, which simulates the evolution of droplet sizes along the axis of a buoyant jet caused by an oil/gas blowout. This "dynamic" model computes droplet size distributions taking into consideration the processes of jet breakup and coalescence, with resistance to breakup consisting of both fluid interfacial tension and viscosity. The model is an extension of Zhao et al. (2014) applied to the longitudinally-varying conditions of a buoyant multiphase jet. The buoyant jet is currently represented by an analytical solution for the relevant plume parameters (e.g., dissipation rate, velocity, width, droplet concentration), but we are evolving to an integral plume model which is somewhat more sophisticated and can include transformation processes such as dissolution. Earlier this year we published a paper on the model in *Marine Pollution Bulletin*. The abstract is included as Attachment 2 to this progress report.

We have completed a second paper in which VDROP-J is applied to conditions at the Deepwater Horizon oil spill. Results for median droplet diameter and droplet size distribution are presented for untreated oil, dispersant–treated oil resulting in a 10 fold decrease in interfacial tension (IFT),

and dispersant-treated oil resulting in a 1000 fold decrease in IFT. Scenarios with varying oil flow rate, gas flow rate, and orifice diameter were also simulated, and results were compared with "static" models based on Weber number or modified Weber number, evaluated at the jet orifice. This paper has been submitted to the *American Institute of Chemical Engineering Journal*, and the abstract is included as Attachment 3 to this progress report.

Brief review of recent SINTEF reports describing API-supported research

We have briefly reviewed three reports. All are in draft form and we look forward to reviewing final copies when they are ready. We also look forward to discussion during the upcoming workshop in Houston, on Nov 19 and 20.

Brandvik et al. (2014b) analyze the effectiveness of chemical dispersants injected through four injection methods: upstream (up to 2000 diameters upstream of the nozzle), simulated injection tool (6 diameters upstream of the nozzle), injection above the nozzle (in the center of the plume 0-30 diameters downstream of the nozzle, and horizontal injection (directed perpendicular to the plume from different radii 3 diameters downstream from the nozzle). Much of the data come from SINTEF's earlier Phase I and II work for API.

The authors find that, while droplet size and IFT are both reduced for all four injection methods, the greatest effectiveness comes from using the simulated injection tool. They hypothesize that, with the simulated injection tool, the dispersant has sufficient time to mix with the oil—over a length of 6 diameters upstream of the nozzle and 6 diameters downstream of the nozzle, the latter constituting the so-called zone of flow establishment—before encountering the area of high turbulence where maximum break-up occurs. By contrast, they argue that with the upstream injection, there is too much time for mixing resulting in the formation of surfactant aggregates that decrease the effective concentration of dispersant as it interacts with the oil. This conclusion is supported by the experimental observation that droplet sizes decrease if the location of the injection is moved closer to the nozzle. Meanwhile, with injection downstream from the nozzle efficacy drops off as the distance from the nozzle increases. This is attributed to the fact that the dispersant becomes diluted, as it must mix with both oil and water. Efficiency for the horizontal injection is also less than that for the simulated injection tool for the same reason. It will be interesting to compare these results with our (Scott Socolofsky and his group at TAMU) measurements documenting the spatial and temporal statistics of the concentration of dye (representing dispersant) as it mixes into a bubble (representing oil) plume after being injected by a number of devices similar to those used by SINTEF.

In order to utilize droplet size formulae based on the Weber or modified Weber number, it is desirable to correlate the decrease in droplet size with the decrease in IFT. This is true for all four injection methods. However, such correlations are confounded by the fact that SINTEF's IFT is measured using oil droplets that have been extracted from their tank and then allowed to

pool (and hence lose their identity as individual droplets) over a period of hours. This brings up the question, which we first heard raised by Steve Masutani, of how and where to measure the IFT. For example, is the effective DOR greater for small droplets versus large droplets? This question is also relevant to the latent breakup stage. Also, dispersant aggregates form and break-up due to surface processes that have time scales that are different from plume time scales so, as the authors remark, there may be an issue with scaling up laboratory results to field scale based on scaling laws that are predicated on plume dynamics.

Davies and Brandvik (2014) describe the experimental setup and some preliminary results regarding their investigation of latent droplet breakup (Phase IV of the API scope). Latent breakup refers to the processes by which dispersant-treated oil droplets continue to break up through tearing and tip-streaming following initial droplet formation. Their study uses an inverted cone, patterned after the one used by Steve Masutani and his group at U. Hawaii. However, the SINTEF cone is taller, uses natural (rather than synthetic) seawater, and operates in a once through (rather than recirculating) mode. The once through configuration allows the seawater to flow by gravity, from a header, without experiencing bends in a piping system. This reduces turbulence and allows for more stable droplets to be observed. In addition, droplets are created using a nozzle similar to that used in SINTEF's earlier Phase I and II tests. This allows them to study droplets whose size is consistent with droplets formed by jet-induced breakup. Careful attention is paid to issues of background illumination, and image analysis, to improve the precision of droplet characterization, including calculation of the equivalent circular diameter, the deformation (ratio of minor to major axes), and the droplet rise velocity (factors important in understanding the onset of secondary droplet splitting), as well as observation s of droplet-droplet coalescence.

Preliminary results show that deformation increases with increasing droplet size and DOR, but not to the extent predicted by a theoretical model (which is not described). Several explanations for the discrepancy involve the notion that the dispersant may not be adequately mixed with the oil, and thus that the bulk IFT which is measured may not correlate with the local IFT. Again, this points to the need to better characterize IFT as a function of space and time. The inverted cone system is being rebuilt to allow use of the simulated insertion tool, which would reduce the mixing time between dispersant and oil.

Finally, the authors comment on a potential bias of diffraction-based droplet sizing instruments, including the LISST-100 they have been using, in overestimating the concentration of small droplets. This is relevant because the process of tip-streaming does produce small droplets, resulting in a bi-modal droplet distribution.

Brandvik et al. (2014a) describe experiments on droplet size distributions conducted at high pressure using facilities at the Southwest Research Institute (SwRI) in San Antonio TX. These tests relate to API-Phase IIIa. Several series of tests were performed.

To check on repeatability between the two facilities, a first set of tests was run with untreated oil at ambient pressure, using the same parameters as used in earlier tests at SINTEF as part of API-Phase I. The data at SwRI showed general smaller values of mean diameter than were observed at SINTEF (e.g., 280 um vs 144 um). While several possible physical/chemical explanations were identified (variation of oil flow rate, quality of artificial salt water, oil temperature and possible wax precipitation), none were sufficient to explain the factor of two change in droplet size. Later tests repeated at SINTEF suggest that the discrepancy might be due to a bias in the LISST DEEP instrumentation used by SwRI which might have resulted in an under-representation of the number of large droplets.

A second set of tests was made comparing untreated oil, with dispersant-treated oil applied using both the simulated insertion tool and upstream injection. Consistent with earlier findings, a greater shift (resulting in smaller droplet sizes) was found using the simulated insertion tool.

Most of the tests compared droplet sizes under ambient versus high pressure. For both untreated and treated oil, most tests showed little effect of pressure. However, the authors are cautious about their preliminary conclusion of no pressure effect pending further investigation of instrument bias.

References

Brandvik, P.J., Bradly, C., Leirvik, F., Farooq, U., Krause, D., and Davies, E., 2014a. "Subsurface oil releases—verification of dispersant effectiveness under high pressure*". Draft report dated August 3, 2014.*

Brandvik, P.J., Johansen, Ø., Leirvik, F., Krause, D., and Daling, P., 2014b. "Subsea injection of dispersants, effectiveness of different dispersant injection techniques—an experimental approach, *Draft manuscript dated August 24, 2014*.

Davies, E. J., and Brandvik, P.J. 2014. "Prelim inverted cone results". *Memo dated July 7, 2014*.

Zhao, L., Torlapati, J., Boufadel, M.C., King, T., Robinson, B., and Lee, K., 2014. "VDROP: a comprehensive model for droplet formation of oils and gases in liquids—incorporation of the interfacial tension and droplet viscosity". *Chemical Engineering Journal* 253: 93-106.

Attachment 1

Case Study: Intercomparison of Oil Spill Prediction Models for Accidental Blowout Scenarios with and without Subsea Chemical Dispersant Injection

Scott Socolofsky, E. Eric Adams, Michel C. Boufadel, plus one or more authors representing API and the respective modeling teams (SINTEF, NETL, RSMAS, U. Maryland, DHI, and Exxon (ASA)).

Abstract

This paper presents the results of a model intercomparison exercise for integrated oil spill models applied to subsea blowouts, including an evaluation of the effect of subsea injection of chemical dispersants. The intercomparison is based on a prescribed test matrix of blowout conditions in deep and shallow water, for high and low gas to oil ratio, and in weak to strong crossflows. Each model included modules for predicting the initial bubble and droplet size distribution (DSD), the nearfield plume stage, and the farfield Lagrangian particle tracking stage of oil and gas transport. Analysis of the intercomparison results quantifies model uncertainty and demonstrates the likely range of effectiveness for subsea dispersant injection. DSD models give predictions accurate to within +/-50% for the volume mean diameter, and the plume stage of transport in deepwater (2000 m release depth) is often minor, extending to a height of 15% of the water depth on average. Hence, most of the transport and degradation of oil is during the Lagrangian particle-tracking phase. Based on the models assessed here, subsea dispersant injection can be expected to reduce the volume mean diameter at the source from 2 to 8 mm without dispersant to 0.1 to 0.4 mm with dispersant, which translates to downstream distances to oil surfacing increasing from less than 1 km without dispersant to a few 10's of km with dispersant.

Under final review before submission to *Marine Pollution Bulletin*

Attachment 2

Evolution of Droplets in Subsea Oil and Gas Blowouts: Development and Validation of the Numerical Model VDROP-J

Lin Zhao, Michel C. Boufadel, Scott A. Socolofsky, E. Eric Adams, Thomas King, and Kenneth Lee

Abstract

The droplet size distribution of dispersed phase (oil and/or gas) in submerged buoyant jets was addressed in this work using a numerical model, VDROP-J. A brief literature review on jets and plumes allows the development of average equations for the change of jet velocity, dilution, and mixing energy as function of distance from the orifice. The model VDROP-J was then calibrated to jets emanating from orifices ranging in diameter, D, from 0.5 mm to 0.12 m, and in cross-section average jet velocity at the orifice ranging from 1.5 m/s to 27 m/s. The d_{50}/D obtained from the model (where d_{50} is the volume median diameter of droplets) correlated very well with data, with an R^2= 0.99. Finally, the VDROP-J model was used to predict the droplet size distribution from Deepwater Horizon blowouts. The droplet size distribution from the blowout is of great importance to the fate and transport of the spilled oil in marine environment.

Marine Pollution Bulletin 83 (2014) 58-69.

Attachment 3

Prediction of the Oil Droplet Size Distribution from the Deepwater Horizon Blowout

Lin Zhao, Michel C. Boufadel, Eric Adams, Scott A. Socolofsky, and Kenneth Lee

Abstract

Knowledge of the droplet size distribution (DSD) from the Deepwater Horizon blowout is an important step in predicting the fate and transport of the released oil. We used a thoroughly calibrated DSD model, VDROP, that is capable of accounting for oil viscous resistance to breakup in the presence of dispersants. VDROP was coupled with jets/plumes equations to produce the model VDROP-J, which was used to consider various realistic scenarios to evaluate the DSD from the DWH blowout within 200 m of the wellhead. For untreated oil, the median droplet size d_{50} was predicted to be between 3 - 7 mm at 200 m. For the dispersant-treated oil, the predicted d_{50} was 0.7 – 1.6 mm for a reduction of oil-water interfacial tension by a factor of 10, and 0.2 – 0.5 mm for a reduction of the interfacial tension by a factor of 1000. The DSD was bimodal near the wellhead, and converted to unimodal as the plume moved away from the wellhead. The change occurred more rapidly for cases of dispersant-treated oil. Scenarios with varying oil flow rate, gas flow rate, and orifice diameter were also simulated. These results, especially for dispersant-treated oil, are very different from recent modeling results in the literature.

Submitted to *American Institute of Chemical Engineering Journal* (2014)

APPENDIX H

EVALUATION OF MODELS FOR SUBSURFACE DISPERSANT INJECTION

PROGRESS REPORT 8

E. Eric Adams, PhD, PE

Scott A. Socolofsky, PhD

Michel Boufadel, PhD, PE

Submitted to

American Petroleum Institute

Oil Spill Response Joint Industry Task Force (JITF)

D3 Subsea Dispersant Injection Modeling Team

Attn: Joe Twomey

patrick.twomey@hdrinc.com

August 18, 2015

Introduction

This report summarizes activity since our Progress Report 7 (November 7, 2014). Note that some of the presented material has been previously transmitted in email correspondence with C. Cooper in January and July, 2015, but it is included here for completeness.

Model development/application

We have coupled NJIT's VDROP-J model (Zhao, et al., 2014b) to TAMU's multiphase plume model so that initial droplet sizes provided by VDROP-J can be used in blowout plume simulations. We are continuing to work on two-way model coupling, with iteration, so that results from the blowout plume simulation can be fed back into VDROP-J droplet predictions.

We are also planning to apply the original VDROP model (Zhao, et al., 2014a), developed for fluids with stationary flow properties, to the experiments of Aman et al. (2015) to explore the transient evolution of the droplet size distribution (DSD).

We submitted to *Applied Mathematical Modeling* a manuscript describing (methane) bubble dynamics (Zhao et al., 2015a). The main conclusions of the paper are 1) dissolution of methane in the surrounding water alters the size distribution and only certain sizes can make it to the water surface, and 2) the mixing energy due to bubbles is not negligible. This latter point might also be a consideration with the Belore (2014) experiments described below as he used a horizontally discharging jet in order to increase the trajectory length and to allow the gas bubbles and oil droplets to fractionate, so that each could be distinguished by the LISST.

Comparison of SINTEF's model against data

We performed an initial comparison of SINTEF's model predictions with experimental data conducted by S.L. Ross at the Ohmsett facility in Leonardo, New Jersey (Belore, 2014; Ross 2014). Briefly, the experiments employed a LISST instrument to measure droplet size distributions for two different oils, plus either air or methane, plus dispersant, jetted horizontally into seawater. They reported volume median diameters (d_{50}) that were considerably smaller than the "SINTEF model" predicts. They also reported that earlier column tests at the Ross Facility in Ottawa showed that the SINTEF model was able to predict d_{50} before dispersants were added. Ideally, we would like to be able to use Belore's data to quantify how well the SINTEF model can predict the observed dependence of d_{50} on the presence of dispersants and gas and possibly to suggests approaches for further calibration.

As a first step, we made a quick analysis of their data in relation to predictions made with the SINTEF model. Using SINTEF'S original model parameters (A = 15 and B = 0.8; Johansen et al., 2013), which is what we believe Belore used when referring to the "SINTEF model", the model over-predicts the 48 measured values of d_{50} by an average factor of 15 (median factor of 8)! Since these experiments were all with dispersants, and Belore implies that reasonable agreement was observed in earlier tests before dispersants were added, it appears that the SINTEF model is not predicting enough of an effect of dispersant addition.

However, there are some issues with Belore's experiments which cloud the comparisons. For example, the LISST instrument truncates the largest droplet sizes, and if this were corrected, the "measured" d_{50}'sould be larger, and at least somewhat closer to the SINTEF predictions. On the other hand, the SINTEF model "takes credit" for the higher exit velocities (hence higher values of We and lower values of d_{50}/D) due to the presence of gas; without the "credit" the predicted droplet sizes would be even larger. We feel the "credit" may be too high, as the SINTEF/API Phase II tests did not seem to show as strong a reduction in droplet size due the presence of gas as predicted, though they acknowledge difficulties distinguishing droplets from bubbles. (See our discussion in Progress Report 6.) And it is difficult to assess the effects of gas in Belore's experiments, since they all contained gas, generally at a GOR, by volume, of about 5 or 10. But it is possible to compare the 20 pairs of experiments in which conditions were similar except for the GOR: in 17 or the 20 the predictions indicated more of a reduction in the d_{50} with the larger GOR, than was observed. This indeed supports the contention that the SINTEF model "takes too much credit" for the presence of gas. The discrepancy between model and data when dispersants are present might plausibly have been resolved if measurements showed that the gas caused a GREATER reduction in d_{50} than was predicted in going from low to high GOR, but the limited amount of data does not seem to support this. Perhaps there are other measurements with and without gas that we should be aware of? Also, in applying the SINTEF model, we followed Belore and used a factor of 1000 reduction in IFT (from untreated to treated oil), and this seems large; use of a smaller reduction factor would lead to even larger predicted d_{50}'s, though not by very much as the treated cases are mostly in the Re controlled regime.

The discrepancy between model and data when dispersants are present could be resulting from the fact that SINTEF's original parameter set (as well as the subsequent one to a lesser degree) are off. In the limit of Re control (high values of the viscosity number, $Vi = U\mu/\sigma$), $d_{50}/D = C\ Re^{-3/4}$ where C is $A^{5/4}B^{3/4}$. Using SINTEF's original parameter set (A = 15 and B = 0.8; Johansen, et al., 2013) yields C = 25, while using their latter set (A = 24.8 and B = 0.08; Brandvik et al., 2012) yields C = 8.3, resulting in droplet sizes that are a factor of 3 smaller. Were the parameters to be changed further (by similar factors such that C ~ 3), the average predictions would be in the same ballpark as the observations.

As an illustration of the difference between measurements and prediction, Table 1 compares SINTEF's predictions with one of Belore's runs: Run 10 using Endicott oil mixed with air (GOR ~2.8:1), and a DOR ~ 1:17, discharged at a rate of 533 ml/min, through a nozzle with orifice

diameter of 0.15 cm. This run was chosen, in part, because it had a smaller GOR than most of the other runs. For this experiment, Belore observed a d_{50} = 0.02 cm. In Table 1 we look at the effects of varying both GOR (0 and 2.8:1) and DOR (0 and 1:17) using SINTEF's model with both sets of parameters and assuming, as Belore did, that dispersants reduce IFT by 1000 fold. In each block of four rows the last row is shaded indicating that these are the conditions (values of GOR and DOR) actually pertaining to Belore's Run 10.

The first four rows of Table 1 shows results using SINTEF's original parameters (A = 15 and B = 0.8). The predicted d_{50}'s with and without gas, and with and without dispersant, range from 0.13 to 0.22, comparable to the orifice diameter and an order of magnitude larger than the observed d_{50}. (The predicted d_{50} for the fourth row is 0.13 cm, about 6.5 times the measured d_{50}.) There is little sensitivity to the presence of dispersants, even with the assumed 1000 fold reduction in IFT, since we are in the Re controlled regime. In the presence of gas, the predicted d_{50}'s show a modest reduction of about 40% due to the increase in the exit velocity of the oil.

The second four rows of Table 1 use SINTEF's newer parameters (A = 24.8 and B = 0.08). The overall reduction in d_{50}, compared with the the previous block, is nearly 3 reflecting the 3 fold decrease in the parameter $C = A^{5/4}B^{3/4}$, and the predicted d_{50} = 0.04 cm shown in the fourth row now exceeds the measurement by only a factor of two. Again, there is a minimal effect of dispersant because we are still in the Re controlled regime, and there is the same ~40% reduction in predicted d_{50} due to the presence of gas.

The last two blocks of rows in the table are for the two values of A, but with B set to zero. This is tantamount to having no viscosity, or complete We control. Values of d_{50} are vastly reduced, compared with the previous two blocks, and the model displays healthy sensitivity to the presence of both gas and dispersant. The fourth rows of these two blocks show values of d_{50} = 0.00019 and 0.0003 cm, two orders of magnitude smaller than the measured d_{50}. Again, this reinforces the notion that SINTEF's calibration could stand tweaking. If they have not already done so, we would be happy to look into this further.

To summarize, experiments we have looked at previously, as well as those reported by Belore (2014), suggest that the SINTEF model adequately predicts the DSD for untreated oil. Conversely, Belore's data suggest that the SINTEF model over-predicts sizes for dispersant treated oil, at least within the parameter range he studied, though this conclusion is confounded by the presence of gas in all of their experiments. Similar conclusions were also found when comparing the SINTEF model with VDROP-J (Zhao, et al., 2015). The explanation seems to be that the SINTEF model over-predicts the role of viscosity in limiting droplet break-up at small interfacial tension (conditions relevant to dispersant application). As a secondary conclusion, it appears from Belore's data, as well as previous data presented in the SINTEF/API Phase II report, that SINTEF's model over-predicts the effect of gas in reducing droplet size.

We are looking forward to re-visiting these calculations, as well as those in SINTEF's API D3 Phase II-III draft reports previously reviewed in our PR 6 and 7, and more recent studies conducted under Phase IV-VI.

Table 1 SINTEF model simulation of Belore (2014) Run 10. Data in cgs units.

IFT, σ	n = GOR/(1+GOR)	A	B	d_{50}
25	0	15	0.8	0.22
0.025	0	15	0.8	0.21
25	0.74	15	0.8	0.13
0.025	0.74	15	0.8	0.13
25	0	24.8	0.08	0.09
0.025	0	24.8	0.08	0.07
25	0.74	24.8	0.08	0.05
0.025	0.74	24.8	0.08	0.04
25	0	15	0	0.03
0.025	0	15	0	0.0004
25	0.74	15	0	0.012
0.025	0.74	15	0	0.00019
25	0	24.8	0	0.05
0.025	0	24.8	0	0.0007
25	0.74	24.8	0	0.02
0.025	0.74	24.8	0	0.0003

Presentations and future manuscripts

We have successfully completed and published our manuscript on the API sponsored Model Intercomparison Workshop (Socolofsky et al., 2015), We were asked to consider making a short video describing the paper, but think our time would be better spent writing a comprehensive journal article on droplet sizes.

We wrote a small piece for HydroLink,, a magazine published by IAHR, on the topic of "Fluid mechanics of oil spilled from a deep ocean blowout: the role of chemical dispersants." (Adams, et al., 2015). A pdf of the paper is attached to the back of this report. Associated with the paper,

E. Adams gave a plenary lecture on this topic at the 36th IAHR World Congress conducted at The Hague (June 29 to July 3, 2015). There was no additional proceedings paper associated with this presentation.

We have outlined a journal article to comprehensively compare measured and predicted droplet size distributions. Both stationary (correlation-based) and dynamic (population-based) models will be included. The article would summarize the state of our understanding, outline areas of needed research, and address errors in the Aman/Paris approach.

We have re-submitted to *Marine Pollution Bulletin* manuscript entitled "Simulation of scenarios of oil droplet formation for Deepwater Horizon blowout" by Zhao et al. (2015b).

References

Adams, E., S. Socolofsky, and M. Boufadel (2015). 'Fluid mechanics of oil spilled from a deep ocean blowout: the role of chemical dispersants", *Hydrolink* 2/2015: 56-57.

Aman, Z.M., C. B. Paris, E. F. May, M. L. Johns, and D. Lindo-Atichati (2015) "High pressure visual experimental studies of oil-in-water dispersion droplet size", *Chemical Engineering Science* 127:392-400.

Belore, R. (2014). "Subsea Chemical Dispersant Research", paper presented to IOSC, Savannah River, GA.

Brandvik, P.J., O. Johansen, U. Farooq, G. Angell and F. Leirvik (2012), "Sub-surface oil releases-experimental study of droplet distributions and different dispersant injection techniques. A scaled experimental approach using the SINTEF Tower basin", Draft report prepared by SINTEF Materials and Chemistry, Aug 2012.

Johansen, O., P.J. Brandvik and U. Farooq (2013), "Droplet breakup in subsea oil releases – Part 2: Prediction of droplet size distributions with and without injection of chemical dispersants", *Marine Pollution Bulletin*, 73: 327-335.

S.L. Ross Environmental Research (2014) "Subsea Chemical Dispersant Research, report prepared for Bureau of Safety and Environmental Enforcement, U.S. Dept. of the Interior, 110 p.

Socolofsky, S., E. Adams, and M. Boufadel and 15 others (2015). "Intercomparison of oil spill prediction models for accidental blowout scenarios with and without subsea chemical dispersant injection", *Marine Pollution Bulletin*, doi:10.1016/j.marpolbul.2015.05.039).

Zhao, L., J. Torlapati, M. Boufadel, T. King, B. Robinson, and K. Lee (2014a). "VDROP: a comprehensive model for droplet formation of oils and gases in liquids—incorporation of the interfacial tension and droplet viscosity", *Chemical Engineering Journal*, 253: 93-106.

Zhao, L., M. C. Boufadel, S. A. Socolofsky, E. Adams, T. King, and K. Lee (2014b), “Evolution of droplets in subsea oil and gas blowouts: Development and validation of the numerical model VDROP-J,” *Marine Pollution Bulletin*, 83(1), 58-69.

Zhao, L., M.C. Boufadel, T. King, S. Socolofsky, E. Adams, N. Loney, and K. Lee, (2015a) “Prediction of bubble formation in jets and plumes: the role of gas expansion, dissolution and mixing”, submitted to *Applied Mathematical Modeling*.

Zhao, L., M. Boufadel, E. Adams, S. Socolofsky, T. King, and K. Lee (2015b) “Simulation of scenarios of oil droplet formation for Deepwater Horizon blowout”, submitted to *Marine Pollution Bulletin.*

Appendix

Fluid Mechanics of oil spilled from a deep ocean blowout: the role of chemical dispersants

FLUID MECHANICS OF OIL SPILLED
THE ROLE OF CHEMICAL DISPERSA

BY E. ERIC ADAMS, SCOTT A. SOCOLOFSKY, AND M.C. BOUFADEL

A silver lining in the Deepwater Horizon oil spill tragedy that occurred five years ago in the Gulf of Mexico has been the opportunity to better understand various physical, chemical and biological factors affecting oil transport and fate. Fluid mechanics has played an important role in this understanding.

Examples include (i) use of PIV-type analysis of video images to estimate the oil flow rate at its source; (ii) theoretical and experimental approaches to predict oil droplet sizes; (iii) laboratory and mathematical models of varying complexity to study the interaction of multi-phase plumes with ambient currents and stratification; (iv) studies of turbulent mixing, dissolution/degradation, and sediment-oil interactions of rising oil droplets; and (v) the capabilities of 3D circulation and transport models to predict Gulf-wide impact. Here we focus on the role of fluid mechanics in helping to determine the effectiveness of subsea injection of chemical dispersants.

Chemical dispersants

As part of the spill response, nearly 3 million liters of chemical dispersant were applied at the spill source, the first time in which dispersants had been used in this manner at a major oil spill. [Figure 1] Dispersants reduce interfacial tension (IFT), allowing smaller droplets to be formed than would be the case otherwise. This, in turn, allows droplets to be broadcast more widely, and to rise more slowly, reducing impacts to rescue workers and biota on the surface and the shoreline. Coupled with their greater surface area, this also leads to greater rates of dissolution and degradation and, over time, less toxic oil in the environment. On the other hand, there is some evidence that chemically dispersed oil and some dispersant compounds are toxic to some marine life, especially early life stages (NAS, 2013). Hence it is helpful to have a clear idea of just how effective dispersants are—i.e., how much they reduce droplet size and how much this matters—so that their use can be optimized.

Modeling droplet sizes

Under the highly energetic environment of a blowout, droplet sizes are determined from a combination of droplet break-up, due to turbulent fluctuations in pressure, and coalescence due to droplet collision. For decades, chemical engineers have studied such processes under equilibrium conditions, such as a stirred reactor, and developed correlations of characteristic droplet size with the non-dimensional Weber number, which involves density, IFT, a velocity scale and a length scale. However, oil emanating from a blowout is not in equilibrium, but instead experiences decreasing turbulence along the buoyant jet trajectory. Two modeling approaches have been taken to address the dynamic conditions in a jet. The first approach calibrates observed droplet diameters, measured in laboratory experiments with oil jetted into seawater, to the Weber number using the orifice diameter and velocity as length and velocity scales, respectively (e.g., Brandvik, et al., 2013; Johansen, et al., 2013). Modifications have also been made to account

Dr. Adams **is a Senior Research Engineer with MIT's Dept of Civil and Environmental Engineering.**

Dr. Socolofsky **is an Associate Professor with Texas A&M University's Zachry Dept of Civil Engineering.**

Dr. Boufadel **is a Professor at the New Jersey Institute of Technology's Dept of Civil and Environmental Engineering.**

The three are members of an American Petroleum Institute research team evaluating models of subsurface dispersant injection.

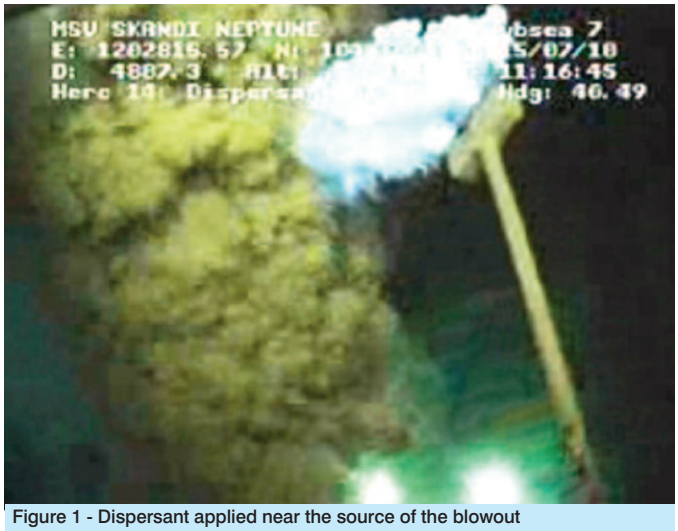

Figure 1 - Dispersant applied near the source of the blowout

FROM A DEEP OCEAN BLOWOUT: NTS

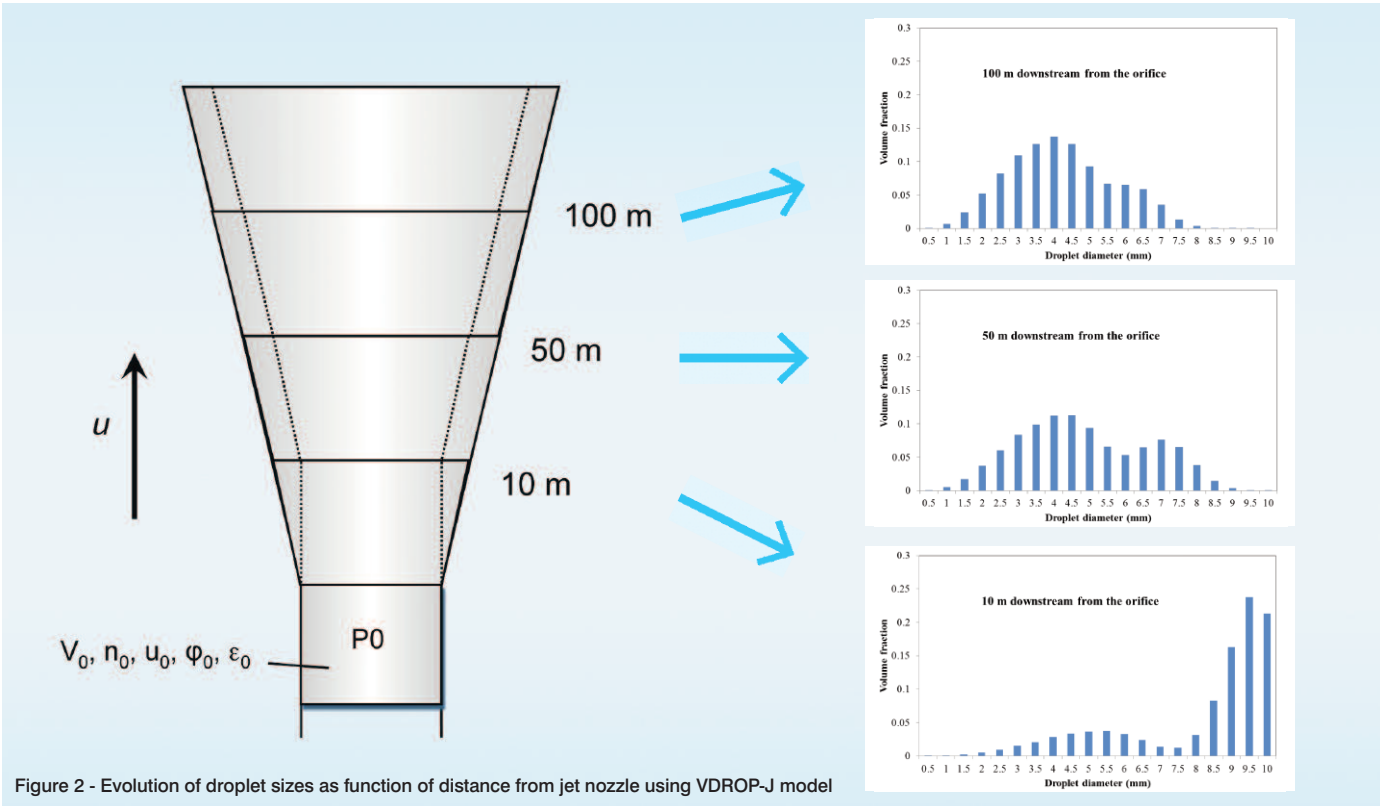

Figure 2 - Evolution of droplet sizes as function of distance from jet nozzle using VDROP-J model

for viscosity (which becomes important when IFT shrinks due to use of dispersants), and the presence of natural gas mixed with the oil. Predicted median droplet sizes from these jet-based correlations agree well with a wide range of laboratory experiments and one small-scale field study, and provide a hopeful method to extrapolate to the scale of a major blowout. They also provide much better agreement with experimental data than correlations based on measurements from a stirred reactor (e.g., Aman et al., 2015). The other approach is use of a dynamic model which simulates droplet breakup and coalescence as oil experiences time-varying turbulence along its trajectory. Recent developments in this field have been captured in the population-based model VDROP (Zhao et al., 2014a), which accounts for the effect of both IFT and oil viscosity in resisting breakup. Zhao et al. (2014b) coupled VDROP to an analytical buoyant jet model and developed the model VDROP-J, whose predicted droplet sizes have been successfully calibrated to available data. [Figure 2] Other models to predict the evolution of the droplet size distribution have been reported by Bandera and Yapa (2011).

A recent model inter-comparison workshop brought together a number of modelers to inter-compare predictions of droplet size and transport for a number of specified test conditions (Socolofsky, et al., 2015). For a large size spill (approximately one third the flow rate of the Deepwater Horizon spill), most models predicted droplet sizes ranging from 1-10 mm without dispersants, and 0.1 to 1 mm if dispersants were uniformly mixed with the oil at a dispersant to oil ratio of 2%. There are still some remaining questions that are being addressed with on-going experiments, such as the effects of using live oil (containing gas), and the dependence on temperature and pressure. Nonetheless, models were in general agreement that the predicted reduction in droplet size and corresponding reduction in droplet rise velocity, could be expected to result in more than an order of magnitude increase in the downstream length to the surfacing oil footprint, a significant measure of the effectiveness of subsea injection of chemical dispersants.

References

Aman, Z. M., C.B. Paris, E.F. May, M.L. Johns, and D. Lindo-Atichati (2015), High-pressure visual experimental studies of oil-in-water dispersion droplet size, Chemical Engineering Science, 127:392-400.
Bandara, U. C., and P. D. Yapa (2011), Bubble sizes, breakup, and coalescence in deepwater gas/oil plumes, J Hydraul Engineering, 137(7), 729-738, doi:10.1061/(asce)hy.1943-7900.0000380.
Brandvik, P. J., Ø. Johansen, F. Leirvik, U. Farooq, and P. S. Daling (2013), Droplet breakup in subsurface oil releases – Part 1: Experimental study of droplet breakup and effectiveness of dispersant injection, Mar Pollut Bull, 73(1), 319-326, doi:http://dx.doi.org/10.1016/j.marpolbul.2013.05.020.
Johansen, O., P. J. Brandvik, and U. Farooq (2013), Droplet breakup in subsea oil releases - Part 2: Predictions of droplet size distributions with and without injection of chemical dispersants, Mar Pollut Bull, 73(1), 327-335, doi:10.1016/j.marpolbul.2013.04.012.
National Academy of Sciences (2013), An ecosystems services approach to assessing the impacts of the Deepwater Horizon oil spill in the Gulf of Mexico, Nat'l Acad Press, Washington, DC.
Socolofsky, S.A, E. E. Adams, M. C. Boufadel , and 15 others (2015), Intercomparison of oil spill prediction models for accidental blowout scenarios with and without subsea chemical dispersant injection, Mar Pollut Bull, accepted for publication.
Zhao, L., J. Torlapati, M. C. Boufadel, T. King, B. Robinson, and K. Lee (2014a), VDROP: A comprehensive model for generating the droplet size distribution from oils—Incorporation of interfacial tension and oil viscosity, Chemical Engineering Journal, 253: 93-106.
Zhao, L., M. C. Boufadel, S. A. Socolofsky, E. Adams, T. King, and K. Lee (2014b), Evolution of droplets in subsea oil and gas blowouts: Development and validation of the numerical model VDROP-J, Mar Pollut Bull, 83(1), 58-69, doi:http://dx.doi.org/10.1016/j.marpolbul.2014.04.020.

APPENDIX I

EVALUATION OF MODELS FOR SUBSURFACE DISPERSANT INJECTION

PROGRESS REPORT 9

E. Eric Adams, PhD, PE

Scott A. Socolofsky, PhD

Michel Boufadel, PhD, PE

Submitted to

American Petroleum Institute

Oil Spill Response Joint Industry Task Force (JITF)

D3 Subsea Dispersant Injection Modeling Team

Attn: Joe Twomey

patrick.twomey@hdrinc.com

September 23, 2016

Introduction

Since Progress Report 8 we have: a) reviewed two additional models for predicting oil droplet sizes (the "ASA" model, Spaulding, et al., 2015; and "Oildroplets", Nissanka and Yapa, 2016); b) reviewed two reports summarizing recent API D3 studies on Phase V (Live oil and natural gas; Brandvik, et al., 2016a) and Phase VI (Upscaling; Brandvik, et al., 2016b); c) initiated a brief comparison of Phase VI experimental results on droplet sizes with the results of the model VDROP-J; and d) coupled more fully the near field plume model TAMOC with the droplet model VDROP-J, with application to the DWH spill. In addition we attended the AMOP conference in June 2016, presenting a paper by Socolofsky, Dissanayake, Adams and Boufadel on "Required accuracy of oil droplet size distribution predictions for fate and transport modeling of subsea accidental oil well blowouts".

Review of Additional Models

We have briefly reviewed two new models.

Spaulding, et al., (2015) of RPS ASA developed a model (called here the ASA model) for NRDA because they thought existing models were inadequate. The reasons for this belief were that: i) they thought operational models (CDOG, Deep Blow and the earlier OILMAP DEEP) based on We scaling predicted droplets for treated discharges that were too small, ii) they thought the modified We scaling proposed by SINTEF predicted droplets for treated discharges that were too large, and iii) they thought population models were not sufficiently tested/available for routine engineering purposes. We believe they are certainly right on i) as viscosity (omitted from early operational models) should be included as a resisting force for break-up when IFT is small. ii) is based on comparisons of model predictions against data from SL Ross and OHMSETT tank tests (Belore, 2014; S.L.Ross (2014). As mentioned by SINTEF (Brandvik, et al., 2016b), and discussed below, these tests were conducted with thin shearing oils at very high shear rates (due to large discharge velocities and small orifices). Hence the *in situ* viscosities during the experiments were likely quite a bit smaller than those measured at lower shear rates outside of the jet, and thus the predicted droplet sizes should have been smaller. So, we don't think ii) should discredit modified We models.

As applied to oil droplets, the ASA model (Eq 17 of Spaulding, et al., 2015) is

$$d_{50}/d_o = r\, We^q\, (1 + 10Oh)^p$$

where d_{50} is the volume median droplet diameter, Oh is the Ohnesorge number = $\mu/(\rho\sigma d_o)^{0.5}$, We is the Weber number = $\rho U^2 d_o/\sigma$, and r, p and q are empirical constants. In their definition of Oh and We, σ is the IFT between oil and water, μ is the viscosity of oil, ρ is the density of water (in We) and oil (in Oh), and U is the oil exit velocity. We presume that no modification is made in

the definition of U for the presence of any gas combined with the oil. Also, d_o is a characteristic length scale equal to either the orifice diameter (as used in most models) or the maximum stable droplet size, whichever is smaller. This is an interesting concept and we wonder if the definition might be suitable for application to other models (e.g., the length in the modified We number or the seed diameter for population models). See also below. The exponents p (0.46) and q (-0.518) come from analysis of droplet sizes of surface oil dispersed by breaking waves, while the constant r (9.67) comes from a fit to droplet sizes measured during the Deep Spill field experiment. The fact that they included data from both surface and submerged oil releases reflects the authors' desire to find a universal equation that applied to both conditions, but we wonder if this is possible, given the somewhat different breakup mechanisms.

As part of their model development, they evaluated several forms of the droplet distribution and argue for log-normal.

With their three constants they were able to fit their predicted droplet sizes to the two data sets reported by Belore (2014) as well as the SINTEF Tower Basin data. When comparing their model with the Belore data, they presumably used Belore's measured viscosities to compute Oh, so we suspect their model, if used with *in situ* viscosities, would predict droplets for treated oil that are too small. See further discussion below.

The maximum stable droplet size is given by:

$$d_{max} = 4(\sigma/g\Delta\rho)^{0.5}$$

Referencing our PR1, if one uses σ = 23 dyne/cm, and $\Delta\rho$ = 0.18 g/cm^3 for the DWH spill, then d_{max} ~ 1.5 cm. This is in contrast to an "orifice" size as large as 50 cm. For untreated oil, the modified (or straight) We model gives d_{50} proportional to $d_o^{0.4}$ so using a d_o of 1.5 versus 50 cm, produces smaller predicted droplets by a factor of $(50/1.5)^{0.4} = 4$.

They also compare the predictions to measurements taken with ROV video and holographic cameras in the aftermath of the DWH spill. These measurements were made within the intrusions which would only have contained droplets less than a critical size (Chan et al., 2015), which is most likely to have occurred during times when dispersant was applied. Thus, while their predictions were in the ballpark, the uncertainty in the discharge and ambient conditions occurring at the time render precise validation impossible.

We have compared the values of d_{50} predicted with the ASA model versus what we believe to be the best available data for oil droplets. See Table 1 and supporting calculations in the appendix, which is an addendum to the appendix of our PR1. We have included: 1) data from SINTEF's Tower Basin in their API Phase I study (designated Block A in the appendix); 2) data from SINTEF's Tower Basin in their earlier BP-supported study (Block B); 3) data from Tang and Masutani for silicone fluids; 4) field experiments with diesel oil and LNG at Deep Spill; and 5) recent larger scale work conducted by SINTEF in their Tower Basin and at Ohmsett (API D3

Phase VI study). Data sets 1) through 4) have been discussed in our PR1, and 5) is discussed below. We have omitted Tang and Masutani's data with oil, due to their concern about the reliability of their PDPA instrumentation applied to opaque fluids, and a recent study by Zhao et al. (2016) at Ohmsett, due to concerns that their LISST instrument may have preferentially sampled smaller droplets at the bottom of their rising horizontally discharged plume. The predictions of both the ASA model and the SINTEF model (with A = 24.8 and B = 0.08) versus data from the five studies are included in the appendix, and the average of observed versus predicted ratios of d_{50} for the five studies are reported in Table 1. We note that the two models define the Weber number slightly differently (ASA bases their definition on the density of water while SINTEF uses the density of oil), and ASA uses d_o as a length scale as described above. (Runs in which $d_o = d_{max} < D$ are shaded in the column labeled d_{max}.) Also, when compared to the large scale data, the SINTEF model was applied explicitly, using the observed value of d_{50}/D in the modified We.

Table 1 Comparison of ASA and SINTEF model predictions of d_{50} versus data

Data Set	No data points	Aver.Obs/Pred d50 for ASA model	Aver Obs/Pred d50 for SINTEF model
A) Tower Basin (API)	17	2.88	1.02
B) Tower Basin (BP)	10	3.28	1.75
C) U. Hawaii silicone fluid	15	1.53	1.28
D) DeepSpill Field Study	4	2.10	0.63
E) Ohmsett/TB (API)	66	2.15	0.88
Average		2.39	1.11

From Table 1 it appears that the ASA model under-predicts droplet size by more than a factor of two, which would be qualitatively consistent with the above discussion concerning their treatment of Belore's data in their model calibration. Meanwhile the SINTEF model predictions are, on average, within about 10% of the data. However, we note that the SINTEF model predicts significantly smaller droplet sizes compared with data, for the BP supported tests as opposed to the API supported tests, which is consistent with the different calibration coefficients (A = 24.8; B = 0.08 found for the API study and A = 16; B = 0.8 for the BP study).

The ASA model was also applied to bubbles from a gas-only release. (There was no mention of a combined gas and oil release.) Full details are missing from Spaulding et al. (2015) and no calculations for bubble size are presented, but they state that phase specific parameters were used in We (including σ = 73 dyne/cm), that a constant (small) value was used for Oh, and that r = 2.99 (based on observations from the Deep Spill field experiment). We presume that exponents p and q were the same as used with oil. There is ambiquity in the literature as to whether the density used in We is that of the jetted fluid (oil or gas) or the seawater. The ASA model predictions use seawater so their calibration must reflect this choice.

Nissanka and Yapa (2016) is a follow-up to an earlier paper (Bander and Yapa, 2011), and describes a dynamic (or population based) oil droplet size model. The model, which the authors dub Oildroplets, computes droplet sizes by simulating the processes of droplet breakup and coalescence as droplets are transported within a plume and experience time varying turbulence along the plume trajectory. Plume properties needed to run Oildroplets are computed using a companion plume model CDOG (Zheng et al., 2003).

The model is semi-empirical. There are several constants involved in the sub-models describing collision frequency and the efficiency of breakup and coalescence. The values for the constants are mostly taken from the literature (i.e., not calibrated to blowout data). However, the most important parameter is the energy dissipation rate ε which is a function of jet mean velocity and radius, i.e., $\varepsilon = c_d V^3/R$. The authors fit the value of c_d separately for each of 9 laboratory experiments conducted by SINTEF as well as limited data from the Deep Spill field experiment. After fitting, the agreement with observed droplet size distributions is good. However, because the functional form of ε is well established, the constant of proportionality c_d should be relatively constant, yet the calibrated values of c_d vary (their Table 2) by a factor of 80! And when the authors tried to correlate the calibrated values of c_d to non-dimensional parameters, their correlations were not as successful as when they correlated c_d with the (dimensional) velocity V. One would prefer a non-dimensional correlation so this remains a limitation of the model.

Oildroplets also requires that a seed diameter be chosen. This is consistent with the major finding of Zhao et al (2016) that the droplets result from primary breakup at the orifice followed by secondary breakup that is based on turbulence. If the seed size was too large, computed droplet sizes were found to be too large, so the authors constrain the seed diameter to be smaller than the orifice diameter. It is not clear how well this constraint works for very large orifice diameters (e.g., 50 cm in the case of DWH) and we wonder if the maximum stable droplet size, described above, would make a better maximum seed size since it represents a maximum achievable droplet size, and is independent of the orifice size.

Review of API supported studies

SINTEF/SwRI's Phase V study (Brandvik, et al., 2016a) was conducted to understand how oil droplets (and to some extent gas bubbles) are formed under combined oil and gas releases. A second objective was to simulate live oil by recombining dead oil with natural gas. Tests were performed at both SINTEF's Tower Basin and a hyperbaric chamber at SwRI. The tests exploit the capabilities of their newly developed color Silhouette camera combined with video imaging to distinguish droplets from bubbles. Details of the instrumentation and analysis software are contained in Davies et al. (2016), but this report is apparently still in preparation. The following are some observations.

The modified We model reproduces the observed decrease in median droplet diameter with increasing gas flow rate (and constant oil rate; Figure 4.11) in the high pressure tests conducted at SwRI. And indeed the predicted median diameters agree quite well for both untreated and treated oil (Figure 4.15). A somewhat milder decrease in droplet size with increasing gas flow was observed in the Tower Basis tests (Fig 4.7), but no predictions are included nor is any explanation offered for the milder trend.

The high pressure tests seemingly validate the extensions of the modified We model dealing with an increased velocity U_c to account for increased plume momentum and buoyancy in the presence of gas. To our knowledge, this is the first data set that actually shows that the added buoyancy and turbulence introduced by the gas decreases droplet sizes. Neither earlier SINTEF studies conducted as part of API D3 Phase II, nor the Belore (2014) data showed a definitive dependence of oil droplet size on gas flow rate, so it would be interesting to understand why such a dependence was observed here and not before. See further discussion under review of Phase VI below.

The behavior of gas bubbles appears more complicated than that of the oil droplets. Figure 4.8 shows that bubble size increases with gas flow rate in the Tower Basin tests when gas was released along with oil, and Figure 4.9 shows similar behavior when water was used in place of oil. Yet, Figures 4.11 and 4.12 show the opposite: in the high pressure SwRI tests, bubble size decreases with increasing gas flow when both oil (Figure 4.11) and water (Figure 4.12) are discharged along with gas. If the modified We model applies to gas bubbles as well as oil droplets, then bubble size should decrease with gas flow. A plausible explanation for the different trends, suggested by the authors, is that, because of the low gas density in the Tower Basin tests (conducted at essentially atmospheric pressure), the We's of these bubbles were much less than those in the high pressure tank, and hence might not have been in the atomization regime. Of course, this explanation assumes that the Weber and modified Weber numbers are computed using the density of the jetted fluid (oil or gas) and not the receiving seawater. The difference in density between oil and seawater is small, but that between gas and seawater is substantial. We note that some researchers going back to Hinze (1955), and including Johansen et al., (2013), Spaulding et al., (2015), and Nissanka and Yapa (2016) base their We on the density of seawater, while others, including Tang and Masutani (2003), Brandvik et al., (2012), and Johansen et al. (2015) base We on the jetted fluid.

Assuming We is based on the density of the jetted fluid, some support for the authors explanation above is provided in Table 2 which shows computed values of gas We for tests conducted in SINTEF's Tower Basin and in the hyperbaric tank at SwRI. The atmospheric pressure tests assume $\rho = 0.002$ g/cm^3, $\sigma = 73$ dyne/cm, $D = 0.3$ cm, $Q_o = 1.5$L/min, $C_g = nQ_o/(1-n)$, where n is the void fraction ($0.1 < n < 0.9$), and $U = 4Q_g/(3.14nD^2)$. For simple comparison, similar parameter values are used for the hyperbaric tests except that the gas density is increased by 100X. Tang and Masutani (2003) report that the threshold value of We separating laminar from transitional jet break up, when oil is jetted into seawater, is 30, while the value separating

transitional from atomized breakup is We = 324. For most values of n, the atmospheric tests were in the laminar regime, and none were in the atomization regime; for the hyperbaric tests, some were in the transitional and some were in the atomization regime. The laminar conditions indicated for the atmospheric pressure tests certainly suggest that the modified We model might not be appropriate for predicting gas bubble sizes, but it is unclear why bubble sizes would increase with We in the laminar regime. Results from Tang and Masutani (2003) suggest that, for laminar conditions, bubble/droplet sizes are scaled by the orifice diameter, so one might expect the bubble sizes to be independent of We. Table 2 also includes roughly calculated values of We for Deep Spill and the DWH spill, both of which exceed 340, suggesting bubble formation is in the atomization range.

Table 2 Calculated values of Weber number for SINTEF experiments with gas

Study/ Facility	Void ratio (n)	D (cm)	ρ_g (g/cm^3)	Q_g (cm^3/s)	U (cm/s)	We
Tower Basin	0.1	0.3	0.002	2.8	390	1.3
	0.3	12	0.002	10.7	510	2.1
	0.5	0.3	0.002	25	710	4.1
	0.7	0.3	0.002	58	1180	11
	0.9	0.3	0.002	225	3540	100
SwRI	0.1	0.3	0.2	2.8	390	130
	0.3	0.3	0.2	10.7	510	210
	0.5	0.3	0.2	25	710	410
	0.7	0.3	0.2	58	1180	1100
	0.9	0.3	0.2	225	3540	10000
Deep Spill	0.33	12	0.1	7000	190	580
DWH	0.5	50	0.2	900000	92	1200

Finally, gas bubble sizes, like oil droplet sizes, were reduced in the presence of dispersants. As with oil, the reduced bubble size would enhance transformation processes such as dissolution and degradation that depend on surface area. The increased dissolution, in turn, would lead to a more rapid decrease in plume buoyancy.

Following are a couple of curiosities. Figure 4.5 shows an interesting skewness toward smaller bubble sizes overlapping with a skewness toward larger droplet sizes. There is also a hint of bi-modality in the oil distribution. Only one graph of droplet size distribution was provided, although more raw data are in the appendix.

One diagnostic they performed is to compute the gas void fraction observed in the plume based on the ratio of integrated bubble volumes divided by integrated bubble plus droplet volumes and compare this with the void fraction in the inflowing fluids. For example, Figure 4.6 shows that, for some tests, the quantified void fraction is consistently higher than input, suggesting that the

measured bubble sizes are a bit too big, or that the measured droplet sizes are a bit too small. If so, is this a basis for a secondary calibration?

SINTEF's Phase VI study on upscaling (Brandvik, et al., 2016b) reports laboratory data on droplet size distributions at significantly larger scale (larger droplet sizes, afforded by the use of larger discharge diameters) than have been available before. In the process they have developed and tested a droplet measurement system (Silhouette camera), and used plume modeling (SINTEF's Plume 3D) to optimize available space and time at OHMSETT. This is potentially a very significant contribution!

Most of the data appear to be of high quality and they have identified procedures to weed out data of unacceptable quality. However, the following are some places where additional information is needed. Some of the ideas come from a conference call with API, SINTEF and us on September 12, 2016

- Perhaps most importantly, they need to report more precisely the camera locations (in all three dimensions) relative to the plume origin and trajectory. The longitudinal separation between discharge and measurement would allow for more informed comparisons with models such as VDROP-J that show DSD evolving with distance.
- The longitudinal position also relates to possible droplet/bubble loss out of the top of the plume. We appreciate that they considered droplet loss this when they chose a vertical discharge. Nonetheless, how sure are they that they have not lost droplets out the top?
- The vertical position of the camera is also related to potential droplet/bubble loss. We understand that the cameras were kept in a single location for each experiment even though the flow rates changed. So apparently the jets were positioned so that the cameras' field of view was similar for each plume. Were there any (regular) camera images taken to show the location of the Silhouette camera relative to the plume for verification? If the field of view was slightly high/low relative to the plume, this would bias the observations to relatively large/small droplets.
- One idea discussed during the Sept 12 teleconference, would be to analyze SilCam images frame by frame (i.e., at discrete times; hence distances along the plume) in addition to ensemble averaging. Plumes are known to meander and the up and down motion of a meandering plume allows a stationary camera to capture droplets residing at different elevations relative to the plume centerline, thus offering a way to estimate the error associated with uncertain camera placement. Also, though this would require more work, the authors could use their plume model to predict the differential transport of large and small droplets within their plume and thereby gauge possible distortions to the measured droplet size distributions. Even if the camera were sitting exactly on the plume centerline, is the DSD on the centerline representative of the DSD averaged over the entire crossection? Perhaps a model could tell?

- What is the smallest droplet size that the cameras(s) can resolve? Are they possibly missing the smallest droplets in the DSD's of the treated oil? For example, the right side of Figure 5.7 seems too grainy to discern the smallest droplets which were reported.
- Unless we are misinterpreting something, there appear to be some small discrepancies between the volume median droplet sizes indicated on Figures 5.8, 5.10, and 5.12 and those in Table C-1.
- Finally, as a summary it would be helpful to include some error bars on the measurements. (We do realize that replicates were taken so some measure of error can be found in the spread of the measurements in Figures 5.14-5.19.)

The authors compare their data with predictions of their previously developed modified Weber number model for a single dispersed phase (oil). Note that this comparison uses the coefficients developed in their Phase I study (A = 25, B = 0.08). Generally good agreement is obtained, which suggests their relationship can be extended to larger modified Weber numbers than were obtained in previous lab experiments, and approaching those achieved in the DeepSpill field experiment. The following are some comments that relate to both the Phase V and VI studies.

As they mention, their Phase VI experiments only included a single dispersed phase (oil). Thus they were unable to test at large scales their theory that the presence of natural gas, which creates higher discharge momentum (because of the added volume flux) and more turbulence (due to the added buoyancy), produces smaller oil droplets. Based on the apparent success of the Silhouette camera combined with video imagie analysis documented in their Phase V study (which we realize was actually conducted after the Phase VI study), it would be nice to see a few additional runs made and analyzed at large scale using both gas and oil.

Because the addition of gas has a significant influence on predicted droplet size, it might be worthwhile to re-examine the only other experimental studies we are aware of that address this topic: SINTEF's Phase II study, and Belore (2014), neither of which provide evidence that the presence of gas decreases droplet size. Both studies are hampered by the fact that the LISST instrumentation they used cannot distinguish between gas and oil, but the Belore study was conducted using horizontal jets so the gas bubbles and oil droplets should have escaped from the jet preferentially, allowing measurements at locations where mainly droplets were present. The gas and oil do not fractionate completely (some oil would escape with the gas) and the oil droplets would tend to escape preferentially in accordance with rise velocity (this was found in the Phase VI study), but perhaps the distributions could be calculated with plume models. It should also be mentioned that the Belore study did not include experiments with only oil for comparison, but they did conducted tests with fixed oil flow rate and varying gas flow rate. Indeed, of the 20 pairs of experiments in which Belore only increased the GOR (increasing the flow rate of gas, but leaving the oil flow rate constant), the measured median droplet diameter *increased or did not change* substantially in 14!

The Phase VI report stresses the need to estimate accurately the *in situ* viscosity in order to properly apply the modified We model. Like most laboratory studies, Belore (2014) used very high discharge velocities and small orifice diameters, resulting in high shear rates, which are roughly proportional to velocity over diameter. To the extent that the oils tested were shear-thinning, this means that the viscosities they measured at shear rates of $1s^{-1}$ and $100s^{-1}$ were likely higher than the *in situ* viscosity, leading to over-prediction of median droplet diameter using the modified We formula. However, while this impacts the author's ability to *predict* droplet sizes, it should not affect a direct comparison of experimental data conducted with varying GORs.

This is a reminder that calculations of droplet size are less reliable for treated oil than for untreated, due to the difficulty of estimating *in situ* values of IFT (and viscosity) in the former. For determining IFT for their OHMSETT tests, it appears that SINTEF simply used constant values of 20 and 0.2 (cgs units) for untreated and treated oil, respectively. The IFT for untreated oil is easy to obtain, but assuming a constant reduction of 100X with treatment (DOR = 1% with application using a SIT) is pretty rough. (We note that in their high pressure tests at SwRI, measured values of IFT for treated oil were often only 5 to 10X smaller than values for untreated oil.). For viscosity, they mention the importance of measuring it at the appropriate shear rate, in case the oil is non-Newtonian. See above discussion. But viscosity can't be measured in the field, so one must rely on laboratory measurements at a specified shear rate. What is the appropriate shear rate? Like other turbulence characteristics (e.g., dissipation rate), velocity gradients in a turbulent jet will be greatest at the edge of the jet within the zone of flow establishment (ZFE), and these gradients are not resolved by models that presume complete mixing across the jet (e.g., VDROP-J). Beyond the ZFE, the velocity shear varies more gradually, and is more likely to be resolved by 1-D models. So one question is whether most of the breakup takes place before or after the ZFE (~ 6 nozzle diameters downstream from release).

This is not just an issue with Belore's tests; most experimental studies have been conducted at high shear rates. Approximating the shear rate as being proportional to the discharge velocity divided by the orifice diameter (U/D), Table 3 summarizes characteristic shear rates for several laboratory and field conditions. The shear rates in the lab are significantly higher.

As a matter of fact, SINTEF's measured viscosities for their Oseberg Blend did not actually vary much with shear rate. Their Figure 4.15 suggests that as shear rate increased from 100 to 1000 s^{-1}, viscosity decreased by only about 4% at 40 ^{o}C to 17% at 5.5 ^{o}C. In the limit of small IFT, where viscosity limits droplet break-up, the modified We model predicts that median droplet diameter is proportional to viscosity to the power ¾, so even a 17% decrease in viscosity would result in only a 13% change in droplet diameter.

And, of course, viscosity is only important for treated oil, as the viscosity number used in the modified We becomes insignificantly small for untreated oil.

Table 3 Approximate shear rates (U/D) for various lab and field conditions

Site/Study	U (cm/s)	D (cm)	U/D (s^{-1})
Deep Water Horizon	65	50	1.3
DeepSpill	147	12	12
OHMSETT (Belore)	300	0.15	2020
SINTEF Tower Basin	1415	0.15	9400
OHMSETT (Phase VI)	250	3.2	78
U. Hawaii	300	0.2	1500

As with previous tests, DSDs were only reported for a single longitudinal position, implicitly assuming that the DSD does not evolve (or that any evolution has taken place upstream of the measurement). Population models such as VDROP-J suggest some evolution, and it would be nice to test this in the lab. Population models have also shown a bi-modal DSD and there is a (slight) hint of bi-modality in some of the measured distributions (e.g., Figures 5.2 and 5.4); it would be nice to explore this further.

A few final small comments:

In the conclusion section (and possibly elsewhere) it is stated that …"the experimental data show a very high correlation with predicted values (d_{50}) from the modified Weber scaling algorithm." This statement could be strengthened. Not only is there a good correlation, but there is also a good fit. (The model could hypothetically predict sizes that are exactly 100 times larger than measured, and there would be a good correlation, but a lousy fit.)

Also, Testa et al., (2016) is listed, but the reference is incomplete. It has now been published and can be cited as listed in the references.

Comparing Phase VI results with VDROP-J

We have performed some preliminary simulations of the Phase VI SINTEF/OHMSETT results using VDROP-J, and we found agreement with data for the higher flow rate, but not for the small flow rate. A power point summary of the comparison was distributed and discussed during the Sept 12, teleconference. It is possible that the disagreement at lower flow rates could be due to uncertainties in the measurements (as discussed above) or inadequacies of the model. We are awaiting additional feedback from SINTEF on their measurements before revisiting this issue.

Coupling of TAMOC and VDROP-J

We have completed simulations for one-way coupling of VDROP-J to TAMOC for hind casting the Deepwater Horizon Accident. For the simulations, TAMOC provides the properties and flow rates of the released oil and gas to VDROP-J based on the equations of state in TAMOC and the published daily flow rate volumes during the accident. VDROP-J uses these properties to predict the gas bubble and oil droplet size distributions during the spill. TAMOC in turn uses the equilibrium size distributions from VDROP-J to simulate the near field plume and buoyant droplet rise in the water column. The results of the simulations are compared to atmospheric chemistry measurements by the USGS and to concentrations measured in the subsurface intrusion layers, with good agreement between the modeled fate and transport processes and the measured data. A manuscript describing the simulations has been submitted to PNAS and is currently under review. This is a collaborative article that also includes authors from the ETH-Lausanne, Switzerland.

References

Bander, U. C. and P.D. Yapa (2011), "Bubble sizes, breakup and coalescence in deewater gas/oil plumes." *J. Hydraul. Eng*. 137(7): 729-738.

Belore, R. (2014) "Subsea chemical dispersant research" paper presented to IOSC, Savannah River, GA.

Brandvik, P.J., O. Johansen, U. Farooq, G. Angell and F. Leirvik (2012), "Sub-surface oil releases-experimental study of droplet distributions and different dispersant injection techniques. A scaled experimental approach using the SINTEF Tower basin", Draft report prepared by SINTEF Materials and Chemistry, Aug 2012.

Brandvik, P.J., E. Davies, C. Storey, F. Leirvik, D. Krause, D. (2016a). "Subsurface oil releases—Verification of dispersant effectiveness under high pressure using combined releases of live oil and natural gas." Final Draft Report prepared for American Petroleum Institute by SINTEF, Trondheim, Norway, and Southwest Research Institute, San Antonio, TX, 14 August, 2016.

Brandvik, P.J., E. Davies, C. O. Johansen, F. Leirvik, and R. Belore. (2016b). Subsurface dispersant injection—Large-scale experiments to improve algorithms for initial droplet formation (modified Weber scaling)." Final Draft Report prepared for American Petroleum Institute by SINTEF, Trondheim, Norway, 25 April, 2016.

Chan, G. K. C., A. C. Chow, and E. E. Adams (2015). “Effects of droplet size on intrusion of sub-surface oil spills”, Environmental Fluid Mechanics”, 15: 959-973.

Davies, et al. (2016) “The use of spectral transmittance imaging to size and classify suspended particulate matter in seawater (in preparation).

HInze, J.O. (1955). “Fundamentals of the hydrodynamic mechanism of splitting in dispersion processes.” *AIChE Journal*, 1(3): 289-295.

Johansen, Ø., M. Reed, M., and N. R. Bodsberg (2015). “Natural dispersion revisited”, *Mar. Pollut. Bull* 93 (2015) 20–26.

Johansen, Ø., Brandvik, P.J., Farooq, U. (2013). Droplet breakup in subsea oil releases – Part 2: Predictions of droplet size distributions with and without injection of chemical dispersants. *Mar. Pollut. Bull.* 73, 327–335.

Nissanka, I. D., Yapa, P. D., Calculation of oil droplet size distribution in an underwater oil well blowout, J. Hydr. Res, http://dx.doi.org/10.1080/00221686.2016.1144656.

Spaulding, M., Mendelsohn, Crowley, D., Li, Zhengkai, and Bird, A. (2015) Technical Reports for Deepwater Horizon Water Column Injury Assessment, WC_TR.13: Application of OILMAP DEEP to the Deepwater Horizon Blowout, Appendix G: Development of OILMAP DEEP droplet size model. Report prepared by RPS ASA, South Kingstown, RI 02879.

S.L. Ross Environmental Research (2014) “Subsea chemical dispersant research”, report prepared for Bureau of Safety and Environmental Enforcement, U.S. Dept of Interior, 110 p.

Tang, L., and Masutani, S. M. (2003). "Laminar and turbulent flow liquid-liquid jet instability and breakup." 13th International Offshore and Polar Engineering Conference Honolulu, HI, 317-324.

Testa, J., E. Eric Adams, E. W. North, and R. He (2016), Modeling the influence of deep water application of dispersants on the surface expression of oil: A sensitivity study, *J. Geophys. Res. Oceans*, 121, doi:10.1002/2015JC011571.

Zhao, L., Boufadel, M.C., Socolofsky, S., Adams, E.E., King, T., Lee, K. (2014). Evolution of droplets in subsea oil and gas blowouts: development and validation of the numerical models VDROP-J. *Marine Pollution Bulletin*. 83 (2014) 58-69.

Zhao, L., F. Shaffer, B. Robinson, T. King, C. D’Ambrose, Z. Pan, F. Gao, R. Miller, R. Conny and M. Boufadel. (2016). "Underwater oil jet: Hydrodynamics and droplet size distribution." *Chemical Engineering Journal* 299: 293-303.

Zheng, L., P.D. Yapa, and F. Chen, (2003). A model for simulating deepwater oil and gas blowouts. Part I: Theory and model formulation”. *J. Hydr. Res*. 41(4):339-351.

APPENDIX J

EVALUATION OF MODELS FOR SUBSURFACE DISPERSANT INJECTION

PROGRESS REPORT 10

E. Eric Adams, PhD, PE

Scott A. Socolofsky, PhD

Michel Boufadel, PhD, PE

Submitted to

American Petroleum Institute

Oil Spill Response Joint Industry Task Force (JITF)

D3 Subsea Dispersant Injection Modeling Team

Attn: Joe Twomey [patrick.twomey@hdrinc.com]

Suzanne M. Lemieux [LemieuxS@api.org]

April 28, 2017

Introduction

Progress Report 9 included a review of a new model which we referred to as the "ASA" model, and which was featured prominently in the recent NRDA process. Here in Progress Report 10 we update the review based on ASA's recent journal publication, (Li et al., 2017).

In January we were sent "most recent" copies of the last two studies SINTEF conducted as part of their API D3 work: Phase V ("Live oil and natural gas"; Brandvik, et al., 2016a) and Phase VI ("Upscaling"; Brandvik, et al., 2016b). These reports are basically the same versions which we reviewed in Progress Report 9, but they also include comments from API reviewers. Our Progress Report 9 contained a number of comments/suggestions on these drafts and, based on our earlier conference call with SINTEF, we sense that most of these are being addressed. We also agree with most of API's comments, and encourage the reports to be finalized if they have not already been so. When this happens we would be happy to take a final look.

While not technically within the scope of our API review study, we can mention two additional studies that we have been involved in. The first concerns the size of gas bubbles, as measured in Texas A&M's Offshore Technology Research Center (OTRC). These data, along with data from other studies in the literature, suggest that bubble size depends not only on a Weber number but also on the maximum stable bubble size even within the atomization breakup regime for compressible fluids like gas. We are preparing a draft manuscript describing this work which includes an empirical method to predict bubble sizes. The second study is an attempt to include the process of tip-streaming in our droplet model VDROP-J. A conceptual model was developed based on calibration to droplet sizes measured in a horizontally directed oil into water jet. We have prepared a draft manuscript on this effort as well, and will be happy to forward copies of both manuscripts if/when they are accepted.

Additional comments on "ASA" model

Our previous review of the ASA model was based on the technical report, Spaulding, et al. (2015). These authors have since published a journal paper, Li et al. (2017). The two documents differ slightly, so we have re-examined our previous conclusions based on the newer document. We focus on several aspects of the model that have been mentioned by Don Danmeier and API's D3 team through personal communications with us.

One comment concerns the model coefficient "r" in the relationship for the volume median droplet size d_{50}. As applied to oil droplets, the ASA model (Eq 17 of Spaulding, et al., 2015; eq 5 of Li et al., 2017) is

$$d_{50}/d_o = r\, We^q\, (1 + 10Oh)^p \qquad (1)$$

where d_o is a characteristic length scale equal to either the orifice diameter (as used in most models) or the maximum stable droplet size, whichever is smaller. Oh is the Ohnesorge number $= \mu/(\rho\sigma d_o)^{0.5}$, We is the Weber number $= \rho U^2 d_o/\sigma$, and r, p and q are empirical constants. In their definition of Oh and We, σ is the IFT between oil and water, μ is the viscosity of oil, ρ is the density of water (in We) and oil (in Oh), and U is the oil exit velocity.

The authors claim their model can be applied to both surface oil, which is dispersed with the help of turbulence from breaking waves, and oil from a blowout, which is dispersed with the help of jet-induced turbulence. For *surface oil*, their exponents p (0.460) and q (-0.518) and their proportionality constant r (1.791) come from empirical fits to data from two studies of droplet sizes of surface oil dispersed by breaking waves. For *subsurface oil* Spaulding et al. (2015) assume the same values of the exponents p and q as for surface oil, but fit their constant r (9.67) to observations of diesel droplets from Release 2 (diesel plus LNG) from the Deep Spill field experiment, which had a reported value of d_{50} = 3.7mm (Johansen et al., 2001). Subsequently, Li et al., (2017) picked a larger value of r (14.05) by calibrating their model to a revised value of d_{50} = 5.4mm as reported by Bandvik et al. (2014). In Progress Report 9 we had used the smaller value of r (9.67) and it is clear from the linearity of the model that, all else equal, the larger value of r (14.05) would predict values of d_{50} that are roughly 45% larger. As shown below, that brings their predicted values of d_{50} closer to observations. It is also worth noting, that as part of our Progress Reports 1 and 3, we calculated our own values of d_{50} for the same DeepSpill experiment using data from Johansen et al., (2001). Figures 7.1.18 and 7.1.19 of that report show histograms of droplet size at four elevations above the release. The volume median diameters ranged from 2.9 to 6.7mm with an average of 4.3mm, a bit closer to the smaller of the two values reported above.

The ASA model defines d_o as a characteristic length scale equal to either the orifice diameter D or the maximum stable droplet size, whichever is smaller. The maximum stable droplet size is given by

$$d_{max} = \{4\sigma/[g(\rho_w - \rho_o)]\}^{0.5} \qquad (2)$$

For most laboratory scale experiments (small D) without chemical dispersants (thus reasonably large σ) d_{max} is around 10 mm and thus tends to be larger than, or comparable to, the orifice diameter D, and the length scale reverts to the orifice diameter D. However, for larger lab settings (e.g., the Ohmsett facility) and/or experiments with dispersant treated oil (large D and small σ respectively), d_{max} may govern. We see this in the comparison of ASA and SINTEF model predictions shown below.

Another question concerns the value of U to use when oil is combined with gas. The SINTEF modified We model identifies two possible influences of gas on the flow of oil out of an orifice and in the near field of the buoyant plume. The first factor is that the gas, which has relatively little mass, creates a void, requiring the oil to exit the orifice through a constricted cross-section.

This in turn gives the oil more velocity, momentum and energy than if there were no gas. The second factor is that the gas increases the buoyancy of the mixed plume causing plume velocities downstream from the orifice to be higher than would be experienced by a less buoyant jet without gas. Since SINTEF's model was calibrated to laboratory data with jet-like flow, adjusting the exit velocity to account for buoyancy leads to a downstream jet velocity that more closely resembles that in an actual plume.

In reading Spaulding et al. (2015) and Li et al. (2017) it was not clear which, if either of these two factors were considered. However, it is clear from the calculations pertaining to the DWH spill described in Li et al. (2017), that they took the co-flowing gas into account. According to Don Danmeier of Chevron, who talked with Deb Crowley of ASA, ASA accounts for the volume occupied by the gas (first factor) but not the buoyancy (second factor). Dan indicated that ASA accounts for the volume occupied by gas by calculating the actual (exit) oil velocity between the voids (gas) or U' = U/(1-n) where n is the void fraction, which can be written as GOR/(1+GOR), where GOR is the *in situ* gas/oil ratio expressed in terms of volumes. This approach has been confirmed by us through personal communication with Deb Crowley.

In Progress Report 9 we compared the ASA model predictions (using nominal values for U and D in their definition of We and Oh and a value of r = 9.67), along with the SINTEF model predictions, against data from five studies: A) SINTEF Tower Basin data conducted for API, B) SINTEF Tower Basin data conducted for BP, C) U. Hawaii silicone fluid data, D) DeepSpill field study, and E) Ohmsett/TB study for API. The justification for choosing these data sets (and omitting others) was discussed in the progress report.

A modification of Table 1 from the previous progress report is repeated here. The second column indicates the range of orifice diameters and the third column indicates the number of experiments (or experimental observations in the case of DeepSpill), how many of the experiments used dispersants, and how many of the experiments had a calculated value of $d_{max} < D$. Column 4 shows that the previously predicted values of d_{50} with the ASA model were generally smaller than observed with an average ratio of predicted to observed d_{50} of 0.63. Column 5 shows ASA calculations with the revised value of r = 14.05 and the different definition of U'=U/(1-n). Note that the different definition of U only affects calculations with gas (data from the DeepSpill test). In general, the newly predicted ASA values are much closer to the observations, with an average ratio of predicted to observed d_{50} of 0.97. The newly predicted values are also broken down into those for experiments without and with chemical dispersants. In general, the predictions without dispersants are quite close to the observations (average predicted to observed ratio of 1.07), while the predictions with dispersants are significantly smaller than observations (average predicted to observed ratio of 0.58). The last column shows that the SINTEF model tends to somewhat over-predict observations without dispersants (average ratio of predicted to observed d_{50} of 1.20) and somewhat under-predict observations with dispersants (ratio of 0.75). While predictions with the ASA and SINTEF models seem to be in the same ballpark for data sets A, B, and C, the ASA predictions are

significantly lower than the SINTEF predictions for data sets D and E. We note from column 2 that all runs in these last two studies had $d_{max} < D$, and hence their calculations used the (smaller) maximum stable droplet size as the characteristic length scale. All other things equal, this suggests that the ASA model will predict a greater reduction in d_{50} due to dispersant application than would the SINTEF model. Based on the data in Table 1 alone, it is hard to say which of the two empirical models (SINTEF or ASA) is better, but it is interesting that they both do fairly well in predicting droplet sizes for oil that has not been dispersed, while both under-predict droplet sizes for dispersed oil. And, as has been discussed previously, both models must prescribe a droplet size distribution, and they both assume that the spread of the distribution is independent of scale and that this distribution does not evolve with the distance downstream from the point of release.

Table 1 Comparison of ASA and SINTEF model predictions of d_{50} versus data, adapted from Progress Report 9 (w/o, w/ are tests without and with chemical dispersants)

Data Set	Range of Orifice dia's (cm)	No. Exps (no. w/ disp; no. w/ $d_{max} < D$)	Aver Pred/Obs d_{50} Prev ASA model	Aver Pred/Obs d_{50} Rev ASA model Tot; w/o; w/	Aver Pred/Obs d_{50} SINTEF model Tot; w/o; w/
A) Tower Basin (API)	0.05-0.15	17 (9, 5)	0.68	1.00; 1.24; 0.79	1.02; 1.02; 1.02
B) Tower Basin (BP)	0.05-0.3	10 (4, 2)	0.49	0.73; 0.97; 0.36	0.66; 0.80; 0.48
C) UH silicone fluid	0.1-0.5	15 (0, 0)	0.97	1.42; 1.42; NA	1.24; 1.24; NA
D) DeepSpill Field Study	12	4 (0, 4)	0.52	0.88; 0.88; NA	1.73; 1.73; NA
E) Ohmsett/TB (API)	2.5-5	66 (0, 66)	0.51	0.82; 0.82; NA	1.24; 1.24; NA
Average			0.63	0.97; 1.07; 0.58	1.18; 1.20; 0.75

Returning to the role of gas mixed with oil, the approach used by ASA is somewhat different from that of SINTEF. In Progress Report 1 we discussed various approaches to account for gas, and we expand on that discussion here. Refer to Table 2.

Assume an orifice has a diameter D and that it discharges oil with a nominal velocity (Q/A) of U. If gas is also present, the void fraction n can be written as GOR/(1+GOR), where GOR is the *in situ* gas/oil ratio expressed in terms of volumes. The cross-sectional area through which the oil actually flows is thus $(1-n)\pi D^2/4$, the actual oil velocity is U/(1-n), and an equivalent actual diameter is $D(n-1)^{0.5}$. Thus, one approach to account for gas is to simply use these values of orifice velocity and diameter in the definitions of Oh and We (for the ASA model) and We or modified We (for the SINTEF model). This is Row 2 of Table 2. However, it appears that both models use the nominal diameter for their analysis (except for ASA when the maximum stable droplet diameter is less than the orifice diameter) and adjust the velocity to constrain agreement with some other variable. For example, ASA constrains the actual velocity to be U/(1-n) (Row 3 of Table 2) while SINTEF constrains the momentum flux by using a modified velocity $U/(1-n)^{1/2.}$ (Row 4 of Table 2). Table 2 suggests a couple of other "equivalent" velocities that conserve other potential quantities of interest (Weber number in Row 5 and dissipation rate ε in Row 6).

Table 2 Approaches to correct for the presence of gas with oil assuming a void ratio of n (U is nominal oil exit velocity through an orifice with nominal diameter D)

Approach	Velocity	Diameter	Momentum	We	Dissipation Rate, ε
Nom velocity & diameter	U	D	U^2D^2	U^2D	U^3/D
Match velocity & diameter	$U/(1-n)$	$D(1-n)^{1/2}$	$U^2D^2/(1-n)$	$U^2D/(1-n)^{3/2}$	$(U^3/D)/(1-n)^{7/2}$
Nom diameter; match velocity	$U/(1-n)$	D	$U^2D^2/(1-n)^2$	$U^2D/(1-n)^2$	$(U^3/D)/(1-n)^3$
Nom diameter; match mom.	$U/(1-n)^{1/2}$	D	$(U^2/D^2)/(1-n)$	$U^2D/(1-n)$	$(U^3/D)/(1-n)^{3/2}$
Nom diameter; match We	$U/(1-n)^{3/4}$	D	$U^2D^2/(1-n)^{3/2}$	$U^2D/(1-n)^{3/2}$	$(U^3/D)^{9/4}$
Nom diameter; match diss rate	$U/(1-n)^{7/6}$	D	$U^2D^2/(1-n)^{7/3}$	$U^2D/(1-n)^{7/3}$	$(U^3/D)/(1-n)^{7/2}$

We should emphasize that the corrections described in Table 2 all ignore the momentum of the gas, essentially assuming negligible gas density. Gas density, of course, increases with depth, and based on calculations in Zhao et al. (2014), reaches approximately 73 kg/m^3 in the 844 m water depth of DeepSpill and 135 kg/m^3 in the 1500 m water depth of Deepwater Horizon. Assuming that the actual gas velocity is the same as the oil velocity, and that the nominal void

fractions (n) are 0.33 and 0.5, the gas momentum, as a percentage of the oil momentum, is approximately 4% and 15%, for DeepSpill and Deepwater Horizon, respectively. The former is negligible, but the latter is comparable to the uncertainty expressed in the variability of the corrections in Table 2. Hence neglect of gas momentum is not always negligible.

Table 3 shows the sensitivity of predicted volume median diameters to the above choices choosing, as a reference case, predicted diameters with n = 0. Calculations are made for n = 0.2, 0.5 and 0.8. While this comparison could be made with either the ASA or the SINTEF models, we use the simple SINTEF Weber number model assuming negligible effect of viscosity for which $d_{50} \sim DWe^{-0.6} \sim D^{0.4}U^{-1.2}$.

Table 3 Sensitivity of predicted d_{50} to assumptions in Table 2. Predictions are relative to a reference d_{50} computed with the nominal orifice velocity and diameter (Row 1)

Approach	d_{50}/d_{ref} with n = 0.0	d_{50}/d_{ref} with n = 0.20	d_{50}/d_{ref} with n = 0.50	d_{50}/d_{ref} with n = 0.80
Nom velocity & diameter	1.00	1.00	1.00	1.00
Match velocity & diameter	1.00	0.73	0.38	0.11
Nom diameter; match velocity	1.00	0.77	0.44	0.14
Nom diameter; match mom.	1.00	0.87	0.66	0.38
Nom diameter; match We	1.00	0.82	0.54	0.23
Nom diameter; match diss rate	1.00	0.73	0.38	0.11

From Table 3 we see that all approaches suggest that the presence of gas decreases droplet size and that the decrease is a strong function of the void ratio, n. We also note that the ASA approach of matching the velocity (Row 3) produces smaller droplets than the SINTEF approach of matching momentum flux (Row 4). Finally, as we argued in Progress Report 1, we see that matching the turbulence dissipation rate (Row 6) by adjusting velocity, while maintaining the nominal orifice diameter, is equivalent to using the actual velocity and diameter. This also gives the largest reduction in droplet diameter of any of the approaches analyzed.

There have only been a few data sets in which oil droplet size has been measured for a release of gas plus oil. One such study is the API D3-Phase V study conducted at SwRI and SINTEF (Brandvik, et al., 2016a). We reviewed this study in our Progress Report 9, and reproduce two figures from that report here. Figure 4.11 of that report is modified here as Figure 1 and shows experimental values of d_{50} for two experiments with a fixed flow rate of untreated oil and varying gas flow rate (open and closed blue circles), and two experiments with a fixed flow rate

of treated oil and varying gas flow rates (open and closed red squares). These experiments were conducted at high pressure. Also shown are predictions with the SINTEF modified We model including effects of both increased momentum and buoyancy due to gas. We focus here on only the results for the untreated oil and plot the values of d_{50} expected from scaling three models (Rows 3, 4 and 6 of Tables 2 and 3) which describe various ways to correct for momentum (but not buoyancy). Model 4 (ASA, which preserves the actual exit velocity) and Model 6 (which matches the actual turbulence dissipation rate) both tend to over-predict the decrease in d_{50} with increasing n, while Model 3 (SINTEF's method of matching momentum but not accounting for buoyancy) does not predict enough decrease in d_{50}. But when buoyancy is included (SINTEF's calculations, not ours), the agreement with observations is good.

Figure 4.7 of Brandvik et al., (2016a), modified here as Figure 2, presents similar data collected at SINTEF's Tower Basin under atmospheric pressure. Again we focus on the data for untreated oil and observe that the predicted decrease in d_{50} with increasing n is significantly greater with all three models in comparison with observations. The closest agreement is with the SINTEF model, but that does not include the effect of buoyancy which would make the predicted droplet sizes even smaller.

A third data set that could be used for comparison is that contained in Belore (2014) and S.L Ross, (2014). But in that study the droplet sizes tended to *increase* with n rather than decrease. So, as we concluded in our previous progress report, the SINTEF (and now the ASA) corrections for co-flowing gas seem to agree with some data and not others.

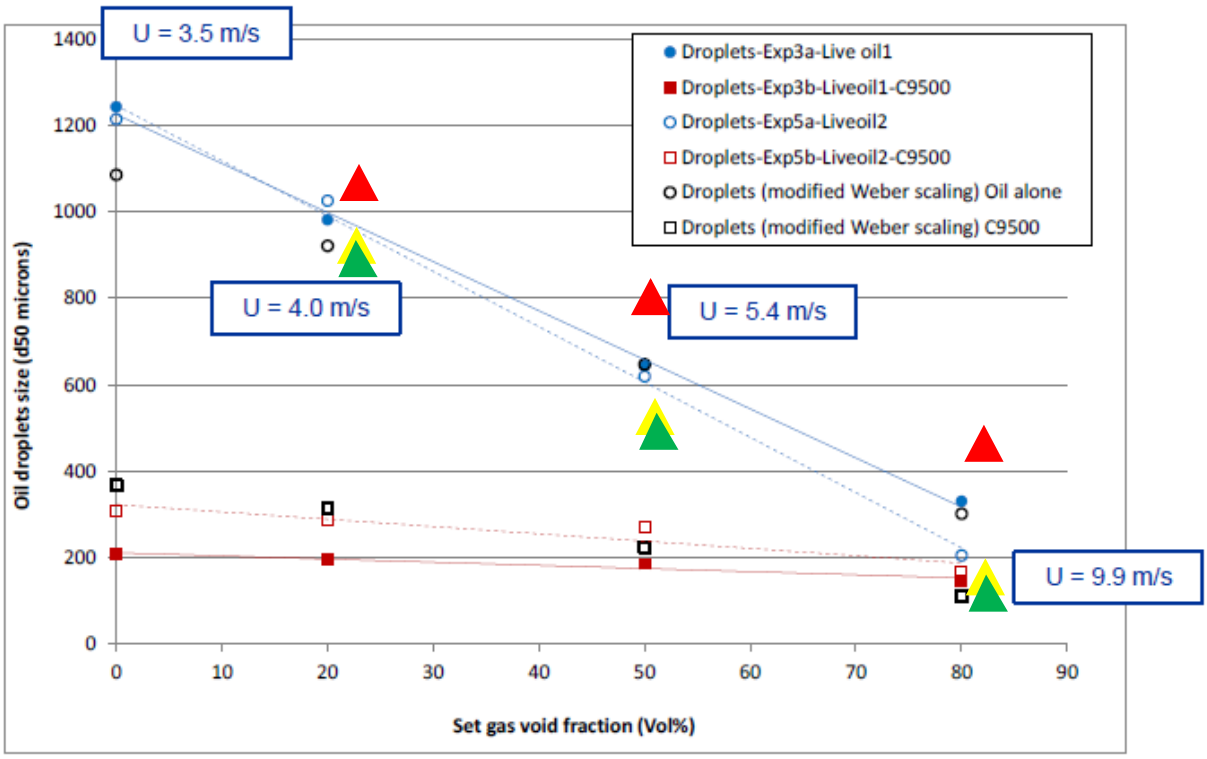

Figure 1 (modification of Figure 4.11 of Brandvik, et al., 2016a). Measured median oil droplet size versus void fraction. Blue circles are data from high pressure tests at SwRI for untreated oil, black circles are SINTEF predictions with their modified We model, and diamonds are diameters scaled from Table 3 for Row 4 (red), Row 3 (yellow), and Row 6 (green).

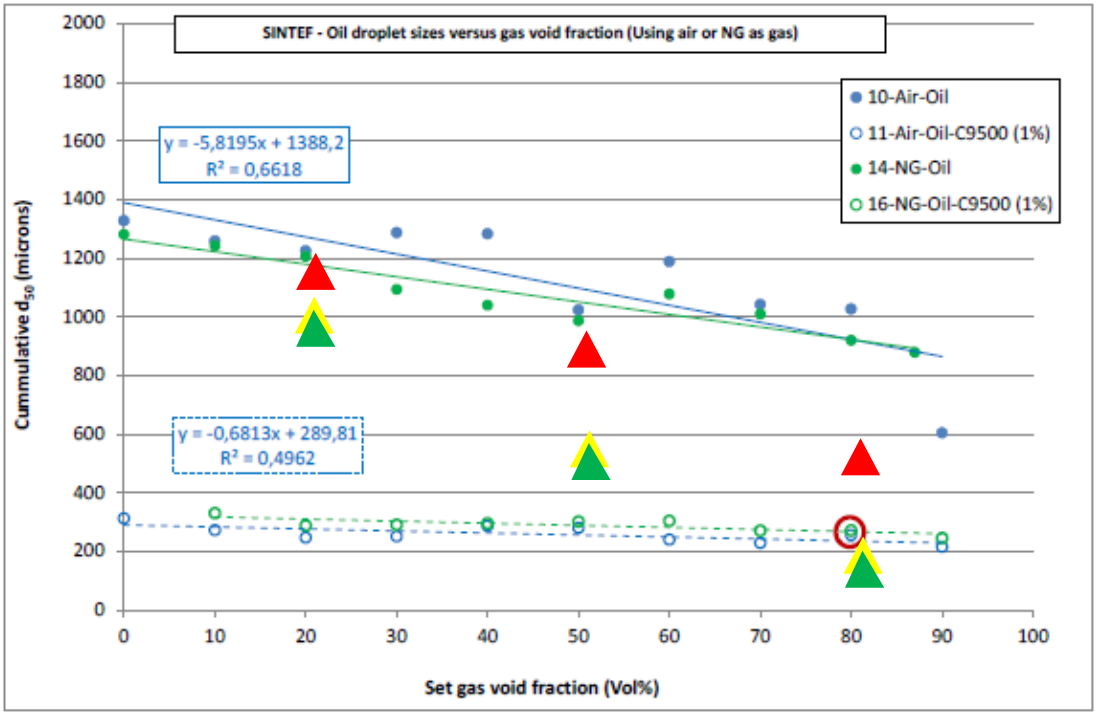

Figure 2 (modification of Figure 4.7 of Brandvik, et al., 2016). Measured median oil droplet size versus void fraction. Solid circles are data from atmospheric pressure tests at SINTEF for untreated oil, and diamonds are diameters scaled from Table 3 for Row 4 (red), Row 3 (yellow), and Row 6 (green).

References

Belore, R. (2014) "Subsea chemical dispersant research" paper presented to IOSC, Savannah River, GA.

Brandvik, P.J.,Ø. Johansen, U. Farooq, G. Angell, F. Leirvik, (2014). "Subsurface oil releases—Experimental study of droplet distribution and different dispersion injection techniques – Version 2. A scaled experimental approach using the SINTEF Tower Basin, SINTEF Report A26122, Trondheim Norway.

Brandvik, P.J., E. Davies, C. Storey, F. Leirvik, D. Krause, D. (2016a). "Subsurface oil releases—Verification of dispersant effectiveness under high pressure using combined releases of live oil and natural gas." Final Draft Report prepared for American Petroleum Institute by SINTEF, Trondheim, Norway, and Southwest Research Institute, San Antonio, TX, 14 August, 2016.

Brandvik, P.J., E. Davies, C. O. Johansen, F. Leirvik, and R. Belore. (2016b). Subsurface dispersant injection—Large-scale experiments to improve algorithms for initial droplet formation (modified Weber scaling).” Final Draft Report prepared for American Petroleum Institute by SINTEF, Trondheim, Norway, 25 April, 2016.

Johansen, O, H. Rye, A. Melbye, H. Jensen, B. Serigstad, and T. Knutsen, (2001). Deep Spill JP Experimental Discharges of gAs and Oil at Jelland Hansen – June 2001. Technical Report SINTEF Applied Chemistry, Trodheim Norway.

Li, Z., M.L. Spaulding, D. French McCay, D. Crowley, and J.R. Payne. (2017). “Development of a unified oil droplet size distribution model with application to surface breaking waves and subsea blowout release considering dispersant effects”. *Marine Pollution Bulletin* 114(1):247-257.

S.L. Ross Environmental Research (2014) “Subsea chemical dispersant research”, report prepared for Bureau of Safety and Environmental Enforcement, U.S. Dept. of Interior, 110 p.

Spaulding, M., D. Mendelsohn, D. Crowley, Z. Li, and A. Bird. (2015) Technical Reports for Deepwater Horizon Water Column Injury Assessment, WC_TR.13: Application of OILMAP DEEP to the Deepwater Horizon Blowout, Appendix G: Development of OILMAP DEEP droplet size model. Report prepared by RPS ASA, South Kingstown, RI 02879.

Zhao, L., M. C. Boufadel, S. A. Socolofsky, E. Adams, T. King, and K. Lee (2014b), “Evolution of droplets in subsea oil and gas blowouts: Development and validation of the numerical model VDROP-J,” *Marine Pollution Bulletin*, 83(1), 58-69.